Resource Allocation Software Algorithms for AMC-OFDM Systems

Muayad Sadik Croock Al-Janabi

School of Electrical, Electronic and Computer Engineering

Newcastle University

Newcastle upon Tyne, UK.

A thesis submitted for the degree of

Doctor of Philosophy

May 2012

Declaration

I declare that this thesis is my own work and it has not been previously submitted, either by me or by anyone else, for a degree or diploma at any educational institute, school or university. To the best of my knowledge, this thesis does not contain any previously published work, except where another person's work used has been cited and included in the list of references.

Muayad Sadik Croock Al-Janabi

To the messenger of Allah (Mohammed) “the praying and peace upon him” and my family.

Whoever treads a path, seeking knowledge therein,
Allah makes easy for him a path to Paradise.
-Mohammed "the praying and peace upon him"

It was tight and when it became even tighter, it suddenly relieved itself
and I had thought it could not do so.
-Alshafiee

Acknowledgements

Foremost, I would like to express my sincere gratitude to my supervisor Dr. Charalampos Tsimenidis for the continuous support of my PhD study and research, his patience, motivation, enthusiasm, and immense knowledge. I am also grateful to my supervisor Prof. Bayan Sharif for all the hope he has put on me, before I thought I could do any research at all. He has enlightened me through his wide knowledge and his deep intuitions about where it should. I also would like to thank my supervisor Dr. Stephane LeGoff for his appreciated efforts. I would like to thank Mrs. Gillian Webber for her support and help.

My deep thanks to my sponsor (Ministry of Higher Education and Scientific Research/IRAQ) for offering me this great opportunity. I also would like to thank Iraqi Cultural Attache'/London for the appreciated support and help throughout my PhD study.

I have been fortunate to come across many funny and good friends, without whom life would be bleak. I thank my colleagues and friends at School of Electrical, Electronics and Computer Engineering, especially Salah, Mohammed, Emad, Chintan, Ahmed, Sabah and Ibrahim. I really appreciate their efforts and help.

My special gratitude is due to my father, my mother for always being there when I needed them most. They deserve far more credit than I can ever give them. I could not imagine the level that I have reached without their warm-heartedness, support and help.

Finally, I owe my thanks to my wife and my children. They have lost a lot due to my research abroad. Without their encouragement and understanding it would have been impossible for me to finish this work.

Abstract

In recent years, adaptive modulation and coding (AMC) technologies, resource allocation strategies and user scheduling for single-cell downlink orthogonal frequency division multiplexing (OFDM) and orthogonal frequency division multiple access (OFDMA) systems have been widely researched in order to ensure that capacity and throughput are maximised. In terms of AMC technologies, the correlation between the channel coefficients corresponding to the transmitted sub-carriers has not been considered yet. In the literature of resource allocation and user scheduling, either channel coding is not considered or only a fixed code rate is specified. Consequently, with a fixed number of data sub-carriers for each user, all these criteria restrict the flexibility of exploiting the available channel capacity, which reflects negatively on system throughput. At the same time, the presented scheduling algorithms so far managed the data of each user regardless the fair services of all users. The philosophy of this thesis is to maximise the average system throughput by proposing novel AMC, resource allocation and user scheduling strategies for OFDM and OFDMA systems based on developed software engineering life cycle models. These models have been designed to guarantee the scalability, extendibility and portability of the proposed strategies. This thesis presents an AMC strategy that divides the transmitted frame into sub-channels with an equal number of sub-carriers and selects different modulation and coding schemes (MCSs) amongst them rather than considering the same MCS for the entire frame. This strategy has been combined with a pilot adjustment scheme that reduces the pilots used for channel estimation in each sub-channel depending on the measured coherence bandwidth, signal to noise ratio (SNR), and SNR fluctuation values. The reduced pilots are replaced with additional data sub-carriers in order to improve the throughput. Additionally, a novel

resource allocation strategy has been introduced in order to maximise the system throughput by distributing the users, transmission power and information bit streams over the employed sub-channels. The introduced method utilises the proposed AMC strategy in combination with pilot adjustment scheme to tackle the problem of channel capacity exploiting efficiently. It presents the throughput as a new cost function in terms of spectral efficiency and bit-error rate (BER), in which both convolutional coding rates and modulation order can be varied. The investigated throughput maximisation problem has been solved by producing two approaches. Firstly, optimised approach that solves the adopted problem optimally using the well known Lagrange multipliers method. This approach requires a huge search processes to achieve the optimal allocation of the resources, which yields a high computational complexity. To overcome the complexity issue, the second approach decouples the considered maximisation problem into two sub-problems based on the decomposition method on the cost of performance particularly for low SNR values. The proposed resource allocation strategy has been developed to work with multi-input-multi-output (MIMO) based AMC-OFDMA systems. In this project, two MIMO transmission criteria are considered, i.e. traditional and eigen-mode. In contrast, a user scheduling algorithm combined with the proposed resource allocation and AMC strategies is presented. The user scheduling algorithm aims to maximize the average system throughput by arranging the users in distinct queues according to their priorities and selecting the best user of each queue individually in order to guarantee a fair user service amongst different priority levels. When the involved users are scheduled, the scheduled users have been passed to the resource allocation to implement the distribution of the available resources. The proposed strategies have been tested over different international telecommunication union (ITU) channel profiles. The obtained simulation results show the superior performance of the introduced approaches in comparison with the related conventional methods. Furthermore, the gradually improvement in the throughput performance of the AMC-OFDM/ODMA system throughout the combination of the proposed strategies is clearly explained.

Contents

List of Figures

List of Tables

Nomenclature

List of Abbreviations

AMC Adaptive Modulation and Coding

AWGN Additive White Gaussian Noise

BER Bit Error Rate

BICM Bit Interleaved Coded Modulation

CDF Cumulative Density Function

CDMA Code Division Multiple Access

CP Cyclic Prefix

CSI Channel State Information

DS Dynamic Sub-Channelling

FEC Forward Error Correction

FER Frame Error Rate

FFT Fast Fourier Transform

FS Fixed Sub-Channelling

HARQ Hybrid Automatic Repeat Requests

ICI Intercarrier Interference

ISI Intersymbol Interference

ITU International Telecommunication Union

LDPC Low Density Parity Check

LS Least Square

MAC Media Access Control

MC-CDMA multi-carrier CDMA

MCS Modulation and Coding Scheme

MIMO Multi-Input-Multi-Output

ML Maximum Log-Likelihood

MMSE Minimum Mean Square Error

MSE Mean Square Error

MWMS Maximum Weight Matching Scheduling

OFDMA Orthogonal Frequency Division Multiple Access

OFDM Orthogonal Frequency Division Multiplexing

OSI Open System Interconnection

PAPR Peak to Average Power Ratio

PEP Pair-Wise Error Probability

PSK Phase Shift Keying

PTS Partial Transmit Sequence

QAM Quadrature Amplitude Modulation

QoS Quality of Service

QPS Queue Proportional Scheduling

QSI Queue State Information

RAI Resource Allocation Information

RA Resource Allocation

RMS Root Mean Square

SCFDE Single Carrier Frequency Domain Equalisation

SE Square Error

SISO Single-Input-Single-Output

SLM Selective Level Mapping

SNR Signal to Noise Ratio

SRAI Scheduling and Resource Allocation Information

SVD Singular Value Decomposition

TDD Time Division Duplex

UBPA User, Bit and Power Allocation

WCDMA Wideband CDMA

WLAN Wireless Local Area Network

List of Symbols

$X(n)$ The OFDM symbols assigned to each sub-carrier in frequency domain

$(.)^H$ The Hermitian operation

$(b)^+$ The maximum of (b,0)

$[.]^*$ The conjugate operation

$\beta(q,r)$ Scheduling matrix element

$\mathbf{H_k^{(m,d)}}$ The channel between k-th user and the assigned BS in terms of the transmit and receive antennas for m-th sub-channel and d-th data sub-carrier

$\delta_d(m)$ The adjusted numbers of data sub-carriers of the m-th sub-channel

$\delta_p(m)$ The adjusted numbers of pilot sub-carriers of the m-th sub-channel

$\eta_k(m)$ Lagrange multiplier

$\eta_m(k)$ Lagrange multiplier

$\gamma(m,z)$ The SNR value of each data sub-carrier within the m-th sub-channel

$\gamma_{\min}(m)$ The minimum SNR value of the m-th sub-channel

γ_{av} The average SNR value

$\hat{\mathbf{H}}_p$ The vector of the estimated channel values corresponding to the pilots

$\hat{H}_d$ The vector of the estimated channel values corresponding to the data

λ The water filling level

$\Lambda_{B_{coh}}(\beta)$ The channel correlation value in terms of B_{coh}

$\mathbf{\Sigma}$ Diagonal matrix containing the singular values as diagonal elements

$\mu_k(m)$ The power adjustment value for m-th sub-channel assigned to k-th user

Ω Lagrange multiplier

$\Pi(m)$ The pilot reduction value of the m-th sub-channel

ψ_g The average system throughput of the g-th transmitted OFDM frame

ψ_{av} Total average system throughput

$\psi_{MIMO,UB}$ Through upper bound of MIMO system

ψ_{UB} Throughput upper bound

ρ_{av} The average spectral efficiency

$\rho_k(m)$ The spectral efficiency for the m-th sub-channel in (bps/Hz)

$\sigma_d^2(m)$ The variance of the MSE of the estimated channel

$\sigma^2_{k,\Xi_k(m,z)}(m)$ The variance of the SNR fluctuation values

$\sigma^2_{W_{k,d}(m,z)}$ The variance of AWGN samples

τ_l The channel delay of the l-th path in (ns)

$\mathbf{H}$ The channel matrix

$\mathbf{U}$ Complex left singular unitary matrix

$\mathbf{V}$ Complex right singular unitary matrix

$\varphi(k,m)$ The user allocation matrix element

$\varpi_{\hat{H}_d(f)}$ The mean values of the frequency response of the channels

$\varrho_d(f)$ The estimation errors of the channel

$\xi_d(m)$ The number of data sub-carriers in the m-th sub-channel

$\Xi_k(m,z)$ The fluctuation values of the channel coefficients corresponding to the involved sub-carriers within the m-th sub-channel assigned to k-th user

$\xi_p(m)$ The number of pilot sub-carriers in the m-th sub-channel

B_T The total channel bandwidth

B_{coh} Channel frequency coherence bandwidth

B_{CSI} The bandwidth required for the feedback CSI

B_{eff} The effective bandwidth

$B_{k,coh}$ The user channel frequency coherence bandwidth

$c_{1_k}(m),\ c_{2_k}(m)$ The selected variables for fitting the theoretical BER to practical values for all employed MCS options

D_{rms} The root mean square (RMS) delay value

$E\{.\}$ The expectation value

K The number of users

$k_{\text{opt}}(m)$ The optimal user to be assigned to the m-th sub-channel

L The total number of channel's paths

M The number of sub-channel

$M(m)$ The selected modulation order for the m-th sub-channel

$MSE^{(full)}(m)$ Channel MSE with full use of pilots

$MSE^{(prop)}(m)$ Channel MSE with adjusted number of pilots

N_c The number of spacial MIMO channels

N_d The number of data sub-carriers

N_g The number of guard sub-carriers

N_p The number of pilot sub-carriers

N_r The number of receive antennas

N_t The number of transmit antennas

N_{coh} The number of frequency coherence bands

$N_{B,CSI}(m)$ The required number of bits that cover the feedback information for each sub-channel in (bits)

N_{FFT} The FFT size

P_l The power of the l-th path in (dB)

P_T The total transmitted power

$P_e(m)$ The BER value of the m-th sub-channel

P_{out} The outage probability

$P_{sc_k}(m)$ The power value of the m-th sub-channel assigned to the k-th user

$P_s(m)$ The average symbol power

Q The number of queues

$q_{\text{opt}}(m)$ Optimal user in the q-th queue

$R_B(m)$ The bit rate for m-th sub-channel in (bit/s)

$R_c(m)$ The selected coding rate for the m-th sub-channel

T_{CSI} The required time for the feedback CSI transmission

$W(n)$ AWGN samples

$x(v)$ The transmitted OFDM waveform samples in time-domain

$Y(n)$ The received OFDM signal in frequency domain

Chapter 1

Introduction

Nowadays, modern communication systems are considered an important part of life. These systems allow people around the world to talk, watch videos and exchange distinct data independently, using telephones, cellular mobile phones and networks, regardless of the distances and surrounding circumstances of the environment [1]. In this context, large numbers of researchers and engineers work towards the designing of efficient communication systems which can guarantee the delivery of the required information packets from the sources to the destinations with a minimum number of errors, through either wired or wireless transmission media. However, significant challenges are faced which restrict the fast development of transmission techniques, such as channel conditions, mobility speed of the transceivers and limited resources. Most of these challenges have been addressed by developing traditional technologies and introducing new techniques which can improve the performance efficiency [2].

1.1 Motivations for The Research

Over the past 60 years, there has been a dramatic progress in the hardware and software development of communication systems over wired and wireless transmission media mainly to exploit the available channel capacity and resources efficiently. The basic digital communication system exhibits two main parts, which are *transmitter and receiver*, as shown in Fig 1.1. The function of the transmitter is to send information from the sources across different types of channel profiles to the receiver of the destinations. The source binary information is optionally encoded with one of the forward error correction (FEC) methods and modulated, utilising the commonly used digital modulation approaches. On the other hand, the receiver is responsible

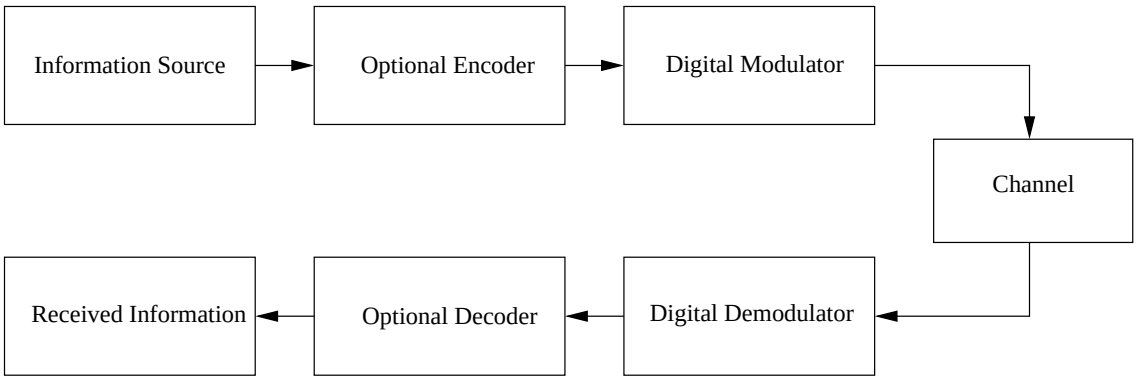

Figure 1.1: Basic digital communication system.

for maintaining the information received by solving the expected transmission problems caused by the multipath channel fading, and performing the required demodulation and decoding [3]. Recent research has focused on enhancing the performance of the digital communication systems, in terms of high transmission rates with a low number of errors, by inventing and developing new technologies and software algorithms [4]. The improvement of such systems is restricted by many constraints, for instance, the capacity, bandwidth and conditions of the channel, as well as the available resources.

In order to overcome the restriction problem of severe channel conditions with high transmission rates, multi-channel and multi-carrier techniques are introduced. The multi-channel technique transmits the same source information several times over different channels, to reduce the interference of transmitted signals. This approach offers a high channel diversity which can be exploited well by the receiver, as shown in Fig 1.2 [3].

In contrast, the multi-carrier systems, such as orthogonal frequency division multiplexing (OFDM) shown in Fig 1.3, can increase the resilience of the transmitted signal to frequency selective fading or narrowband interference. This is carried out by splitting the considered frequency selective fading channel into multiple narrowband flat fading sub-channels and then sending the information bit streams over these sub-channels in parallel. It is well known that in the single carrier systems, a single fade can cause the entire link to fail, while in the multi-carrier systems, a low ratio of the transmitted sub-carriers can be influenced. OFDM systems consider the fast Fourier transform (FFT) to orthogonalise the sub-carriers. The orthogonality represents the mathematical relationship between the frequencies of the carriers in the OFDM systems. In a normal frequency-division multiplex system, sub-carriers

are spaced by adding guards between them, in which the received signals can be detected at the receiver using conventional filters and demodulators. However, the sub-carriers of the transmitted OFDM frame can be arranged orthogonally, in which the sidebands of the individual sub-carriers overlap and the signals are able to be received without carrier interference problem. In addition, these systems are commonly used for multiuser transmission scenarios, due to the high efficiency of user allocation and detection. Furthermore, wireless single and multiuser OFDM systems can adapt to different transmission media environments with lower implementation costs and a high quality of service (QoS), in comparison with other technologies. They are shown to tackle one of the most important multipath fading channels problems, which is inter symbol interference (ISI) [5], [6], [7]. A cyclic prefix (CP) is added to the original OFDM symbol in order to reduce ISI. It is a repetition of the first section of the OFDM frame that has been appended to the end of such frame. It enables multi-path representations of the OFDM symbol to fade, in which the subsequent transmitted symbols have not interfered. Although OFDM systems have solved numerous transmition problems, they suffer from other issues, such as inter carrier interference (ICI) and high peak to average power ratio (PAPR). ICI is caused by the Doppler shift, which occurs as a result of the mobility, and oscillator synchronisation of the transmitter and the receiver [8], [9]. In presence of ICI problem, the orthogonality of the sub-carriers of the transmitted OFDM frame has not been maintained. In multi-path channels, the complexity of ICI issue is become worst and can influence the received signal negatively if it has not been compensated. PAPR of OFDM systems is more than that of single carrier systems due to multiple additions of the involved sub-carriers at the modulator represented by FFT and the use of non-linear amplifiers in the power amplification stage. These additions and power amplifier increase the peak power magnitude. At the same time, the average power value can be low due to destructive interference between the included sinusoids. In communication systems, the high PAPR signals are undesirable due to the exhaustive hardware complexity in practical implementation. Therefore, PAPR problem of OFDM system should be solved by utilising the well known reduction methods, for example selective level mapping (SLM) and partial transmit sequences (PTS) [9].

OFDM systems combined with adaptive modulation and coding (AMC) have been adopted in several modern radio transmission standards, including WiMAX

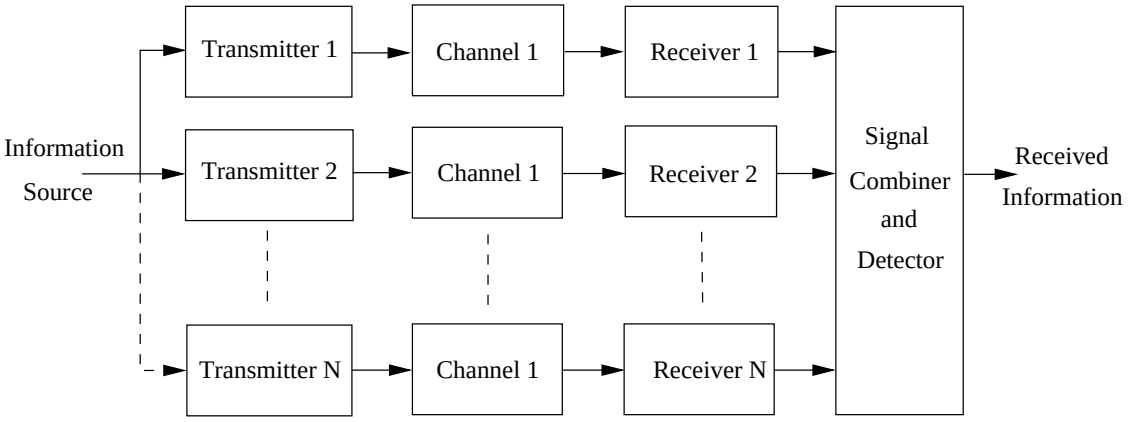

Figure 1.2: Multi-channel system.

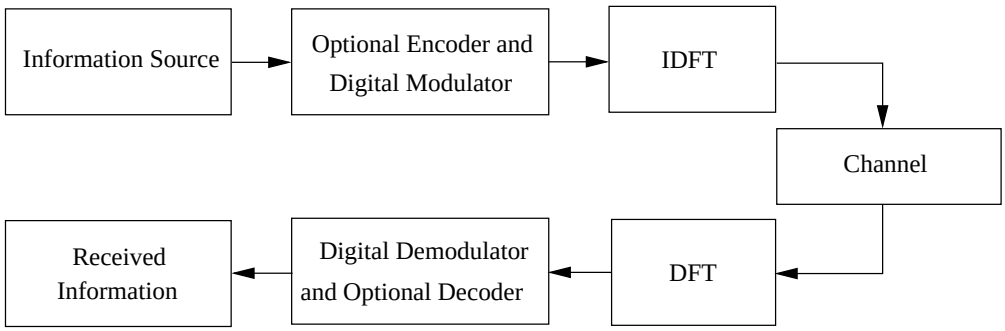

Figure 1.3: Basic OFDM system.

IEEE 802.16 and WiMAX IEEE 802.16e. AMC technique adopts different modulation types and FEC methods with distinct coding rates. This technique matches the conditions of the underlying channels by selecting the suitable modulation and coding scheme (MCS) in order to maximise the data rate depending on the computed signal to noise ratio (SNR) [10]. In contrast, different pilot patterns have been produced to improve the performance of the applied systems by enhancing the accuracy of the channel estimation.

Although the AMC technique improves the performance of single and multiuser OFDM systems, this approach suffers from significant distortion for sub-carriers which are assigned to long distance destinations due to the severe effects of the multipath channels in terms of the delay spread. To overcome this drawback, resource allocation strategies have been considered in order to optimally allocate the user, information bit streams and transmission power amongst the sub-carriers of the transmitted multiuser OFDM frame, called orthogonal frequency division multiple access (OFDMA) frame. These strategies assign the optimal MCS and power value for each group of sub-carriers, in which the adopted optimisation constraints and channel conditions are satisfied.

On the other hand, user scheduling algorithms are utilised to sort the information of the involved users in queues. This information has been served according to different conditions including the priority, the size of the transmitted data, queue state, required time and arrival time of the considered users. The user scheduling algorithms are combined with the AMC and resource allocation strategies in order to exploit the available channel bandwidth efficiently and to enhance the throughput performance of OFDMA systems. As a result, OFDMA systems based on AMC, user scheduling and resource allocation strategies can achieve a significant performance improvement for different transmission scenarios [11].

In contrast, software engineering life cycle methodologies has been defined numerously in literature in the context of communications [12], [13], [14], [15], [16]. The communication systems, designed based on life cycle methodologies, are *scalable*, *extendible* and *portable*. *Scalability* means that the same performance is obtained for different traffic demands, i.e. the systems which are able to handle 100 destinations simultaneously can also deal with 1000 or more efficiently. It is an important aspect of software engineering used for communication systems, due to the dynamic change in the surrounding conditions and the number of destinations. Moreover, *extendibility* is adopted to produce comprehensive systems which can include different communication standards and protocols depending on the transmission media conditions. Finally, the *portability* aspect allows the system to be used for a long lifetime effectively, even with the rapid advances in terms of hardware and software. These aspects are considered throughout the *analysis, design, implementation, and testing* phases of the adopted software engineering life cycle models [17], [18].

1.2 Literature Survey

The focus of this Section is on the recent research publications which fall within the considered areas of this thesis. It studies the up-to-date literature regarding the presented AMC technologies for OFDM and OFDMA systems. In addition, the research work so far of pilot based sub-channelling methods for the same transmission systems are presented. In contrast, the literatures of the resource allocation strategies and scheduling algorithms for single-input-single-output (SISO) and multi-input-multi-output (MIMO) techniques based OFDM and OFDMA systems have been also highlighted in this Section.

1.2.1 AMC Technology

Recently, AMC technologies have attracted substantial research attention. In [19], optimal criterion for MCS selection was proposed in order to maximise the user throughput in cellular systems. The incremental redundancy and chase combining methods of hybrid automatic repeat requests (HARQs) were adopted by the presented criterion. The achieved simulation results proved that employing the proposed method with HARQ can improve the system throughput for slow fading channels. In [20], an AMC technology for bit-interleaved coded modulation based on OFDM (BIC-OFDM) systems was introduced. This technology followed a pair-wise error probability (PEP) analysis approach, to maximise the transmission bit rate by selecting the optimal MCS and allocating the available power over the sub-carriers in the frequency domain. In [21], the transmitted OFDM frame was divided into fixed sub-channels with the same number of sub-carriers. The frequency coherence bandwidth was considered as indicator to show the ability of implementing the AMC technology. The authors of [22] presented a new spreading technique for OFDM frame sub-banding to implement the adopted adaptive modulation method. In [23], the performance analysis of a cross-layer design based approaches with hybrid ARQ (HARQ) protocol for wireless system has been presented. This protocol employed AMC in combination with adaptive cooperative diversity that was subject to fading time correlated of the channels. The authors of [24] developed a general framework in terms of the link delay and loss performance caused by channel fading. This framework was used to design a cross-layer approach that optimised the physical layer AMC and the link layer packet fragmentation.

For the employing of AMC technologies in resource allocation and scheduling strategies, the authors of [25] used the link adaptation schemes, such as AMC and HARQ, to transmit the resource allocation information to the destinations. In addition, the simulation results of the introduced system provided a notable improvement in the spectral efficiency as a function of SNR, in comparison with the traditional methods. In [26], a modified Fischer's loading algorithm for sub-band bit and power allocation has been introduced. The OFDM frame was divided into fixed sub-bands depending on normal sub-carrier indices and sorting the sub-carriers based on channel gain. Additionally, in [27], the AMC and ARQ technologies were adopted to develop a cross-layer strategy which guaranteed the required QoS at traffic trans-

mission. Moreover, the AMC was employed to produce a user scheduling algorithm for downlink wideband code division multiple access (WCDMA) networks in [28]. The analysis and results, in terms of system throughput, scheduling fairness and data rate, proved that the proposed algorithm outperformed the existing approaches. In [29], an efficient scheme based on AMC technology was proposed. Furthermore, an upper bound analytical method was proposed, and the simulation results validated the outcome of this method, as well as showing a significant improvement in throughput and bandwidth exploiting.

In contrast, the authors of [30] compared the performance of AMC based single carrier transmission with frequency domain equalisation (AMC-SCFDE) and AMC-OFDM systems over non-linear and time varying Rayleigh fading channels. The simulation results showed that the performance of an AMC-OFDM system was better if the distance between the transmitter and receiver was close, while the AMC-SCFDE showed a superior performance for long transmission distances.

1.2.2 Pilot Pattern Design

The ability of the design of the optimal pilot pattern to efficiently improve the accuracy of channel estimation has been researched thoroughly. In [31], two pilot aspects were considered for OFDM systems. The analytical and simulation results proved that the proposed pilot aspects improved the bit error rate (BER) performance in comparison with the traditional methods. On the other hand, the problem of data sub-carriers and pilot tones interference in data-pilot-multiplexing schemes was solved by proposing a new scheme in [32]. This scheme was shown to achieve a better performance in terms of mean square error (MSE) for channel and frequency offset estimation. The authors of [33] presented a new channel estimation method based on compressed sensing technology. It exploited the channel delay Doppler sparsity to reduce the number of pilots. In [34], the number and positions of pilots were optimised as well as the power of the pilots and data sub-carriers has been optimally distributed in order to minimise the BER. In addition, a pilot reduction method, presented as a trade-off criterion between the channel estimation accuracy and bandwidth efficiency, was introduced in [35]. This method decided the optimal number of pilots in OFDM transmission. In [36], the number of pilot tones used for channel estimation of OFDM systems was minimised based on the prediction

of the channel estimation errors and the required QoS. The authors of [37] improved the throughput performance of the mobile IEEE 802.16e OFDMA systems by introducing a dynamic sub-channelisation scheme. Simulation results of this scheme appeared to show a superior throughput performance over the traditional sub-channelisation approaches.

1.2.3 Resource Allocation for SISO Based Systems

In terms of the goodput maximisation problem, the authors of [38] presented a bit and power allocation strategy for parallel sub-channels systems using the ARQ technique to maximise the number of delivered information bits without errors to the destination. The simulation results showed the superior performance of the proposed approach in comparison with the waterfilling based methods. In [39], the bit and power allocation strategy presented by [38] was introduced for BICM-OFDM systems. The goodput of the investigated BICM-OFDM for a wireless local area network (WLAN) scenario was improved significantly, as demonstrated by the analytical and simulation results. On the other hand, the same strategy was expanded to work over decode and forward relay based OFDM systems in [40].

The authors of [41] proposed an optimal power allocation for relayed transmissions, in order to exploit the available power efficiently over all the stages of the systems. Numerical results showed that the introduced strategy enhanced the system performance for the links, with unbalanced average fading power and with a high number of relay hops. Moreover, the bit loading and power allocation problem for downlink multiuser OFDM systems was tackled by the authors of [42], who presented an iterative algorithm which removed all of the sub-carriers that needed more power than was allowed from the transmitted frame. This algorithm caused an insensible reduction in the average transmission bit rate, while the BER performance was significantly improved.

In contrast, the bit rates obtained for many continuous and discrete bit loading schemes for OFDMA systems were studied in [43]. Moreover, an efficient power allocation algorithm for a fixed coding rate based coded OFDM was proposed by [44], in order to minimise the BER and frame error rate (FER) under the constant power constraint. Simulation results proved that the BER and FER were significantly reduced. In [45], optimal and sub-optimal power allocation algorithms were

introduced for multi-relay OFDM systems, with efficient exploiting of the cooperation gain of distributed antenna array. The required feedback and results were also analysed for a specific, desired accuracy. In [46], a low complexity optimal power allocation algorithm for OFDM based ad-hoc networks was presented. It aimed to maximise the weighted rate-sum of the involved users with full consideration to the power constraint. The proposed idea was supported by the simulation results introduced. Furthermore, another low complexity power allocation method for OFDM based clustered multi-band ultra wideband networks was proposed by [47]. The key contribution of this method was to allocate the optimal power value for each cluster, in which the average system throughput was maximised.

Regarding the sub-carrier allocation strategies, two algorithms were presented and analysed by [48], in order to overcome the problem of limited bandwidth assignment of the equal allocation of the sub-carriers for users in OFDMA systems. In [49], the total transmitted power was minimised, while satisfying the required bit rate of each user in OFDMA systems by proposing a sub-carrier allocation strategy. Simulation results showed a superior performance of the proposed system in comparison with traditional methods. The authors of [50] developed the performance upper bound and heuristic algorithms for sub-carrier and slot allocation. The performance of the proposed algorithms was improved significantly, as demonstrated in the simulation results.

The authors of [51] and [52] investigated the maximisation problem of continuous and discrete ergodic weighted sum rates of OFDMA systems, subject to power and BER constraints, with a partial channel state information (CSI). Numerical and simulation results showed the achievement of the required bit rates by users in a high percentage ratio. In addition, three strategies for OFDMA systems were proposed by [53], [54] and [55], in order to tackle the resource allocation problem over multi-cells, relay networks and WiMAX environments. The claim of authors has been proved by the numerical and simulated results presented. In [56], the holes exit between the frequency bands of multi-primary-user was studied, and a new user, bit and power allocation algorithm, was introduced for OFDMA based cognitive radio systems. Simulation results demonstrated that the performance of the investigated algorithm outperformed the equal resource distributed methods. On the other hand, the total transmit power was optimally minimised in [57], by presenting a multiuser sub-carrier, bit and power allocation strategy for OFDMA systems which employed

the adaptive modulation technology. In addition, a throughput maximisation problem subjected to packet error rate constraints was investigated in [58]. The proposed algorithm which solved this problem was based on the varying data rate and payload size. In [59], adaptive bit loading and power allocation algorithms based on mutual information for coded OFDM systems were introduced, in order to maximise the average system throughput under the packet error rate constraint. In [60], a developed resource allocation strategy was introduced. In one data stream, this strategy considered multiple BER requirements for different types of packet to overcome the channel estimation error caused by Doppler shift in the high speed train environment. The authors of [61] investigated the problem of power assignment and sub-carrier allocation in a two-cell downlink OFDMA system in presence of the multi-cell interference. The proposed strategy considered the effects of multi-cell interferences on the resource allocation.

It is observed that the maximisation and minimisation problems are often complex and require high complexity algorithms to be solved. Therefore, numerous complex issues have been tackled by decoupling the main problem into sub-problems, and solving each one individually following the decomposition method [62]. The authors of [63], [64] and [65] divided the complex maximisation problem into sub-problems and solved each one individually, by proposing independent algorithms. In [66], a resource allocation strategy was proposed to maximise the sum rate of homogeneous OFDM systems under the constraints of delayed and non-delayed traffic. Numerical results showed the performance of the proposed strategy in terms of service outage probability, transmission rate and multiuser diversity for both constraint conditions.

The division of the transmitted OFDMA frame into chunks depending on the frequency coherence bands of the channels was adopted by [67], to introduce a resource allocation strategy for OFDMA systems subject to BER and SNR constraints. A comparison between the performance of BER-constraint algorithms and SNR-constraints has been presented through the results. Additionally, a combination of cooperation and resource allocation strategies for OFDMA systems was introduced by [68]. The complexity of these strategies increased linearly with the increase in the number of sub-carriers.

1.2.4 Resource Allocation for MIMO Based Systems

The authors of [69] and [70] have considered the ergodic capacity maximisation problem for MIMO-OFDMA and MIMO-multi carrier(MC)-CDMA systems. In the simulation results, the effect of the number of used antennas, path loss and different user scenarios were studied. It was apparent that the MIMO-OFDMA system outperformed the other scheme for delay sensitive applications. In [71], a dynamic spatial sub-channel allocation strategy for MIMO-OFDMA systems was introduced. This strategy selected the eigenvectors corresponding to the large value of spatial sub-channel eigenvalues, to obtain the beamforming weight vector at the mobiles and base stations. In [72], an efficient ordering approach for the detector of ordered successive interference cancellation was presented. A BER minimisation problem was adopted in the proposed approach, and was solved using the power control methods. In contrast, three resource allocation algorithms for beamforming technology based on MIMO-OFDM systems were proposed and examined over multipath fading channels, with perfect and imperfect CSI knowledge cases in [73]. In [74], the maximisation of the sum rate in terms of performance, complexity, and fairness of suboptimal resource allocation strategies was investigated. Two resource allocation methods were introduced in sub-optimal models. In [75], a novel power allocation strategy for multiuser MIMO relay network was proposed. The interference is cancelled by employing a combination of transmit-receive weights and Tomlinson Harashima precoding. Additionally, the authors of [76] minimised the total transmission power, while maintaining the required bit rate for each user. Simulation results showed the superior performance of the proposed system over traditional beamforming MIMO-OFDM schemes.

1.2.5 Scheduling for OFDMA Systems

In [77], a queue proportional scheduling (QPS) policy was adopted to achieve optimal throughput scheduling for OFDM systems over broadcasting channels. The proposed algorithms were compared with different scheduling approaches, such as maximum weight matching scheduling (MWMS). The authors of [78] presented a low complexity QoS based proportional fairness policy for information packets scheduling. The efficiency of the proposed scheduling algorithm was proven by the simulation results, which included the system throughput, queuing delay and packet

dropping probability.

In [79], a combination of scheduling and resource allocation strategy for the downlink of OFDM based mobile networks was introduced. Different scheduling and resource allocation methods were compared with the proposed strategy in the results presented. Moreover, a fair scheduling based resource allocation algorithm was introduced for OFDMA systems in [80]. The optimality of the proposed algorithm was shown in the provided simulation results. In [81], joint adaptive resource allocation and cumulative density function (CDF) based scheduling strategies were presented for OFDMA systems. The simulation results showed that the proposed strategy outperformed the related conventional approaches. In contrast, a cross-layer scheduling and resource allocation strategy for space time block coding based MIMO-OFDMA systems with imperfect knowledge of CSI was proposed in [82]. The aim of this strategy was to maximise the system throughput which had been verified by the simulation results. Additionally, a low complexity scheduling strategy based on genetic algorithms was extended to work with MIMO-OFDM systems, and developed to tackle the problem of exhaustive computations required for dirty paper coding in [83]. Simulation results demonstrated that the performance of the proposed strategy was better than the conventional dirty paper coding based MIMO-OFDM systems. In [84], the utility maximisation problem in the downlink mesh OFDMA networks was investigated. This problem has been formulated as a cross-layer design of rate control and OFDMA scheduling. It exhibited the rate-control problem at the transport layer and the scheduling problem at the media access control/physical layer. The authors of [85] formulated an optimisation problem for secure resource allocation and scheduling in OFDMA decode and forward relay networks in terms of artificial noise generation in slow fading. The investigated optimisation problem has been solved in a highly scalable resource allocation algorithm based on dual decomposition.

On the other hand, a scheduling and resource allocation strategy for uplink OFDMA based broadband networks was proposed in [86]. Analysis of the complexity and performance of the presented algorithms was provided in the results. In [87], an advanced scheduling algorithm for AMC based systems was introduced, in order to maximise the resulting throughput. In addition, the authors of [88] introduced a combination of threshold based power allocation and multiuser scheduling schemes for downlink transmissions, to maintain the unacceptable users. Simulation results,

in terms of BER as a function of SNR, were provided to show the achieved gain of the proposed strategy in comparison with the traditional approaches.

1.3 Research Gap

In terms of the AMC strategies in the literature [19]-[37], the same MCS for all sub-carriers, different MCS for each sub-carrier and dividing the OFDM frame into fixed sub-bands methods were adopted regardless the coherence bandwidth of the experienced channels. These methods presented an enhancement in the performance on the cost of bandwidth, capacity and high complexity. In contrast, most of the introduced resource allocation strategies, [41]-[76], considered the Shannon capacity formula, which provides inaccurate expectation to the real available channel capacity. Additionally, these strategies have not adopted the changeable coding rates, yet the uncoded or fixed coding rate systems. On the other hand, the presented user scheduling algorithms, [77]-[87], focused on sorting the data packets and solving the traffic problem and ignored the fairness in user data serving.

It is important to note that the research work so far, [19]-[87], focused on solving the problems of the channel bandwidth exploiting, resource allocation and transmission traffic. This was carried out by proposing different AMC, resource allocation and user scheduling strategies, in which the individual related problems were solved. However, in practical systems all these issues, which can be changed from transmission environment to other depending on the channel conditions and available resources, are existed at the same time. Therefore, the need for introducing communication systems that are able to deal with the existing problems is increased.

The objective of this thesis is to introduce comprehensive OFDM and OFDMA systems based on combining the proposed AMC, resource allocation and user scheduling strategies that can solve the limitation problems of exploiting the channel bandwidth and available resources efficiently. These strategies have been designed based on developed software engineering life cycle models. In contrast, the modulation types and coding rates of the proposed strategies can be changed for each group of sub-carriers, i.e. sub-channel, individually based on the related channel condition and resource constraints within each transmitted OFDM/OFDMA frame in order to increase the channel adaptation flexibility. Additionally, the average system throughput, presented as a new cost function, is maximised and the transmission

user traffic problem with fairness service has been tackled.

1.4 Contributions

The aim of this thesis is to design OFDM and OFDMA based wireless communication systems, which adapt to different channel conditions for SISO and MIMO technologies in order to maximise the average system throughput. This has been accomplished by proposing different algorithms for the AMC techniques, resource allocation and user scheduling. The target of these algorithms is to improve the average throughput performance of such systems, in which the related channel conditions and transmission power constraints are satisfied.

In terms of AMC for OFDM systems, numerous algorithms and methods have been introduced by many researchers, such as [19], [20], [25], in order to improve the throughput performance of these systems. The proposed AMC strategy is different from the existing work, as it divides the transmitted OFDM frame into sub-channels, which includes the same number of sub-carriers, depending on the measured frequency coherence bandwidth. Each sub-channel selects the suitable MCS based on the corresponding SNR value, in which the expected BER is achieved. The minimum SNR of the involved sub-carriers in each sub-channel is selected to be the sub-channel SNR value. Additionally, a developed software engineering life cycle model is considered to design the proposed AMC strategy. This strategy employs two MCS scenarios. The first one utilises two digital mapping types of quadrature phase shift keying (QPSK) and sixteen states of quadrature amplitude modulation (16-QAM), combined with three low density parity check (LDPC) coding rates of 1/2, 3/2 and 3/4. The second scenario uses three modulation types of QPSK, 16-QAM and 64-QAM, combined with three convolutional coding rates of 1/2, 3/2 and 3/4. These modulation types and coding methods are adopted following the WiMAX standard of IEEE802.16e. In contrast, the proposed strategy is expanded for SISO and spatial multiplexing MIMO based OFDMA technologies. It is also combined with a novel pilot adjustment scheme which reduces the number of utilised pilots for channel estimation in each sub-channel, and replaces the redundant pilots with additional data sub-carriers in order to improve the average throughput performance instead of designing a pilot pattern expressed by [31] and [32]. This is carried out based on the measured frequency coherence bandwidth computed using

the autocorrelation operation between the neighbouring sub-carriers, the variance of the SNR fluctuation values and the minimum SNR for each sub-channel over the involved sub-carriers. It is important to note that the OFDM and OFDMA which use the full number of pilots are called fixed sub-channelling systems, while the rest are dynamic sub-channelling systems.

On the other hand, the proposed resource allocation strategy for single-cell downlink SISO/MIMO based OFDMA systems allocates the available resources including users, power and information bits optimally amongst the transmitted sub-carriers. This is to improve the average system throughput, in which the channel conditions and power constraints are satisfied. A developed software engineering life cycle model is introduced to design the proposed resource allocation strategy. This strategy has been introduced as a throughput maximisation problem, which is solved by providing two approaches. The first approach, called optimised, tackles the investigated problem optimally using Lagrange multipliers method with high complexity. Additionally, the second approach, called decoupled, divides the considered problem into two sub-problems and presents a solution for each one individually based on Lagrange multipliers method to reduce the computational complexity in expense of performance. The proposed resource allocation strategy is motivated by the existing work of [38], [44], [48], [51], [69], [70] and [76] by the following key points. Firstly, it is combined with the AMC strategy and pilot adjustment scheme in order to increase the flexibility and adaptivity of the system. Secondly, it aims to maximise the average throughput as a new cost function of spectral efficiency and BER, subject to the constraints of power and channel conditions. Both spectral efficiency and BER are evaluated for different modulation types, combined with distinct coding rates selected for the sub-channels within each transmitted OFDM and OFDMA frame based on the employed AMC technique. As a result, the modulation type and coding rate can be changed instead of using adaptive modulation with/without fixed coding rate [38]. Finally, the approximated BER evaluation approach presented by [89] is developed to incorporate the employed channel coding.

User scheduling has been widely researched in order to solve the problems of information management, transmission traffic and priorities [77], [83] and [88]. In this thesis, the proposed user scheduling algorithm considers the user scheduling with the proportional queuing method. It sorts the users into different queues depending on their priority levels, and then selects the best user in each queue, in which the av-

erage throughput of the applied system is maximised. In contrast, the empty queues are employed to serve the users with high priority levels to offer more bandwidth for them. The proposed scheduling algorithm differs from the literature work in three aspects. Firstly, it has been combined with the proposed resource allocation, AMC method and pilot adjustment scheme to produce a cross-layer strategy that works through three different layers, which are data link, media access control (MAC) and the physical layers. Secondly, it arranges different users within each queue based on their priority levels instead of utilising a queue for the data of each user. Finally, the proposed strategy is designed based on a developed life cycle model to provide it with high scalability, extendibility and portability.

In summary, the contribution of the work can be listed as:

1. In Chapter two, a novel fixed and dynamic sub-channelling based AMC strategy for OFDM and OFDMA systems has been introduced to improve the system throughput.

2. In Chapter three, a new resource allocation strategy for SISO-OFDMA systems was produced to maximise the average system throughput.

3. In Chapter four, the SISO based resource allocation strategy has been expanded for spatial multiplexing MIMO-OFDMA systems to maximise the average system throughput by exploiting the available MIMO channel diversity and resources.

4. In Chapter five, a user scheduling algorithm has been proposed to maximise the throughput performance of OFDMA systems and solve the transmission traffic problems.

1.5 Publications Arising From This Research

1. **Muayad S. Al-Janabi**, Charalampos C. Tsimenidis, Bayan S. Sharif and Stéphane Y. Le Goff, "Adaptive MCS Selection with Dynamic and Fixed Sub-channelling for Frequency-Coherent OFDM Channels," *International Journal on Advances in Telecommunications,*, vol. 2, no. 4, pp. 131-141, 2009, http://www.iariajournals.org/telecommunications.

2. **Muayad S. Al-Janabi**, Charalampos C. Tsimenidis, Bayan S. Sharif and Stéphane Y. Le Goff, "Scheduling and Resource Allocation Strategy for OFDMA Systems over Time-Varying Channels," *International Journal of Wireless Information Networks,*, vol 18, no 3, pp. 119-130, 2011, DOI: 10.1007/s10776-011-0158-9.

3. **Muayad S. Al-Janabi**, Charalampos C. Tsimenidis, Bayan S. Sharif and Stéphane Y. Le Goff, "Adaptive Resource Allocation for Single-Cell Downlink OFDMA Systems," accepted for publication by *IET SMT,* doi: 10.1049/iet-smt.2011.0136, 2011.

4. **Muayad S. Al-Janabi**, Charalampos C. Tsimenidis, Bayan S. Sharif and Stéphane Y. Le Goff, "Adaptive MCS Selection in OFDM Systems Based on Channel Frequency Coherence," in *Proc. IEEE AICT*, Venice, Italy, pp. 177-182 May 2009. (Awarded as a best paper).

5. **Muayad S. Al-Janabi**, Charalampos C. Tsimenidis, Bayan S. Sharif and Stéphane Y. Le Goff, "Simulated and semi-analytical throughput evaluation for AMC-OFDMA systems," in *Proc. IEEE IET CSNDSP*, Newcastle upon Tyne, UK, 184-188 July 2010.

6. **Muayad S. Al-Janabi**, Charalampos C. Tsimenidis, Bayan S. Sharif and Stéphane Y. Le Goff, "Optimal user scheduling and allocation for WiMAX OFDMA systems," in *Proc. IEEE ISWCS*, York, UK, pp. 290-294 September 2010.

7. **Muayad S. Al-Janabi**, Charalampos C. Tsimenidis, Bayan S. Sharif and Stéphane Y. Le Goff, "Optimal user scheduling and resource allocation strategy for AMC based OFDMA systems," in *Proc. IEEE PIMRC*, Istanbul, Turkey, pp. 1298-1302, September 2010. (Awarded as a best paper).

8. **Muayad S. Al-Janabi**, Charalampos C. Tsimenidis, Bayan S. Sharif and Stéphane Y. Le Goff, "Bit and power allocation strategy for AMC-based MIMO-OFDMA WiMAX systems," in *Proc. IEEE WiMob*, Niagara Falls, Canada, pp. 575-579, October 2010.

1.6 Thesis Outline

The thesis is organised as follows:

Chapter 2 presents the proposed AMC technology for OFDM and OFDMA systems based on a developed software engineering life cycle model. It also introduces dynamic and fixed sub-channelling based on the proposed pilot adjustment scheme for such systems. Simulation results are included and discussed for various channel profiles.

Chapter 3 focuses on the proposed resource allocation strategy for SISO-OFDMA systems. It includes the developed software life cycle model, used for designing the proposed strategy. The related simulation results are provided to assess the performance of the investigated systems over different channel conditions.

Chapter 4 introduces the expansion of the proposed resource allocation strategy to MIMO technology based OFDMA systems, with a discussion of the corresponding simulation results.

Chapter 5 provides the proposed developed software engineering life cycle model based user scheduling algorithm, which is combined with the introduced AMC and resource allocation strategies. All of the related simulation results and discussions are included in the final part of this Chapter.

Chapter 6 conclusions and future work are drawn.

Chapter 2

AMC Software Algorithms for OFDM and OFDMA Systems

As highlighted earlier, the AMC technologies are considered for the modern communication systems in order to efficiently exploit the channel capacity with high transmission rates and low errors. This Chapter introduces the proposed AMC strategy for downlink OFDM and OFDMA systems. It also describes the presented pilot adjustment scheme that employs the measured frequency coherence bandwidth, SNR and the variance of SNR fluctuation values of each sub-channel to reduce the number of required pilots for channel estimation. Consequently, the reduced pilots are replaced with additional data sub-carriers in order to increase the average system throughput. It is important to note that the proposed methods are based on a developed software engineering life cycle model. In this Chapter, two MCS scenarios are adopted. The first one utilises the digital mapping methods of QPSK, 16-QAM and 64-QAM combined with three LDPC based coding rates of 1/2, 2/3 and 3/4. Furthermore, the second scenario uses three mapping methods of QPSK, 16-QAM and 64-QAM associated with convolutional based coding rates of 1/2, 2/3 and 3/4 [90]. The provided simulation results investigate the performance of the introduced AMC strategy for OFDM and OFDMA systems over different channel conditions.

The proposed AMC strategy and pilot adjustment scheme are different from existing research works of [19]-[37] in numerous aspects. Firstly, the proposed AMC strategy exploits the detected frequency coherence bandwidth to divide the transmitted OFDM frame into sub-channels with the same number of sub-carriers. Then each sub-channel selects the optimal MCS option. Secondly, the pilot adjustment

scheme reduces the number of pilots in each sub-channel depending on the measured coherence bandwidth, SNR, and the variance of the SNR fluctuation values. Subsequently, the redundant pilots are replaced by additional data sub-carriers in order to increase the data transmission rate.

2.1 Developed Life Cycle Model for AMC Algorithm

The proposed AMC strategy is designed based on a developed software engineering life cycle methodology. This life cycle methodology is structured based on a cyclic evolutionary methodology [17], [18]. Moreover, it includes four phases, which are requirements, design, implementation and testing.

Fig. 2.1 explains the block diagram of the considered software life cycle. At the transmitter side, the collection of the system requirements, such as the transmitted data and the required CSI, have been performed by the first block. Additionally, the second block designs the optimal system structure, in which the requirements can be satisfied. The designed structure is implemented using the available software. Subsequently, the implemented algorithm is tested over different channel conditions and the obtained results at the receiver side show the performance. Therefore, the testing phase is included in two stages, which are the channel and receiver. In contrast, the feedback information is returned from the receiver to the transmitter using CSI that allows the first three phases of the transmitter to address the required corrections and developments.

2.2 Fixed Sub-Channelling AMC-OFDM

The key contribution of the proposed AMC strategy for the fixed sub-channelling based AMC-OFDM (FS-AMC-OFDM) systems is to exploit the detected frequency coherence bands of the channel in order to divide the downlink single user OFDM frame into sub-channels that include the same number of data and pilot sub-carriers. Subsequently, each individual sub-channel chooses the suitable MCS. In order to estimate the channel coefficients efficiently, pilots are inserted and interleaved across the data sub-carriers using the well known comb method [11]. As mentioned before,

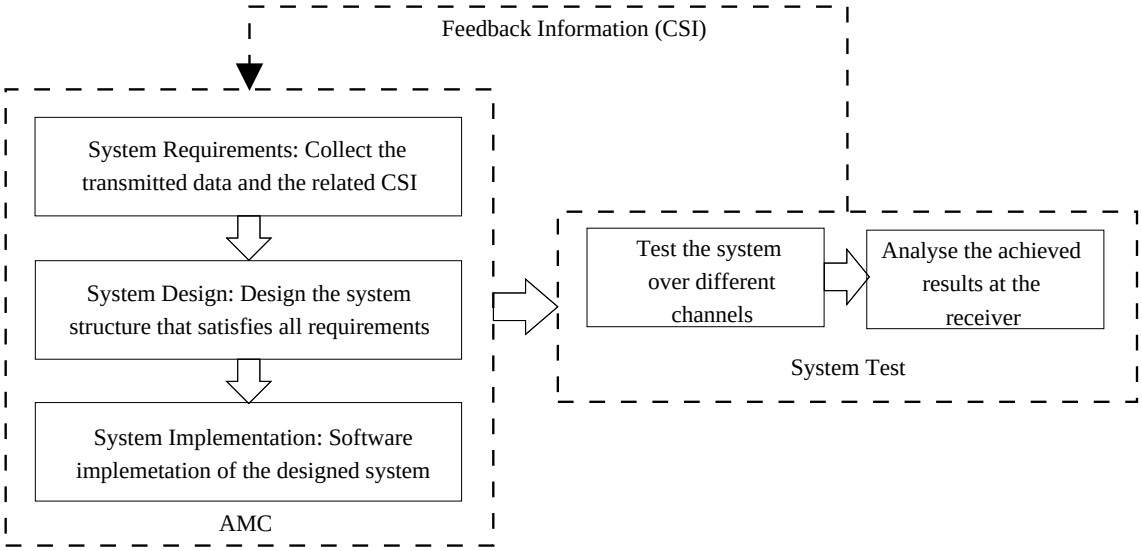

Figure 2.1: The developed software life cycle for the proposed AMC algorithm.

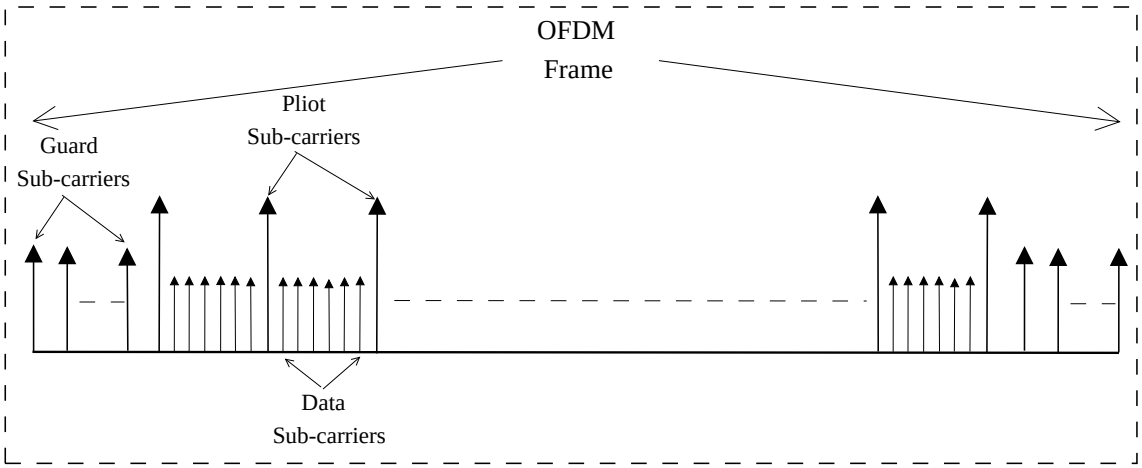

Figure 2.2: OFDM frame structure.

the AMC strategy employs two MCS scenarios, each of which exhibits ten MCS options.

2.2.1 FS-AMC-OFDM System Model

This Section outlines the proposed FS-AMC-OFDM system. The transmitted OFDM frame of the proposed system contains N_{FFT} sub-carriers, which are divided into N_p pilots, N_d data, and N_g guard sub-carriers as shown in Fig. 2.2 [91], [92].

The data and pilot sub-carriers are distributed equally into groups, called sub-channels, corresponding to the number of detected frequency coherence bands, N_{coh}, of the channel as explained in Fig. 2.3. Each sub-channel adopts a distinct MCS and contains $\xi_d(m) = N_d/N_{coh}$ data and $\xi_p(m) = N_p/N_{coh}$ pilot sub-carriers, where $m = \{1, ..., N_{coh}\}$ is the index of the sub-channels. The utilised MCS options are

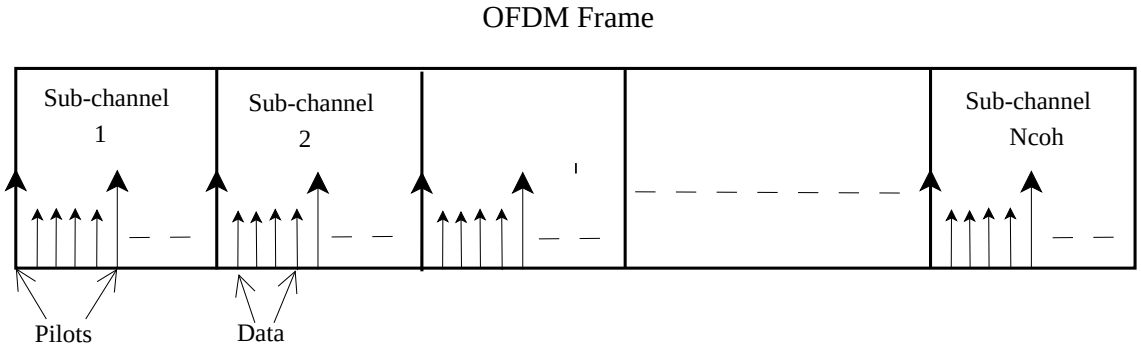

Figure 2.3: OFDM frame sub-channelling.

numbered and the number of the selected MCS for each sub-channel is returned to the transmitter via the feedback CSI instead of sending the entire channel coefficients, which leads to reduce the size of the feedback information. The CSI is assumed to be sent using time division duplex (TDD) link. The process of sending the feedback information over TDD link requires a limited time, which restricts the continuous transmission. In this work, a Mobile WiMAX IEEE 802.16e system is considered for downlink OFDM system with the parameters listed in Table 2.1.

Table 2.1: System parameters

No	Parameter	Value
1	Bandwidth	20 MHz
2	Number of FFT	2048
3	Number of data carrier	1440
4	Number of pilot carrier	240
5	Number of guard sub-carrier	368
6	Cyclic prefix	1/4

The transmitter comprises three main blocks as shown in Fig. 2.4. The first and second blocks generates from the binary data different coded and mapped symbol groups that are assigned to different sub-channels. The third block assembles the OFDM frame from the mapped data and the pilots, which are modulated using binary phase shift keying (BPSK) and inserted at uniform positions in a range of $\frac{\xi_d(m)}{\xi_p(m)}$ using a comb approach. This type of modulation is selected to guarantee the sensitivity to channel effects at both low and high SNR levels. The final part of the transmitter implements the IFFT and CP insertion operations. The transmitted OFDM frame can be mathematically represented as [3], [93]

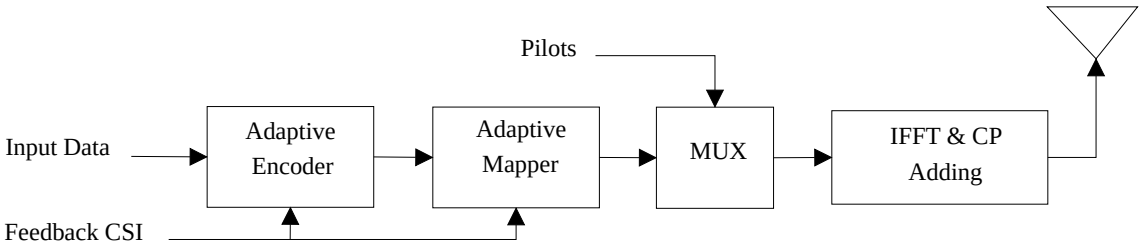

Figure 2.4: Transmitter block diagram of the proposed FS-AMC-OFDM system.

$$x(v) = \frac{1}{\sqrt{N_{\mathrm{FFT}}}} \sum_{n=1}^{N_{\mathrm{FFT}}} X(n) e^{\frac{j2\pi vn}{N_{\mathrm{FFT}}}}, \tag{2.1}$$

where $x(v)$ are the transmitted OFDM waveform samples in time-domain, $X(n)$ denotes the OFDM symbols assigned to each sub-carrier. In addition, $v = \{1, \ldots, N_{\mathrm{FFT}}\}$ and $n = \{1, \ldots, N_{\mathrm{FFT}}\}$ are the time and frequency domain indices, respectively.

It is well known that there are many types of channels, such as time variant and invariant channels for both fast and slow fading. The frequency response of these channels can be more or less selective in terms of the corresponding sub-carriers [2], [94], [95]. This selectivity can decrease the coherence bandwidth, which in turns increases the utilised sub-channels in the proposed system. The frequency coherence bandwidth of the channel can be evaluated either as a function of the root mean square (RMS) delay value, D_{rms} [10]

$$B_{\mathrm{coh}} = \frac{1}{50 D_{rms}}, \tag{2.2}$$

or by measuring the correlation values between the channel coefficients corresponding to the neighbour sub-carriers, in which these values should be over 0.9 [36]. It is important to note that the correlation method is adopted in this thesis. Fig. 2.5 demonstrates the impulse and frequency response of the utilised channel with 20 MHz bandwidth suited to propagate one OFDM frame. This channel model is generated randomly to simulate an urban area channel under three conditions. Firstly, the attenuation values are formed in Rayleigh distribution and the phase is uniformly distributed. Secondly, the frequency selectivity is low, in which this channel should exhibit coherence bandwidth. Finally, this channel is varied slowly. Therefore, the generated channels are time-varying but flat in terms of attenuation for all sub-carriers within the same band and correlated between subsequent symbols

The receiver structure is illustrated in Fig. 2.6. After the CP has been removed

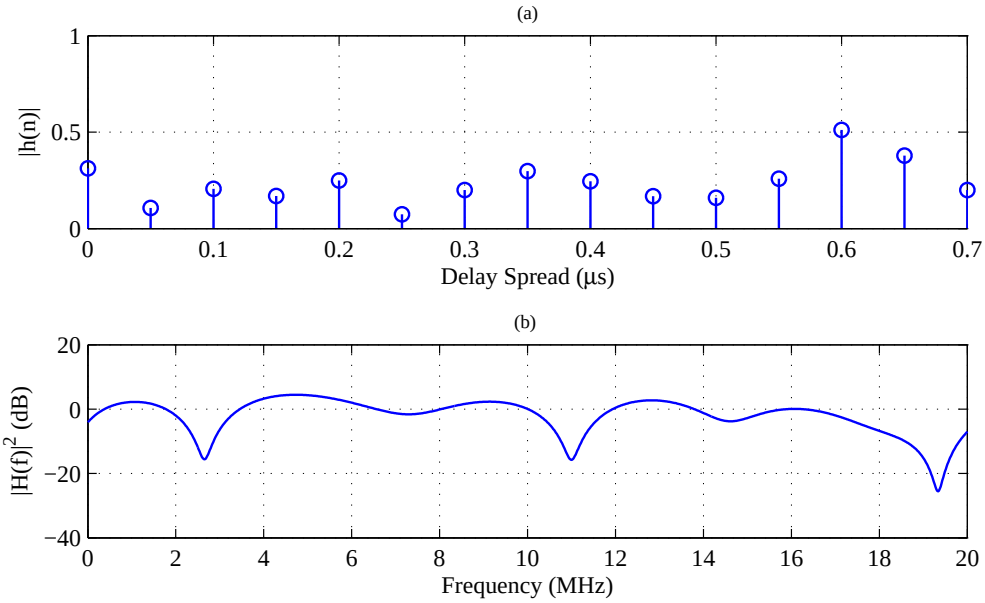

Figure 2.5: Channel model.

and applying the FFT operation, the received OFDM frame can be mathematically represented as

$$Y(n) = X(n)H(n) + W(n), \tag{2.3}$$

where $Y(n)$, $X(n)$, $H(n)$ and $W(n)$ are the received, transmitted, corresponding channel coefficients and additive white Gaussian noise (AWGN) samples, respectively. Following the FFT operation, the pilots are extracted from the received OFDM frame. These pilots are utilised in the *Channel Estimation and CSI* unit to estimate the channel coefficients for each sub-channel using the well-known least square (LS) method [96]. Moreover, the SNR value is evaluated and the decision of suitable MCS for each sub-channel is taken for each sub-channel, individually. This unit also measures the coherence bandwidth of the estimated channel to specify the number of sub-channels for the next OFDM frame. Finally, the data are demodulated and decoded according to the selected MCS at the transmitter using soft maximum log-likelihood (ML) demapper and either Viterbi or LDPC decoder [4], [5], [93]. The feedback CSI can reduce the available channel bandwidth due to the waiting CSI delay. The overhead analysis of the feedback CSI has been considered.

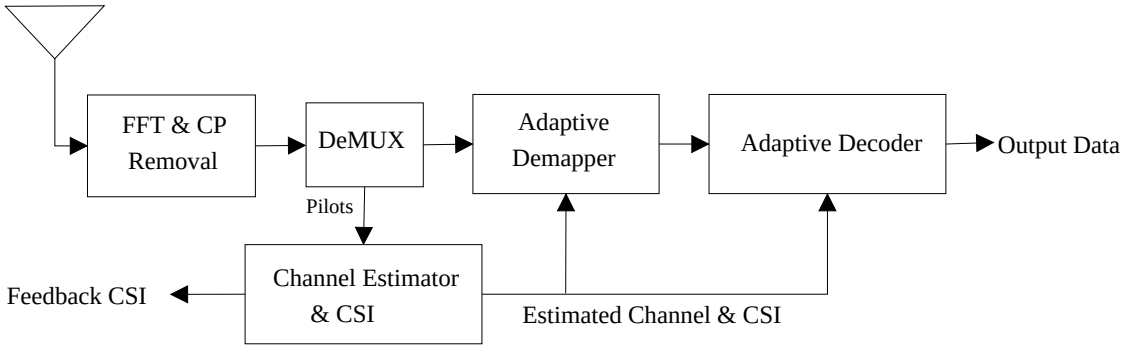

Figure 2.6: Receiver block diagram of the proposed FS-AMC-OFDM system.

2.2.2 Feedback CSI Analysis for FS-AMC-OFDM

The feedback CSI includes the numbers, which are set as a vector, of the optimal MCSs selected for different sub-channels. It is important to note that the optimal MCS for each sub-channel is selected based on the minimum SNR value among the involved sub-carriers in such sub-channel. Then, this minimum SNR is selected to be the sub-channel SNR value.

At the transmitter, the number of the detected coherence bands can be obtained from the length of the returned MCS vector. As mentioned before, CSI is assumed to be returned using TDD link. The use of a TDD link to feedback the CSI implies that the required time for each feedback CSI transmission, T_{CSI}, can reduce the system effective bandwidth. This time is based on the bit rate and the size of CSI. The bit rate for m-th sub-channel in (bit/s) can be calculated as

$$R_B(m) = \rho(m)\xi_d(m)\frac{B_T}{N_{FFT}},\ \forall m \in \{1, ..., N_{coh}\}, \tag{2.4}$$

where B_T is the total channel bandwidth and $\rho_k(m)$ is the spectral efficiency for the m-th sub-channel in (bps/Hz) that is given as

$$\rho(m) = R_c(m)\log_2[M(m)], \tag{2.5}$$

where $R_c(m)$ and $M(m)$ are the selected coding rate and modulation order for the m-th sub-channel, respectively. Consequently, the required number of bits that cover the feedback information for each sub-channel is $N_{B,CSI}(m) = 4$ (bit) as there are ten MCS levels. As a result, the required time for feeding back CSI of each

sub-channel, $T_{CSI}(m)$, can be calculated as

$$T_{CSI}(m) = \frac{N_{B,CSI}(m)}{R_b(m)}. \tag{2.6}$$

From (2.6), the effective channel bandwidth is evaluated as

$$B_{eff} = N_d \frac{B_T - \sum_{m=1}^{N_{sc}} \frac{1}{T_{CSI}(m)}}{N_{FFT}}, \tag{2.7a}$$

$$= N_d \big[\frac{B_T - B_{CSI}}{N_{FFT}}\big], \tag{2.7b}$$

where B_{CSI}, is the total bandwidth of the required feedback CSI for all sub-channels. It should be noted that the channel is assumed to be constant for more than T_{CSI}, which is the time required for sending back the CSI, to guarantee that the CSI is still valid for the next OFDM frame.

2.2.3 Proposed AMC Strategy for OFDM

The key novelty of the proposed AMC strategy is the introduction of distinct MCSs that correspond to the detected frequency coherent sub-channels. In other words, the correlation between the channel coefficients is considered to allocate the frequency bands and then selects the optimal MCS for each one independently. At the receiver, channel and SNR estimation as well as the decision on MCS selection for each sub-channel are performed. Additionally, the frequency coherence bandwidth is measured. The channel estimation is implemented for each sub-channel individually using the LS method as [96]

$$\hat{\mathbf{H}}_p = \frac{\mathbf{Y}_p}{\mathbf{X}_p}, \tag{2.8}$$

where $\hat{\mathbf{H}}_p$ is the vector of the estimated channel values corresponding to the pilots, $\mathbf{X}_p$ is the known transmitted pilot symbols, and $\mathbf{Y}_p$ are the received pilot symbols after the FFT operation. The final channel values are obtained by implementing the 1^{st} order interpolation methods as

$$\hat{H}_d(r+s) = \hat{H}_p(r) + \frac{s\ N_p}{N_d}[\hat{H}_p(r+1) - \hat{H}_p(r)],\ \forall s \in \{1, ..., \frac{N_d}{N_p}\}, \tag{2.9}$$

where $\hat{H}_d(r+s)$ represents the estimated channel values that corresponding to the data sub-carriers between the pilots and $r \in \{1, ..., N_p\}$ is the pilot index. In this work, the channel estimation error is considered as additional noise. Thus the received signal of the data sub-carriers can be written as [36]

$$\mathbf{Y}_d = \mathbf{X}_d\hat{\mathbf{H}}_d + \mathbf{X}_d[\mathbf{H}_d - \hat{\mathbf{H}}_d] + \mathbf{W}_d, \tag{2.10}$$

where $\mathbf{X}_d$ and $\mathbf{Y}_d$ are the transmitted and received data sub-carriers, respectively. The term $\mathbf{W}_d$ is the corresponding AWGN samples.

On the other hand, the SNR value of the z-th data sub-carrier within the m-th sub-channel in terms of the channel estimation error is evaluated as

$$\gamma(m,z) = \frac{E\{|\hat{H}_d(m,z)|^2|X_d(m,z)|^2\}}{E\{|H_d(m,z) - \hat{H}_d(m,z)|^2|X_d(m,z)|^2 + |W_d(m,z)|^2\}}, \tag{2.11a}$$

$$= P_s(m)\frac{|\hat{H}_d(m,z)|^2}{\sigma_d^2(m)P_s(m) + \sigma^2_{W_d(m,z)}(m)}, \ \forall z \in \{1, ..., \xi_d(m)\}, \tag{2.11b}$$

where $\sigma^2_{W_{k,d}(m,z)}$ is the variance of AWGN samples, $P_s(m) = E\{|X_d(m,z)|^2\}$ is the average symbol power and $\sigma_d^2(m)$ is the variance of the square error (SE) of the estimated channel. In practice, $E\{|\hat{H}_d(m,z)|^2\}$ can be replaced by its instantaneous value of $|\hat{H}_d(m,z)|^2$. The minimum SNR of each sub-channel is selected to guarantee that the required performance is maintained as

$$\gamma_{\min}(m) = \min\{\gamma(m,z)\}. \tag{2.12}$$

In literature, the selection of the best SNR is varied between minimum, mean and maximum values. Each method deals with different design criterion and surrounding conditions. In this work, the minimum value is selected to guarantee that the worst case of the channel coefficients corresponding to sub-carriers included in each sub-channel is tackled. In contrast, the coherence bandwidth, B_{coh}, is measured by computing the correlation values between the neighbour channel coefficients in the frequency domain. By assuming that the correlation between the channel coefficients with respect to the channel estimation error depends only on B_{coh}, the correlation values can be obtained as

$$\Lambda_{B_{coh}}(\beta) = \frac{E\{[\hat{H}_d(f) + \varrho_d(f) - \varpi_{[\hat{H}_d(f)+\varrho_d(f)]}]}{E\{|\hat{H}_d(f) + \varrho_d(f)|^2\}} \cdot [\hat{H}_d(f+\beta) + \varrho_d(f+\beta) - \varpi_{[\hat{H}_d(f+\beta)+\varrho_d(f+\beta)]}]^*\}, \tag{2.13}$$

where $\varpi_{\hat{H}_d(f)}$ and $\varpi_{\hat{H}_d(f+\beta)}$ are the mean values of the frequency response of the channels. The terms $\varrho_d(f) = H_d(f) - \hat{H}_d(f)$ and $\varrho_d(f+\beta) = H_d(f+\beta) - \hat{H}_d(f+\beta)$ are the estimation errors of the channel, f is the frequency index and β is the correlation lag. The uniformly distributed phases of the Rayleigh fading channels result in $\hat{H}_d(f)$ and $\hat{H}_d(f+\beta)$ to be zero-mean, thus, (2.13) can be rewritten as

$$\Lambda_{B_{coh}}(\beta) = \frac{E\{[\hat{H}_d(f) + \varrho_d(f)][\hat{H}_d(f+\beta) + \varrho_d(f+\beta)]^*\}}{\sigma^2_{\hat{H}_d(f)+\varrho_d(f)}}, \tag{2.14}$$

where $\sigma^2_{\hat{H}_d(\beta)+\varrho_d(\beta)} = E\{|\hat{H}_d(\beta) + \varrho_d(\beta)|^2\}$ represents the channel variance within a sub-band in terms of the channel estimation error. By varying β iteratively while keeping the correlation value over 0.9, the coherence bandwidth can be obtained, where the channel attenuation value for frequencies separated by B_{coh} or less, are nearly equal.

It is important to note that the coherent time of the channel is assumed to be more than the time required for measuring the coherence bandwidth and sending back the CSI, T_{CSI}. In other words, the channel is assumed to be almost constant for more than T_{CSI}. After obtaining B_{coh}, the number of sub-channels corresponding to the detected coherence bands is evaluated as

$$N_{coh} \approx \frac{B_T}{B_{coh}}. \tag{2.15}$$

From (2.12) and the LDPC based MCS scenario, the suitable MSC of each sub-channel in the next OFDM symbol is selected at the receiver according to Table 2.2. The SNR threshold values shown in this table are achieved from the simulation results of the utilised MCS levels over Rayleigh fading channel at BER level of 10^{-5} following [97].

It is important to note that this work follows the IEEE802.16e standard, which includes the LDPC coding method with limited range of the allowed codewords sizes

Table 2.2: SNR threshold values for different LDPC based MCS options

Modulation type	Code rate	Threshold SNR (dB)
No transmission		$\gamma_{\min}(m) < 2$
QPSK	1/2	$2 \leq \gamma_{\min}(m) < 5.6$
QPSK	2/3	$5.6 \leq \gamma_{\min}(m) < 8.2$
QPSK	3/4	$8.2 \leq \gamma_{\min}(m) < 10.5$
16-QAM	1/2	$10.5 \leq \gamma_{\min}(m) < 11.9$
16-QAM	2/3	$11.9 \leq \gamma_{\min}(m) < 12.5$
16-QAM	3/4	$12.5 \leq \gamma_{\min}(m) < 14.2$
64-QAM	1/2	$14.2 \leq \gamma_{\min}(m) < 15.5$
64-QAM	2/3	$15.5 \leq \gamma_{\min}(m) < 16.3$
64-QAM	3/4	$\gamma_{\min}(m) \geq 16.3$

of $[576, 672, ..., 2304]$ in increment of 96. This limitation can restrict the flexibility of utilising the available MCS options. Therefore, the second MCS scenario that is established on the recommended convolutional coding method is adopted as there are no specific sizes of the resulting codewords. The selection of the suitable convolutional based MCS for each sub-channel assigned to a coherence band based on the corresponding minimum SNR value is based on Table 2.3 [98], [99].

Table 2.3: SNR threshold values for distinct convolutional based MCS options

Modulation type	Code rate	Threshold SNR (dB)
No transmission		$\gamma_{\min}(m) < 4$
QPSK	1/2	$4 \leq \gamma_{\min}(m) < 10.25$
QPSK	2/3	$10.25 \leq \gamma_{\min}(m) < 13.25$
QPSK	3/4	$13.25 \leq \gamma_{\min}(m) < 14.52$
16-QAM	1/2	$14.52 \leq \gamma_{\min}(m) < 16.1$
16-QAM	2/3	$16.1 \leq \gamma_{\min}(m) < 20.25$
16-QAM	3/4	$20.25 \leq \gamma_{\min}(m) < 22.5$
64-QAM	1/2	$22.5 \leq \gamma_{\min}(m) < 28.5$
64-QAM	2/3	$28.5 \leq \gamma_{\min}(m) < 39.1$
64-QAM	3/4	$\gamma_{\min}(m) \geq 39.1$

The diversity of the fading values for distinct sub-channels and MCS selection is expected to improve the average system throughput, ψ_{av}. The term ψ_{av} is evaluated by averaging the throughput of N_{fr} transmitted OFDMA frames, ψ_g, where $g = 1, ..., N_{fr}$, is the frame index. This enhancement is the result of increasing the

average spectral efficiency, $\rho(m)$, expressed by (2.5), for each sub-channel individually. The system throughput for the g-th OFDMA symbol can be mathematically expressed as

$$\psi_g = \sum_{m=1}^{N_{coh}} \xi_d(m)\rho(m)[1 - P_e(m)], \tag{2.16}$$

where $P_e(m)$ denotes the BER value of each sub-channel. Additionally, the reduction of $P_e(m)$ can lead to an increase in the system throughput, as shown in (2.16).

2.3 Dynamic Sub-Channelling AMC-OFDM

A dynamic sub-channelling (DS) for downlink single user AMC based OFDM system, called DS-AMC-OFDM, is provided in this Section. This is carried out by proposing a pilot adjustment scheme that reduces the utilised pilots for channel estimation of each sub-channel according to the measured channel coherence bandwidth and the related SNR value. Furthermore, the unused pilots for each sub-channel are replaced by additional data sub-carriers, in which the sum of data and pilot sub-carriers in each band is kept the same. The number of the required pilots and optimal MCS level of each sub-channel is returned to the transmitter utilising the feedback CSI. As a result, the system throughput is improved by increasing the data transmission for the sub-channels with stable profiles.

In order to describe the investigated system structure and the proposed algorithm, this Section is divided into three parts.

2.3.1 DS-AMC-OFDMA System Model

This Section considers the developments applied to the receiver structure of the FS-AMC-OFDM system shown in Fig. 2.6 [8], [100]. The transmitter block diagram of the proposed FS-AMC-OFDM system is adopted by the DS-AMC-OFDM system. The only difference is that the number of the pilot and data sub-carriers can be reduced or increased for each sub-channel. The number of required pilots is included in the feedback CSI.

Fig. 2.7 illustrates the receiver of the DS-AMC-OFDM system. From this figure, the number of the pilot and data sub-carriers for each sub-channel is adjusted in the *Pilot Adjustment* block. The main function of this block is to decide the optimal

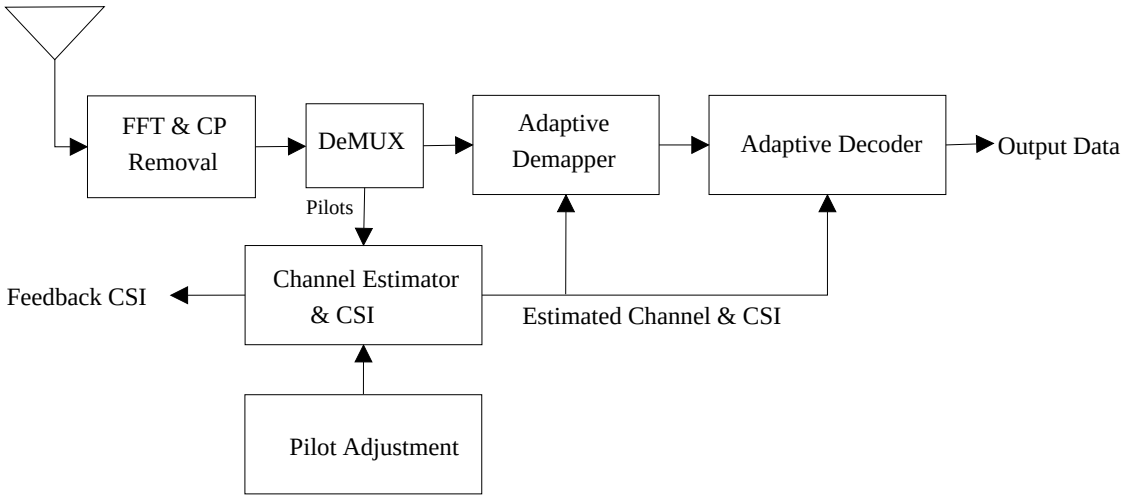

Figure 2.7: Receiver block diagram of the proposed DS-AMC-OFDM system.

number of the data and pilot sub-carriers across the sub-channels individually by applying the proposed pilot adjustment scheme. Moreover, the other blocks of the receiver have the same functions of the FS-AMC-OFDM system. For stable channel profiles, the number of utilised pilots is reduced and the available size from this reduction is filled with additional data symbols at the transmitter to increase the system throughput. The selected number of the pilots of each sub-channel is included in the feedback CSI.

2.3.2 Proposed Pilot Adjustment Scheme for DS-AMC -OFDM

As mentioned earlier, the proposed DS-AMC-OFDM system is based on the introduced pilot adjustment scheme. This scheme reduces the number of employed pilots for channel estimation of each sub-channel assigned to a frequency coherence band depending on the measured frequency coherence bandwidth and the related SNR value. This technique can be divided into two parts to improve the readability of the thesis as follows.

Problem Formulation

The proposed pilot adjustment scheme is based on the scalability of OFDM systems, such as Mobile WiMAX, which endorses the variation of the number of pilots [92]. The throughput of the proposed system is improved by replacing unnecessary pilots

within the sub-channels with additional information data streams. This reduction in the number of pilots for each sub-channel depends on the measured coherence bandwidth, B_{coh}, and the minimum SNR, $\gamma_{\min}(m)$, of the frequency bands. It is important to note that the range of the pilot reduction value, $\Pi(m)$, for each sub-channel can be varied between zero and $\xi_p(m) - 2$. This value is evaluated as

$$\Pi(m) = \zeta(m) B_{coh} \gamma_{\min}(m), \tag{2.17}$$

where the terms $\delta_d(m)$ and $\delta_p(m)$ designate the new numbers of data and pilot sub-carriers achieved after applying the proposed pilot adjustment scheme. These values can be computed based on the pilot reduction value, $\Pi(m)$, and the initial numbers of the data and pilot sub-carriers for the m-th sub-channel, $\xi_d(m)$ and $\xi_p(m)$, respectively, as

$$\delta_d(m) = \xi_d(m) + \Pi(m), \tag{2.18}$$

$$\delta_p(m) = \xi_p(m) - \Pi(m). \tag{2.19}$$

In addition, $\zeta(m)$ is a variable selected to satisfy the condition, $\mod [\delta_d(m), \delta_p(m)] = 0$, that guarantees uniform distribution of new sets of pilot and data sub-carriers within each sub-channel. The evaluation of $\zeta(m)$ is illustrated in Algorithm 1.

Step 1. Initialisation:
Set $\zeta(m) = 0.01$
Step 2. New numbers of pilot and data sub-carriers evaluation:
foreach m **do**
  $\Pi(m) = \zeta(m) B_{coh} \gamma_{\min}(m)$,
  $\delta_d(m) = \xi_d(m) + \Pi(m)$,
  $\delta_p(m) = \xi_p(m) - \Pi(m)$.
end
if $\mod [\delta_d(m), \delta_p(m)] = 0$ **then**
  Go to step 3
end
Increase $\zeta(m)$,
Go to step 2.
Step 3. End.

Algorithm 1: $\zeta(m)$ evaluation for DS-AMC-OFDM

Since the proposed strategy is locally implemented and the related information is fedback to the transmitter via CSI, the receiver of each user is aware of the structure

for the next OFDM frame in terms of the indices of the data and pilot sub-carrier for each sub-channel. Therefore, there is no need for sending forward information from the transmitter to the receiver regarding the structure of the transmitted OFDM frame.

In contrast, the frequency coherence bandwidth, B_{coh}, is evaluated following the mathematical expressions of (2.13), (2.14) and the related explanations. Additionally, $\gamma_{\min}(m)$ can be computed based on (2.12).

Pilot Adjustment Algorithm

Algorithm 2 demonstrates the proposed pilot adjustment method. This algorithm contains two levels of constraints. The constraints of the first level that can be mathematically expressed as

$$B_{coh} \geq \frac{B_{eff}}{2N_{coh}}, \tag{2.20}$$

and

$$\gamma_{\min}(m) \geq 10 \text{ dB}, \tag{2.21}$$

control the variation of the pilot and the data sub-carriers particularly at low SNR levels, i.e. under 10 dB, where the channel estimation error is high due to noise that effects the performance of the utilised LS method [101]. Therefore, the system preferably uses the full number of pilots to recover the expected high channel estimation error that influences the accuracy of the correlation operation of the coherence bandwidth measurements. Additionally, these constraints restrict the pilot reduction for narrow frequency coherence bandwidth. It is important to note that the two constraints values are selected empirically from simulations. This is accomplished by performing a huge number of simulation runs with a range of different possible values and then selecting the optimal values. If the first level constraints are satisfied, the proposed pilot adjustment algorithm continues to decrease or increase the number of allocated pilots for the continuous transmitted OFDM frames. At this stage, the pilot reduction value, $\Pi(m)$, as well as the optimised new number of data and pilot sub-carriers for each sub-channel are achieved following (2.17)-(2.19).

The acceptance of the refined number of the utilised pilots for each sub-channel is controlled by the second level constraint of

$$\Upsilon(m) \leq 0.001. \tag{2.22}$$

This constraint, which is also evaluated empirically from simulations, can decide either the new number of pilots is enough or not based on the channel estimation error, $\Upsilon(m)$, between the MSE of full-use of pilots, $MSE^{(full)}(m)$, and the proposed scheme, $MSE^{(prop)}(m)$. The $\Upsilon(m)$ can be evaluated as

$$\Upsilon(m) = MSE^{(full)}(m) - MSE^{(prop)}(m). \tag{2.23}$$

Step 1. Parameter Evaluations:
foreach m **do**
  Compute B_{coh} using (2.14).
  Compute $\gamma(m, z)$ using (2.11).
  Compute $\gamma_{\min}(m)$ using (2.12).
end
Step 2. First level constraints:
foreach m **do**
  if $B_{coh} \geq \frac{B_{eff}}{2N_{coh}}$, $\gamma_{\min}(m) \geq 10\ dB.$ **then**
    $\Pi(m) = \zeta(m) B_{coh} \gamma_{\min}(m)$,
    $\delta_p(m) = \xi_p(m) - \Pi(m)$,
    $\delta_d(m) = \xi_d(m) + \Pi(m)$,
    The second level constraint:
    if $\Upsilon(m) \leq 0.001$. **then**
      Go to step 3.
    end
    else
      Transmit with full-use of pilots.
      Go to step 3.
    end
  end
  else
    Transmit with full-use of pilots.
    Go to step 3.
  end
end
Step 3. Feedback CSI Generation:
Return $\delta_p(m)$ and the number of the selected MCS to the transmitter.
.

Algorithm 2: Pilot adjustment algorithm for DS-AMC-OFDM

The refined number of the pilots and the selected MCS number of each sub-channel are included in the corresponding feedback CSI to enable the required adjustment at the transmitter.

2.3.3 Feedback CSI Analysis for DS-AMC-OFDM

The same feedback CSI overhead analysis of FS-AMC-OFDM system is applied for DS-AMC-OFDM with additional information bits that express the adjusted number of pilots of each sub-channel for performing the channel estimation efficiently. Therefore, the required number of bits that cover the feedback information for the m-th sub-channel is evaluated as

$$N_{B,CSI}(m) = N_{B,MCS}(m) + N_{B,ps}(m), \tag{2.24}$$

where $N_{B,MCS}(m)$ is the required number of bits to represent the selected MCS for the m-th sub-channel. Additionally, $N_{B,ps}(m)$ denotes the maximum number of bits required to transmit the optimal number of pilots used for efficient channel estimation in each sub-channel. In this case, the consumed bandwidth for feedback CSI is dramatically increased and, as a result, the performance of the proposed DS-AMC-OFDM system is also affected. Additionally, the effective bandwidth can be evaluated based on the refined number of data sub-carriers for each sub-channel, $\delta_d(m)$, as

$$B_{eff} = \big[\sum_{m=1}^{M} \delta_d(m)\big] \left[\frac{B_T - \sum_{m=1}^{M} \frac{1}{T_{CSI}(m)}}{N_{FFT}}\right], \tag{2.25a}$$

$$= \big[\sum_{m=1}^{M} \delta_d(m)\big] \big[\frac{B_T - B_{CSI}}{N_{FFT}}\big]. \tag{2.25b}$$

2.4 Fixed Sub-Channelling AMC-OFDMA

The proposed AMC strategy applied for fixed sub-channelling based downlink single user OFDM system has been expanded to accommodate the dimension of multiuser transmission. In this case, the investigated system that employs such strategy is called FS-AMC-OFDMA. Furthermore, the OFDMA frame is divided into sub-channels and each sub-channel is assigned to a user. Therefore, the numbers of sub-channels and users are identical and different MCS options are selected for the involved users depending on the related SNR values.

2.4.1 FS-AMC-OFDMA System Model

Fig. 2.8 illustrates the block diagram of FS-AMC-OFDMA system. Throughout this work, the scenario of a downlink transmission from a base station (BS) to a set of K users is adopted. The investigated system allocates each user to a single sub-channel so that fair service is guaranteed for all users [67], [65], [70]. The mobile WiMAX standard is also adopted as a reference.

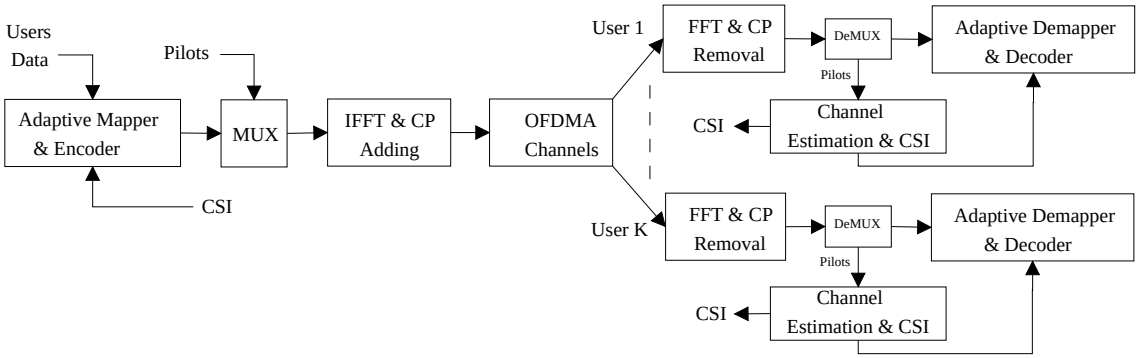

Figure 2.8: Block diagram of an FS-AMC-OFDMA system.

All M sub-channels contain the same number of data and pilot sub-carriers according to the principle of fair service [65]. Thus, the number of data sub-carriers, $\xi_{d_k}(m)$, allocated to user k over sub-channel m is given by $\xi_{d_k}(m) = N_d/K$, for any $k \in \{1, ..., K\}$, whereas the number of pilot sub-carriers, $\xi_{p_k}(m)$, allocated to user k over sub-channel m is given by $\xi_{p_k}(m) = N_p/K$, for any $k \in \{1, ..., K\}$.

At the transmitter, the same sequence of blocks and functions adopted by FS-AMC-OFDM system is considered. Thus, the resulting OFDMA frame is composed of K sub-streams of symbols, each of which corresponds to the data symbols of a particular user $k \in \{1, ..., K\}$. Each sub-stream is encoded and modulated depending on the selected MCS. The optimal selection of the MCS for each sub-channel assigned to a user based on the related SNR value is achieved following Table 2.2 for the LDPC based MCS scenario and Table 2.3 for the convolutional based MCS scenario.

The channel profiles of pedestrian international telecommunication union (ITU)-B, vehicular ITU-A and ITU-B have been considered with different mobility speeds in order to achieve a wide range of user categories in terms of physical location and mobility speed. The parameters of the considered channel profiles in terms of the spread delay, τ_l, and power, P_l, for the $[l]_{l\in\{0,...,L-1\}}$-th channel path are listed in table 2.4 [102].

Table 2.4: ITU channel parameters

Path	Pedestrian ITU-B		Vehicular ITU-A		Vehicular ITU-B	
	τ_l (ns)	P_l (dB)	τ_l (ns)	P_l (dB)	τ_l (ns)	P_l (dB)
1	0	0	0	0	0	-2.5
2	200	-0.9	310	-1	300	0
3	800-	-4.9	710	-9.0	8900	-12.8
4	1200	-8.0	1090	-10.0	12900	-10.0
5	2300	-7.8	1730	-15.0	17100	-25.2
6	3700	-23.9	2510	-20.0	20000	-16.0

At the receiver of the user k, the frequency-domain data sample $Y_k(m,z)$, $z \in \{1,...,\xi_{d_k}(m)\}$, corresponding to the z-th data sub-carrier of sub-channel m in prescience of channel estimation error is given by

$$Y_k(m,z) = X_k(m,z)\hat{H}_k(m,z) + X_k(m,z)[H_k(m,z) - \hat{H}_k(m,z)] + W_k(m,z), \quad (2.26)$$

where $X_k(m,z)$ designates the symbol of user k transmitted over the (z)-th data sub-carrier of sub-channel m, whereas the sample $H_k(m,z)$ and $\hat{H}_k(m,z)$ represents the real and estimated fading experienced by this particular sub-carrier, respectively. The term $W_k(m,z)$ is a complex Gaussian noise sample with zero mean. The SNR value for the user k assigned to the sub-channel m is selected to be the minimum value over the data sub-carriers within such sub-channel based on (2.12) as

$$\gamma_{k,\min}(m) = \min[\gamma_k(m,z)] = \min\left[\frac{P_{s_k}(m)|\hat{H}_k(m,z)|^2}{\sigma^2_{d,k}(m)P_{s_k}(m) + \sigma^2_{W_k(m,z)}(m)}\right], \quad (2.27)$$

where $P_{s_k}(m)$ is the power value of the coded and modulated symbol of the k-th user. The terms $\sigma^2_{W_k(m,z)}(m)$ and $\sigma^2_{d,k}(m) = E\{|H_k(m,z) - \hat{H}_k(m,z)|^2\}$ designate the variance of the AWGN samples and that of the MSE of the fading sample estimate, respectively.

In contrast, the channel estimation for each sub-carrier is performed using LS method [103]. Finally, the information regarding the selected MCS, that can be referred to as feedback CSI, is sent from each user to the base station (transmitter) after each transmitted OFDMA frame using a TDD uplink in order to overcome the problem of outdated CSI. The feedback CSI is received by the base station with a

delay of $T_{k,CSI}(m)$ seconds. In this work, it is assumed that the channel remains constant for more than T_{CSI} seconds, which is the total required time for feeding back the CSI.

The system throughput for g-th OFDMA frame can be mathematically expressed based on (2.16) as a function of the BER, $P_{e_k}(m)$, and spectral efficiency, $\rho_k(m)$, as

$$\psi_g = \sum_{k=1}^{K} \sum_{m=1}^{M} \varphi(k,m) \xi_{d_k}(m) \gamma_{k,\min}(m) [1 - P_{e_k}(m)], \tag{2.28}$$

where $\varphi(k,m)$ is an element in the user allocation matrix. Each row in this matrix represents a user, while each sub-channel is addressed by a column. In this Chapter, the sequential user allocation is considered, i.e. the first user is allocated over the first sub-channel and so on.

2.4.2 Feedback CSI Analysis for FS-AMC-OFDMA

As highlighted before, the delay $T_{k,CSI}(m)$ can significantly degrade the effective bandwidth used for the transmission of data sub-carriers. The feedback delay $T_{k,CSI}(m)$ for each user $k \in \{1, ..., K\}$ can be expressed based on (2.6) as

$$T_{k,CSI}(m) = \frac{N_{B,CSI}^{(k)}(m)}{R_{b,k}(m)}, \tag{2.29}$$

where $R_{b,k}(m)$ is the bit rate of the corresponding feedback link and $N_{B,CSI}^{(k)}(m)$ designates the number of bits that are required to cover the feedback CSI associated with sub-channel m. The bit rate $R_{b,k}(m)$ is given by $R_{b,k}(m) = \rho_k(m) B_k$, where $\rho_k(m)$ denotes the spectral efficiency of the m-th sub-channel assigned to the k-th user and B_k is the bandwidth available for the same user. It can be shown that the bandwidth required for feedback CSI, B_{CSI}, can be expressed as a function of the feedback delays $T_{k,CSI}(m)$, $k \in \{1, ..., K\}$ and $m \in \{0, ..., M\}$, using

$$B_{CSI} = \sum_{k=1}^{K} \sum_{m=1}^{M} \frac{\varphi(k,m)}{T_{k,CSI}(m)}, \tag{2.30}$$

where the user allocation matrix element $\varphi(k,m) = 1$ if the signal of user k is transmitted over sub-channel m, and $\varphi(k,m) = 0$ otherwise. Based on the fair service that allocates one user for each sub-channel, the constraints of

$$\sum_{k=1}^{K} \varphi(k,m) = 1, \quad m = 1, ..., M, \tag{2.31}$$

and

$$\sum_{m=1}^{M} \varphi(k,m) = 1, \quad k = 1, ..., K, \tag{2.32}$$

are employed [70]. These constraints can guarantee the occupation of one user per sub-channel. In contrast, the effective bandwidth can be computed based on (2.7).

2.5 Dynamic Sub-Channelling AMC-OFDMA

The proposed dynamic sub-channelling strategy, based on the introduced pilot adjustment scheme, has been also expanded to work with multiuser OFDM system, which is called DS-AMC-OFDMA. As mentioned earlier, the FS-AMC-OFDMA system allocates one user per sub-channel and the same aspect is followed by the DS-AMC-OFDMA. In contrast, the pilot adjustment scheme includes the variance of the SNR fluctuation values as a selectivity metric of the channels corresponding to different users to reduce or increase the number of utilised pilots.

2.5.1 DS-AMC-OFDMA System Model

The receiver of the FS-AMC-OFDMA system shown in Fig. 2.8 is developed by adding a new function to the *Channel Estimation and CSI* block. This function is the evaluation of the variance of the SNR fluctuation values in addition to measure the frequency coherence bandwidth and SNR for the estimated fading coefficients of the experienced channel. These values are employed to obtain the optimal number of pilot and data sub-carriers for each sub-channel.

2.5.2 Proposed Pilot Adjustment Scheme for DS-AMC-OFDMA

An additional parameter, which is the variance of the SNR fluctuation values, has been included in the pilot adjustment scheme for DA-AMC-OFDMA to measure the selectivity of the corresponding channels. This sub-Section is divided into two parts to ease the understanding of the presented scheme as follows.

Problem Formulation

As highlighted earlier, the reduction in the number of pilots considers the user channel measured coherence bandwidth, $B_{k,coh}$, the variance of the SNR fluctuation values, $\sigma^2_{k,\Xi_k(m,z)}(m)$, and the minimum SNR, $\gamma_{k,\min}(m)$, of each sub-channel assigned to a user. For the DS-AMC-OFDMA system, the pilot reduction value, $\Pi_k(m)$, is computed as

$$\Pi_k(m) = \zeta_k(m)\frac{B_{k,coh}\gamma_{k,\min}(m)}{\sigma^2_{k,\Xi_k(m,z)}(m)}. \tag{2.33}$$

The $\Pi_k(m)$ value amends the initial number of data and pilot sub-carriers, $\xi_{k_d}(m)$ and $\xi_{k_p}(m)$, of the m-th sub-channel assigned to the k-th user as

$$\delta_{p_k}(m) = \xi_{p_k}(m) - \Pi_k(m), \tag{2.34}$$

and

$$\delta_{d_k}(m) = \xi_{d_k}(m) + \Pi_k(m). \tag{2.35}$$

On the other hand, the correlation value of the channel coefficients, used to evaluate $B_{k,coh}$, can be rewritten in terms of multiuser dimension based on (2.14) as

$$\Lambda_{B_{k,coh}}(\beta) = \frac{E\{[\hat{H}_{d,k}(f) + \varrho_{d,k}(f)][\hat{H}_{d,k}(f+\beta) + \varrho_{d,k}(f+\beta)]^*\}}{\sigma^2_{\hat{H}_{d,k}(f)+\varrho_{d,k}(f)}}. \tag{2.36}$$

In addition, the variance of SNR fluctuation values for each sub-channel, $\sigma^2_{k,\Xi_k(m,z)}(m)$, is evaluated as

$$\sigma^2_{k,\Xi_k(m,z)}(m) = \mathrm{var}[\Xi_k(m,z)], \tag{2.37}$$

where $\Xi_k(m,z)$ is the fluctuation value of the channel coefficient of the z-th data sub-carrier within m-th sub-channel assigned to k-th user that can be evaluated depending on the related estimated SNR, $\gamma_k(m,z)$, and the average SNR value, $\Gamma_{k,av}(m) = E\{\gamma_k(m,z)\}$, as

$$\Xi_k(m,z) = \gamma_k(m,z) - \Gamma_{k,av}(m). \tag{2.38}$$

Pilot Adjustment Algorithm

The pilot adjustment algorithm for DS-AMC-OFDMA system is illustrated in Algorithm 3. This algorithm is established on Algorithm 2 with the consideration of multiuser dimension and the variance of the SNR fluctuations values.

Step 1. Parameter Evaluations:
foreach k **do**
  foreach m **do**
    Compute $B_{k,coh}$ using (2.36).
    Compute $\sigma^2_{k,\Xi_k(m,z)}(m)$ using (2.37).
    Compute $\gamma_{k,\min}(m)$ using (2.27)
  end
end
Step 2. First level constraints:
foreach k **do**
  foreach m **do**
    if $B_{k,coh} \geq \frac{B_{eff}}{2M}$,
    $\gamma_{k,\min}(m) \geq 10\ dB$ *and*
    $\sigma^2_{k,\Xi_k(m,z)}(m) \leq 0.2.$ **then**
      $\Pi_k(m) = \zeta_k(m)\frac{B_{k,coh}\gamma_{k,\min}(m)}{\sigma^2_{k,\Xi_k(m,z)}(m)}$,
      $\delta_{p_k}(m) = \xi_{p_k}(m) - \Pi_k(m)$,
      $\delta_{d_k}(m) = \xi_{d_k}(m) + \Pi_k(m)$,
      The second level constraint:
      if $\Upsilon_k(m) \leq 0.001.$ **then**
        Go to step 3.
      end
      else
        Transmit with Full-use of pilots.
        Go to step 3.
      end
    end
    else
      Transmit with Full-use of pilots.
      Go to step 3.
    end
  end
end
Step 3. Feedback CSI Generation:
Return $\delta_{p_k}(m)$ and the selected MCS to the transmitter.

Algorithm 3: The proposed pilot adjustment algorithm for DS-AMC-OFDMA

The constraints of the first level are reformulated as

$$B_{k,coh} \geq \frac{B_{eff}}{2M}, \tag{2.39}$$

$$\gamma_{k,\min}(m) \geq 10 \text{ dB}, \tag{2.40}$$

and

$$\sigma^2_{k,\Xi_k(m,z)}(m) \leq 0.2, \tag{2.41}$$

These constraints restrict the pilot reduction for the low SNR values, high selectivity of the corresponding channel coefficients and narrow coherence bands. After satisfying these constraints, the main parameters are computed following the formulas of (2.27), (2.36) and (2.37) in order to find the pilot reduction value, $\Pi_k(m)$, that provides the new numbers of the data and pilot sub-carriers based on (2.33)-(2.35).

The second level constraint can be formulated as

$$\Upsilon_k(m) \leq 0.001, \tag{2.42}$$

where $\Upsilon_k(m)$, which is the evaluated error between the channel estimation MSE of full use and the adjusted value of pilots, can be computed as

$$\Upsilon_k(m) = MSE_k^{(full)}(m) - MSE_k^{(prop)}(m). \tag{2.43}$$

As mentioned earlier, the first and second level constraints are evaluated empirically from simulations. In order to explain the proposed pilot adjustment scheme in more detail, a channel with five users is selected as an example. Table 2.5 shows the suggested $\Pi(m)$ values per sub-channel in terms of the constraints described by (2.39)-(2.41).

Table 2.5: The number of the data and pilot sub-carriers for each sub-channel

$\delta_{k_p}(m)$	$\delta_{k_d}(m)$	$\Pi_k(m)$	$\sigma^2_{k,\gamma_k(m,z)}(m)$	$\gamma_{k,\min}(m)$	$B_{k,coh}$
48	288	0	otherwise		
28	308	20	$[0.2, 0.15)$	≥ 10	$\geq \frac{B_{eff}}{2M}$
8	328	40	$[0.15, 0.1)$	≥ 10	$\geq \frac{B_{eff}}{2M}$
4	332	44	$[0.1, 0.05)$	≥ 10	$\geq \frac{B_{eff}}{2M}$
2	334	46	≤ 0.05	≥ 10	$\geq \frac{B_{eff}}{2M}$

Based on Table 2.5, Fig. 2.9 shows the distribution of pilots over data sub-carriers in the cases of using 48 and 28 pilots per sub-channel, respectively.

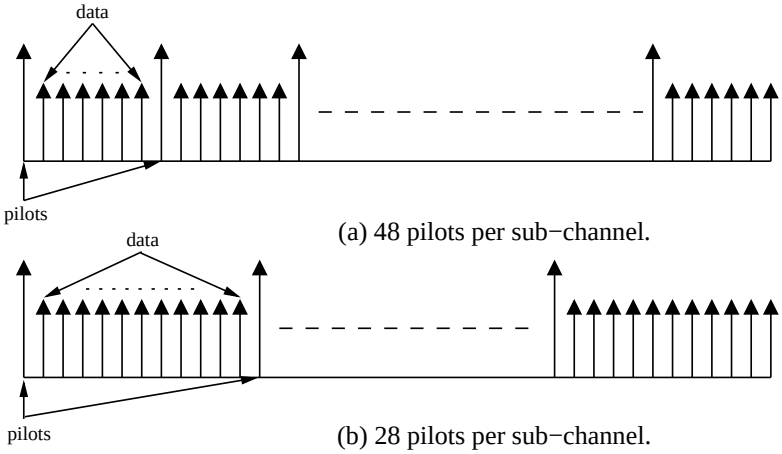

Figure 2.9: (a) Using 48 pilots and 288 data sub-carriers per sub-channel, (b) Using 28 pilots and 308 data sub-carriers per sub-channel.

2.5.3 Feedback CSI Analysis for DS-AMC-OFDMA

The feedback CSI analysis of DS-AMC-OFDM system is adopted for DS-AMC-OFDMA with respect to the multiuser dimension. In addition, the effective bandwidth can be rewritten based on (2.25) as

$$B_{eff} = \big[\sum_{k=1}^{K}\sum_{m=1}^{M}\varphi(k,m)\delta_{d_k}(m)\big]\left[\frac{B_T - \sum_{k=1}^{K}\sum_{m=1}^{M}\frac{\varphi(k,m)}{T_{CSI}(m)}}{N_{FFT}}\right], \tag{2.44a}$$

$$= \big[\sum_{k=1}^{K}\sum_{m=1}^{M}\varphi(k,m)\delta_{d_k}(m)\big]\big[\frac{B_T - B_{CSI}}{N_{FFT}}\big]. \tag{2.44b}$$

2.6 Simulation Results and Discussion

This Section studies the performance of the proposed systems over different channel profiles. Moreover, a detailed discussion, which shows the reason behind the superior performance of the proposed systems, is presented. The introduced two MCS scenarios are employed to obtain these results. In order to make this Section more readable, it has been divided into the following sub-Sections.

2.6.1 LDPC Based AMC-OFDM System

The simulation performance of the LDPC based FS-AMC-OFDM system has been demonstrated and discussed in this sub-Section. The system parameters listed in

Table 2.1 have been adopted. Additionally, two different systems are considered as follows:

1. Conventional adaptive system which adopts the same MCS for the entire OFDM frame based on the minimum SNR value amongst the included sub-channels [20]. This system is called 'Conventional AMC-OFDM'.

2. Proposed AMC-OFDM system that adopts the proposed AMC strategy.

These systems are tested over Rayleigh fading channel with five different frequency coherence bands as shown in Fig. 2.5.

Fig. 2.10 shows the average system throughput comparison between the two systems under investigation. Furthermore, the average throughput is evaluated for $N_{fr} = 1 \times 10^6$ transmitted OFDMA frames, with respect to the real effective bandwidth, B_{eff}, expressed in (2.7) as

$$\psi_{av} = \frac{B_{eff}}{N_d} \frac{1}{N_{fr}} \sum_{g=1}^{N_{fr}} \psi_g. \tag{2.45}$$

It is observed from Fig. 2.10 that the proposed scheme provides a throughput performance gain between 5-15 Mbps over the conventional adaptive system for a SNR range between 5 and 35 dB. The enhancement in performance is due to the fact that the proposed strategy exploits the channel conditions to construct the transmitted OFDM frame by selecting different MCS options assigned to distinct sub-channels. Therefore, the transmitted OFDM frame contains different types of modulation and coding rates that are related to the status of the measured coherence bands in the underlying channel. Moreover, the selection of different MCS options based on the fading diversity of sub-channels can increase the spectral efficiency, which in turn improves system performance by increasing the employed coding rate and modulation level as indicated in (2.16). It is worth observing that at high SNR levels above 30 dB the performance of the adaptive systems approximately converges to the same value because they select the highest MCS for all sub-channels.

Fig. 2.11 presents a comparison of the throughput outage probability, P_{out}, obtained with Conventional AMC-OFDM and Proposed AMC-OFDM systems. Note that P_{out} is evaluated by taking the average, over N_{fr} transmitted OFDM frames, of the outage probability achieved with the g-th frame as

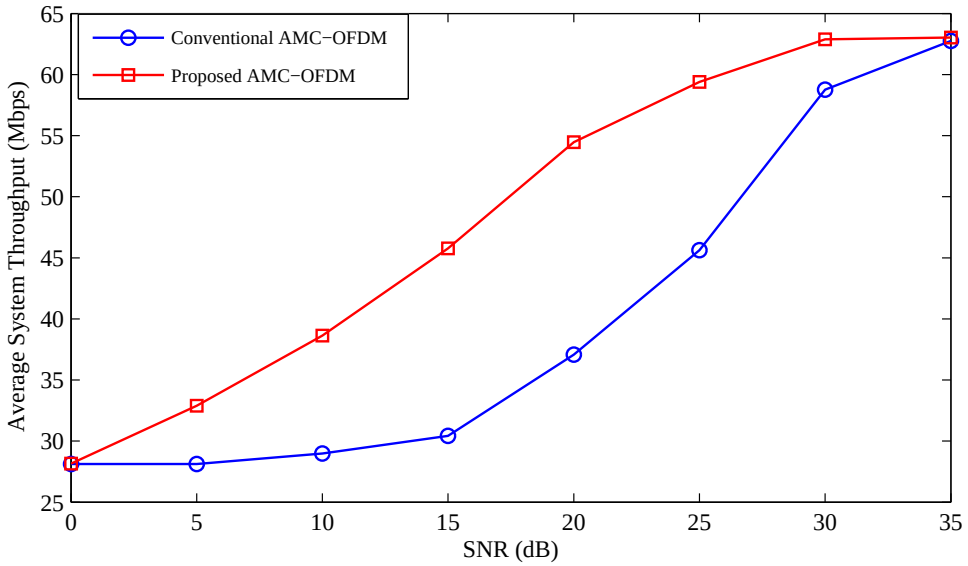

Figure 2.10: Average system throughput for conventional and proposed LDPC-AMC-OFDM systems.

$$P_{out} = 1 - E\left\{\frac{\psi_g}{\psi_{UB}}\right\}, \forall g \in \{0, ..., N_{fr}\}, \tag{2.46}$$

where the throughput upper bound, ψ_{UB}, represents the maximum average system throughput that can be achieved. Furthermore, it can be evaluated as

$$\psi_{UB} = B_{eff}\rho_{max}, \tag{2.47}$$

where $\rho_{max} = 4.5$ bps/Hz is the maximum spectral efficiency achieved by the highest MCS option (64-QAM combined with 3/4 coding rate). It is observed from Fig. 2.11 that the performance of Proposed AMC-OFDM system is better than the other approach. It is also remarked that the proposed AMC strategy adopted by Proposed AMC-OFDM system can achieve the lowest outage probability at SNR values less than the conventional method due to the high flexibility of considering different MCS options throughout distinct ranges of SNR.

The usage probability of the utilised MCS options in terms of different SNR ranges is measured in Fig. 2.12. It is obtained for the Conventional AMC-OFDM and Proposed AMC-OFDM systems by considering four SNR values of 5, 15, 25 and 35 dB. In this figure, the ten MCSs are sorted from the lowest to the highest level as: 1) null transmission, 2) QPSK and 1/2 coding rate, 3) QPSK and 2/3 coding rate, 4) QPSK and 3/4 coding rate, 5) 16-QAM and 1/2 coding rate, 6)

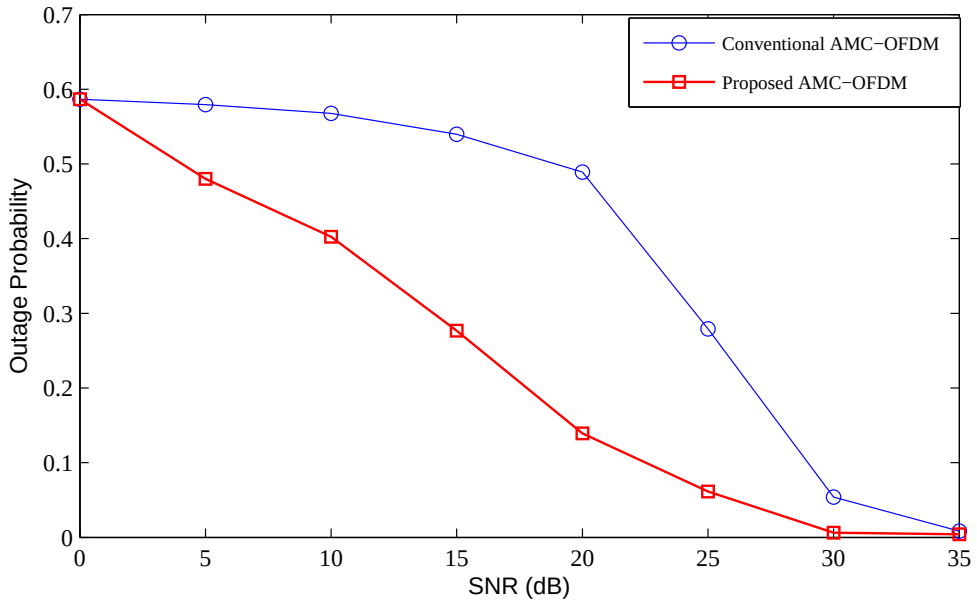

Figure 2.11: Outage probability of conventional and proposed LDPC-AMC-OFDM systems.

16-QAM and 2/3 coding rate, 7) 16-QAM and 3/4 coding rate, 8) 64-QAM and 1/2 coding rate, 9) 64-QAM and 2/3 coding rate and 10) 64-QAM and 3/4 coding rate. Fig. 2.12(a) demonstrates the statistical evaluations for the investigated systems at SNR = 5 dB. It can be observed that the Proposed AMC-OFDM system uses more MCS options than the other approach and the no transmission option is utilised by the Conventional AMC-OFDM scheme in a high usage probability in comparison with the Proposed AMC-OFDM. Moreover, Fig. 2.12(b) illustrates the superior diversity in MCS selection by the proposed AMC strategy for SNR=15 dB. This strategy utilises the higher MCS options, while the conventional method is restricted by the minimum SNR value of the transmitted OFDM frame. The result of Fig. 2.12(c) shows that the Proposed AMC-OFDM system selects the 64-QAM based MCS options in high usage probability compared to the Conventional AMC-OFDM approach for SNR value of 25 dB. In contrast, both investigated systems choose the 64-QAM associated with 3/4 LDPC coding rate for SNR=35 dB as expressed in Fig. 2.12(d).

2.6.2 Convolutional Based AMC-OFDM System

As highlighted in sub-Section 2.2.3, the limited codeword size of the LDPC method restricts the flexibility of considering channels with different frequency coherence

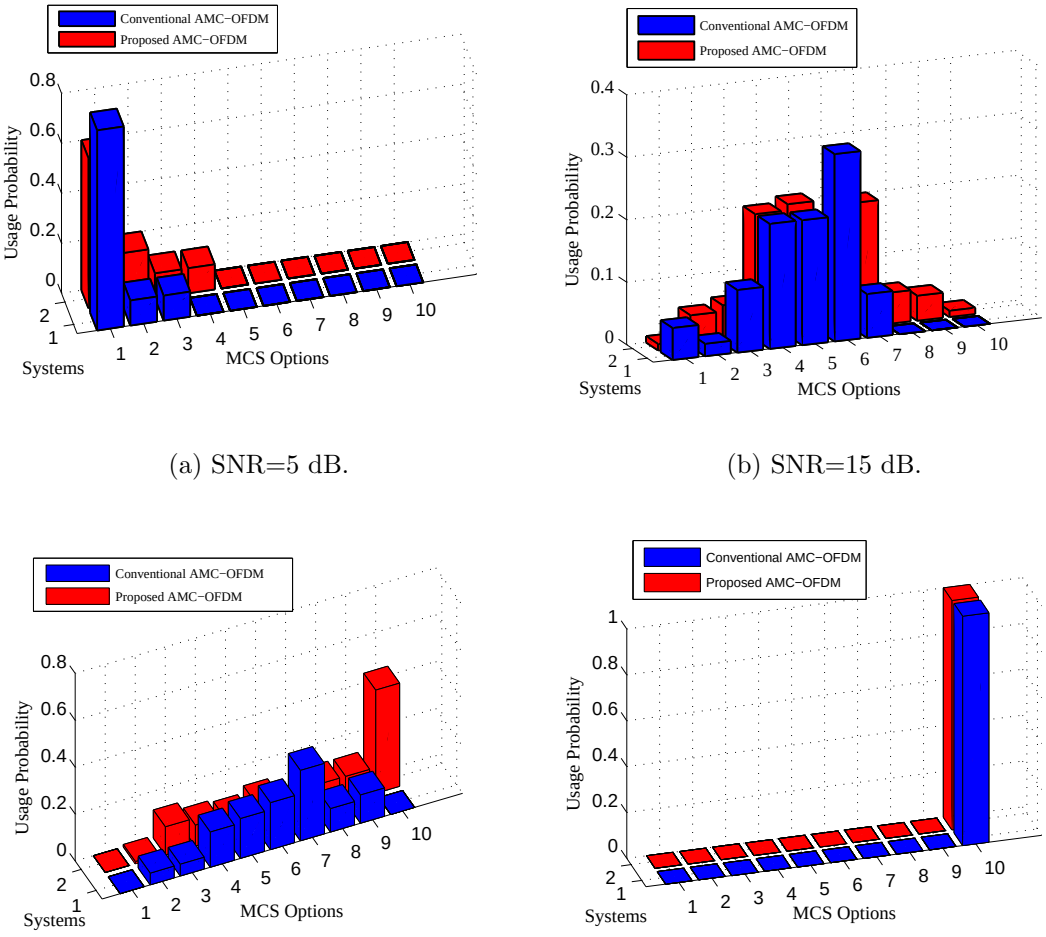

(a) SNR=5 dB.

(b) SNR=15 dB.

(c) SNR=25 dB.

(d) SNR=35 dB.

Figure 2.12: Usage probability of the utilised MCS options for the conventional and proposed LDPC-AMC-OFDM systems.

bandwidth and the required MCS options as well as applying the proposed dynamic sub-channelling. Therefore, the convolutional coding approach has been adopted to accommodate different channel profiles and the proposed pilot adjustment scheme that changes the number of data and pilot sub-carriers within each sub-channel individually. The simulation results are achieved for three systems based on convolutional coding method as follows:

1. Conventional FS-AMC-OFDM that adopts the same MCS option for all sub-channels within the transmitted OFDM frame depending on the minimum SNR value with fixed sub-channelling [20].

2. Proposed FS-AMC-OFDM, which employs the proposed AMC strategy with fixed sub-channelling.

3. Proposed DS-AMC-OFDM that utilises the proposed AMC strategy with dynamic sub-channelling based on pilot adjustment scheme.

It is also important to note that the system parameters of Table 2.1 and the channel model shown in Fig. 2.5 are considered by all investigated systems.

Fig. 2.13 demonstrates the throughput performance of the Conventional FS-AMC-OFDM, Proposed FS-AMC-OFDM and Proposed DS-AMC-OFDM systems. The average throughput values in terms of different SNR ranges are evaluated based on (2.45). It is important to note that the throughput of Proposed DS-AMC-OFDM system outperforms the Proposed FS-AMC-OFDM scheme by 1-7 Mbps over an SNR range of 5-30 dB. At the same time, the Proposed FS-AMC-OFDM system can achieve 5-15 Mbps gains over the Conventional FS-AMC-OFDM scheme across the same SNR range. The improvement in the performance of the proposed dynamic sub-channel allocation strategy over the fixed strategy is the result of increasing the transmitted data size achieved by applying the pilot adjustment scheme. The pilots number is reduced for the stable sub-channel profiles individually, followed by replacing the unused pilot symbols with additional data symbols based on (2.17)-(2.19). On the other hand, the throughput improvement of the Proposed FS-AMC-OFDM and DS-AMC-OFDM schemes in comparison with the conventional AMC method is due to the optimal MCS selection for each sub-channel. It is observed that the obtained performance of the Proposed FS-AMC-OFDM and Conventional FS-AMC-OFDM based on convolutional coding method is less than the same systems

with the LDPC approach, shown in Fig. 2.10. This is due to the behaviour of the LDPC method that can efficiently reduce the number of error bits at low SNR values in comparison with the convolutional approach.

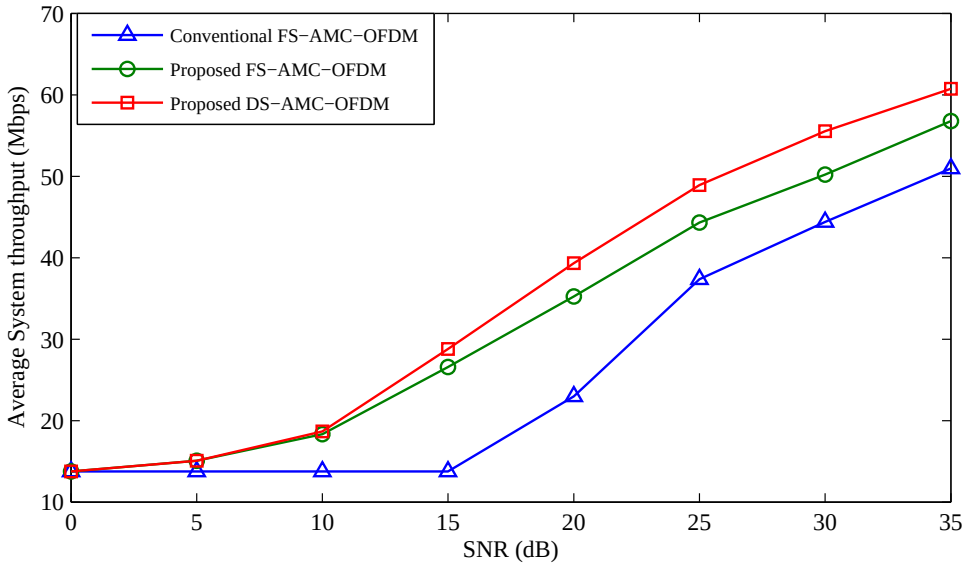

Figure 2.13: Average system throughput for the fixed and dynamic sub-channelling based conventional and proposed convolutional-AMC-OFDM systems.

The throughput outage probability, which is computed based on (2.46), of the investigated systems is illustrated in Fig. 2.14. From this figure, the superior performance of the Proposed FS-AMC-OFDM and DS-AMC-OFDM systems among the conventional method is shown clearly. In contrast, these two systems achieve almost the same performance over different SNR values, which means that both approaches can be close to the related upper bound performance with the increase in the SNR.

Fig. 2.15 illustrates the difference in the channel estimation MSE between the Proposed FS-AMC-OFDM and DS-AMC-OFDM approaches. The figure shows that the reduction in the number of pilots for the sub-channels with stable profile affects the estimation accuracy after 10 dB, in which the second level constraint as defined by (2.22) has not been exceeded. However, the degradation in terms of data recovery errors is acceptable, and hence the performance of the proposed system in terms of average system throughput is improved significantly for the SNR values above 10 dB in comparison with the conventional approaches as demonstrated in Fig. 2.13. Based on Fig. 2.15, the channel estimation error increases gradually after 10 dB for the Proposed DS-AMC-OFDMA system with respect to the FS-AMC-OFDMA scheme. However, since the pilot reduction is additionally constrained by (2.22), the

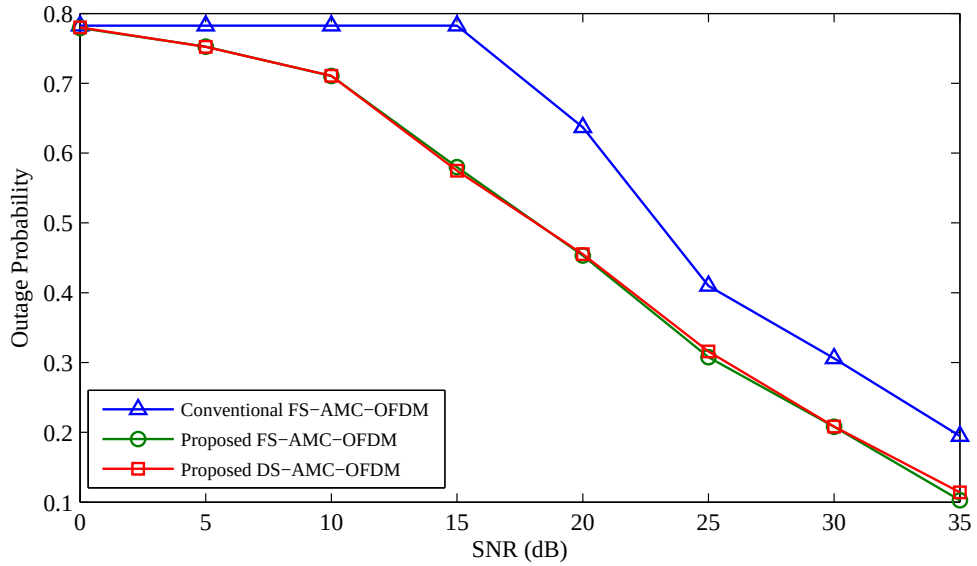

Figure 2.14: Outage probability for the fixed and dynamic sub-channelling based conventional and proposed convolutional-AMC-OFDM systems.

channel estimation error can be arbitrarily controlled.

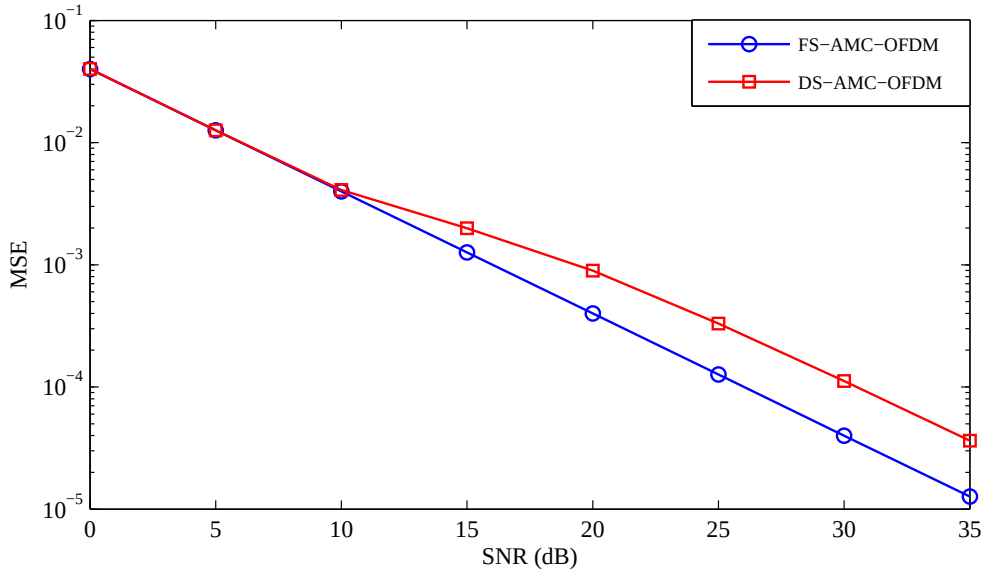

Figure 2.15: MSE for the conventional and proposed dynamic sub-channelling based convolutional-AMC-OFDM systems.

The statistical evaluations in terms of the usage probability of the convolutional based MCS options for the investigated systems is presented in Fig. 2.16. This figure consider the MCS selection ratio for SNR values of 5, 15, 25 and 35 dB in order to cover the behaviour of the considered systems over low and high SNR ranges. It is important to note that the performance of the proposed systems is identical in most cases except in SNR of 15 dB due to wide SNR threshold range of each MCS option.

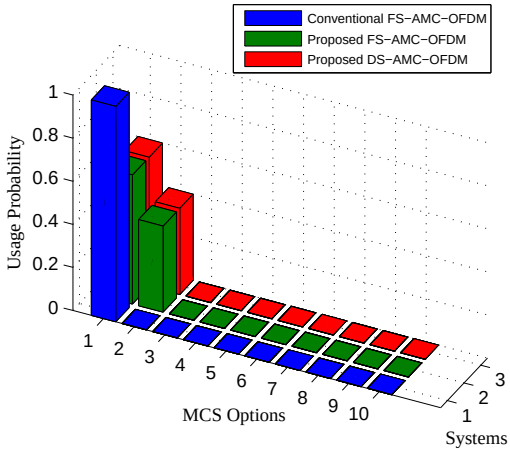

(a) SNR=5 dB.

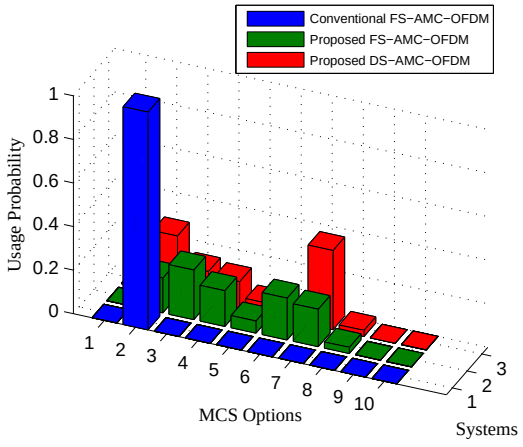

(b) SNR=15 dB.

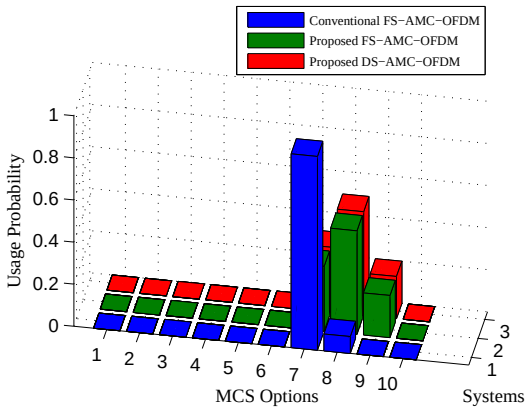

(c) SNR=25 dB.

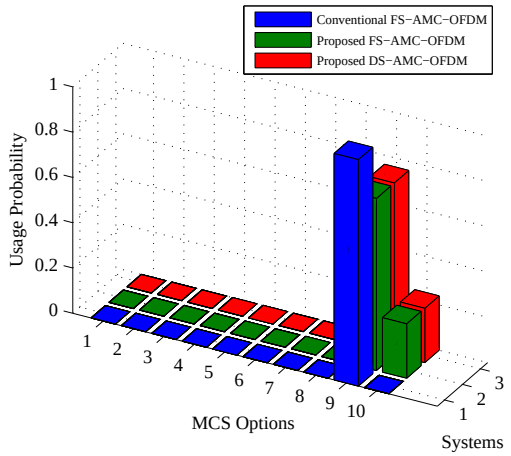

(d) SNR=35 dB.

Figure 2.16: Usage probability of the utilised MCS options for the the fixed and dynamic sub-channelling based conventional and proposed convolutional-AMC-OFDM.

It is also observed that the selection of higher MCS options is less than the LDPC based schemes as these options require more SNR threshold values to be addressed.

2.6.3 Convolutional Based AMC-OFDMA System

The simulation results for the OFDMA systems based on the proposed and conventional methods is introduced in this sub-Section. The simulation model is adopted from the Mobile WiMAX IEEE 802.16e standard with the parameters listed in Table 2.1. Additionally, the simulation results are obtained for 30 users i.e. $K = 30$ over three users scenarios, which adopt the considered three ITU channel profiles

expressed by Table 2.4. Three schemes are considered for comparison as follows:

1. Conventional FS-AMC-OFDMA, which adopts the same MCS for the entire OFDMA frame with a full-use of pilots [19].

2. Proposed FS-AMC-OFDMA that considers different MCS for each sub-channel based on Table 2.3 with the full-use of the pilots.

3. Proposed DS-AMC-OFDMA system that employs the AMC strategy associated with the proposed pilot adjustment scheme and selects the suitable MCS for each sub-channel depending on Table 2.3.

Fig. 2.17 shows the throughput comparison between the investigated approaches. This throughput is computed based on (2.45). It is observed that the throughput performance of the Proposed DS-AMC-OFDMA scheme exhibits gains between 2-30 Mbps over the proposed FS-AMC-OFDMA and Conventional FS-AMC-OFDMA systems for the considered SNR range. In addition, the Proposed FS-AMC-OFDMA scheme outperforms the conventional approach by 2-20 Mbps over the same SNR range. It is noting that the Proposed DS-AMC-OFDMA exploits the diversity of the channels conditions of distinct users more than other approaches. Furthermore, the replacement of redundant pilots by additional data sub-carrier across the OFDMA frame produces a significant improvement in the system throughput.

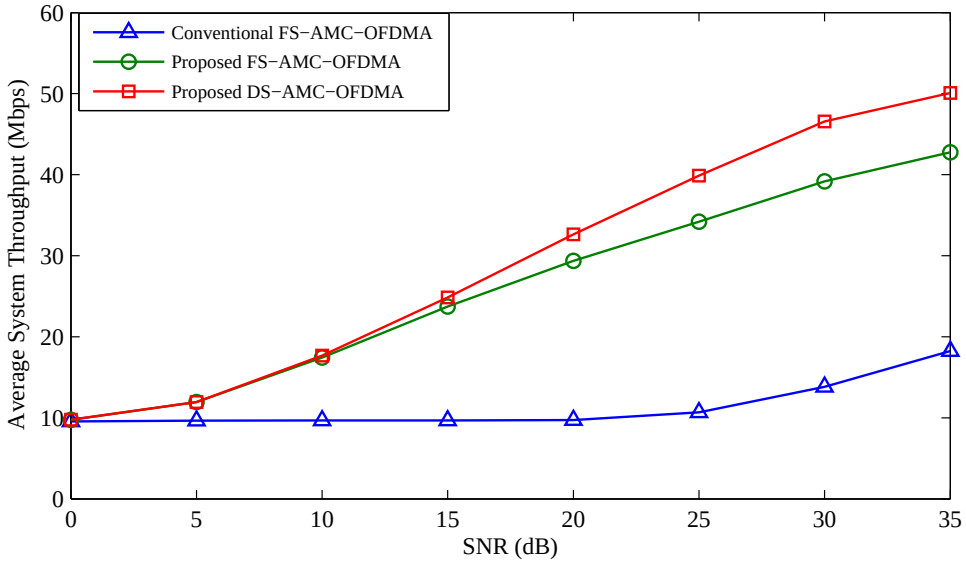

Figure 2.17: Average system throughput for the fixed and dynamic sub-channelling based conventional and proposed convolutional-AMC-OFDMA systems.

In contrast, the average throughput outage probability, evaluated using (2.46), of the three considered systems is demonstrated in Fig. 2.18. This figure shows that the throughput outage probability of the Proposed FS-AMC-OFDMA and DS-AMC-OFDMA systems is significantly less than the conventional approach. This is the results of the high flexibility of MCS selection and the multiuser diversity exploiting.

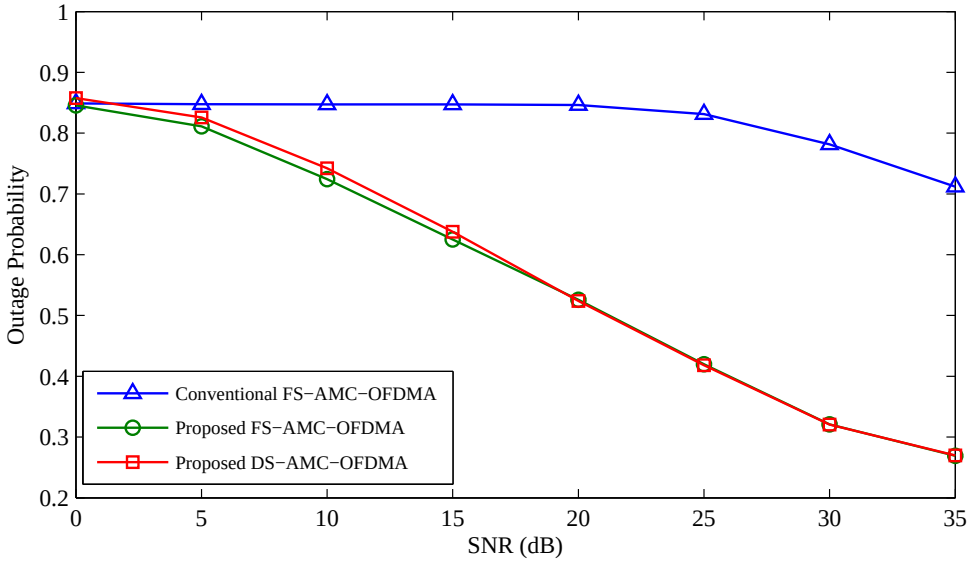

Figure 2.18: Outage probability of the fixed and dynamic sub-channelling based conventional and proposed convolutional-AMC-OFDMA systems.

Fig. 2.19 investigates the effect of the number of users on the average system throughput performance of the considered systems at SNR value of 20 dB. It is shown that the performance of the investigated systems is increased accordingly with the number of users, while the same performance is achieved after 30 users due to the user diversity saturation. This diversity allows the systems to select higher MCS options for distinct users in the same transmitted OFDMA frame. The selection of different MCSs within the same frame can increase the average system throughput. Additionally, it should be noted that the Proposed DS-AMC-OFDMA system outperforms the other systems for distinct number of users since the employed pilot adjustment algorithm increases the number of data sub-carriers exploiting the rich diversity of multi-user environments.

Fig. 2.20 shows the evaluated usage probability of the considered convolutional based MCS options in terms of the three investigated systems. It is observed from this figure that the multiuser channel diversity has been exploited efficiently by the

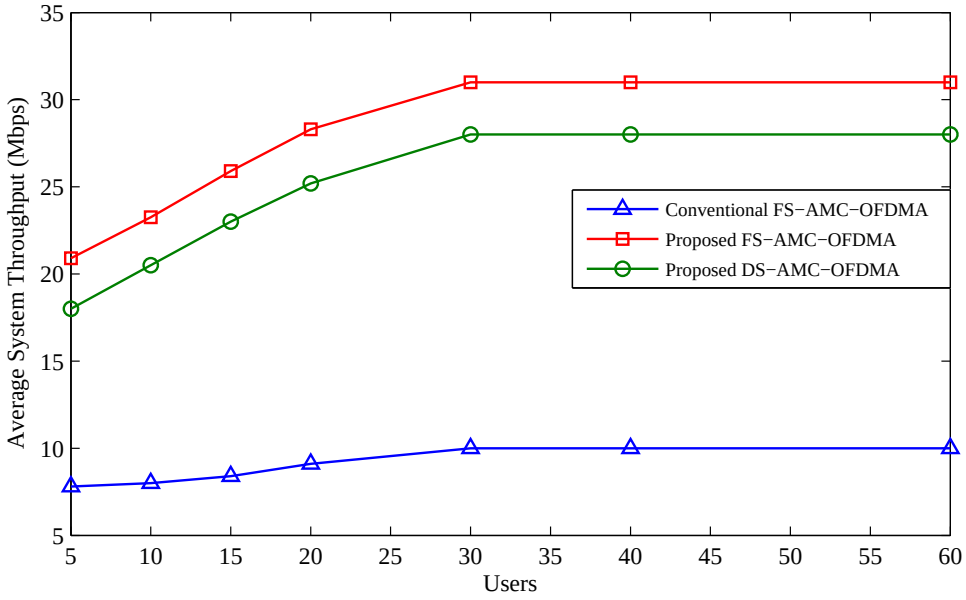

Figure 2.19: Average system throughput vs. users for the fixed and dynamic sub-channelling based conventional and proposed convolutional-AMC-OFDMA systems.

proposed systems in comparison with the conventional approach. In addition, Fig. 2.20(a) illustrates that these systems are able to select the medium levels of the MCSs even for low SNR value of 5 dB. At the same time, the higher MCS options are mostly selected in the SNR value of 35 dB as shown in Fig. 2.20(d).

2.7 Chapter Summary

This Chapter presented the proposed AMC strategy for fixed and dynamic sub-channelling based single and multi-user downlink OFDM systems. The proposed strategy was designed based on the developed software engineering life cycle model, presented in this Chapter. The division of the transmitted OFDM frames into sub-channels depending on the measured frequency coherence bandwidth for fixed sub-channelling single user OFDM system was introduced. Moreover, each sub-channel exhibited the same number of pilot and data sub-carriers. The selection of the optimal MCS for each sub-channel was based on the related SNR value, which has been selected to be the minimum over the involved sub-carriers. In addition, the presented AMC strategy employed two MCS scenarios. The first scenario used the modulation types of QPSK 16-QAM and 64-QAM combined with three LDPC coding rates of 1/2, 2/3 and 3/4, while the second utilised the same modulation types associated with convolutional coding rates of 1/2. 2/3 and 3/4. In contrast, the

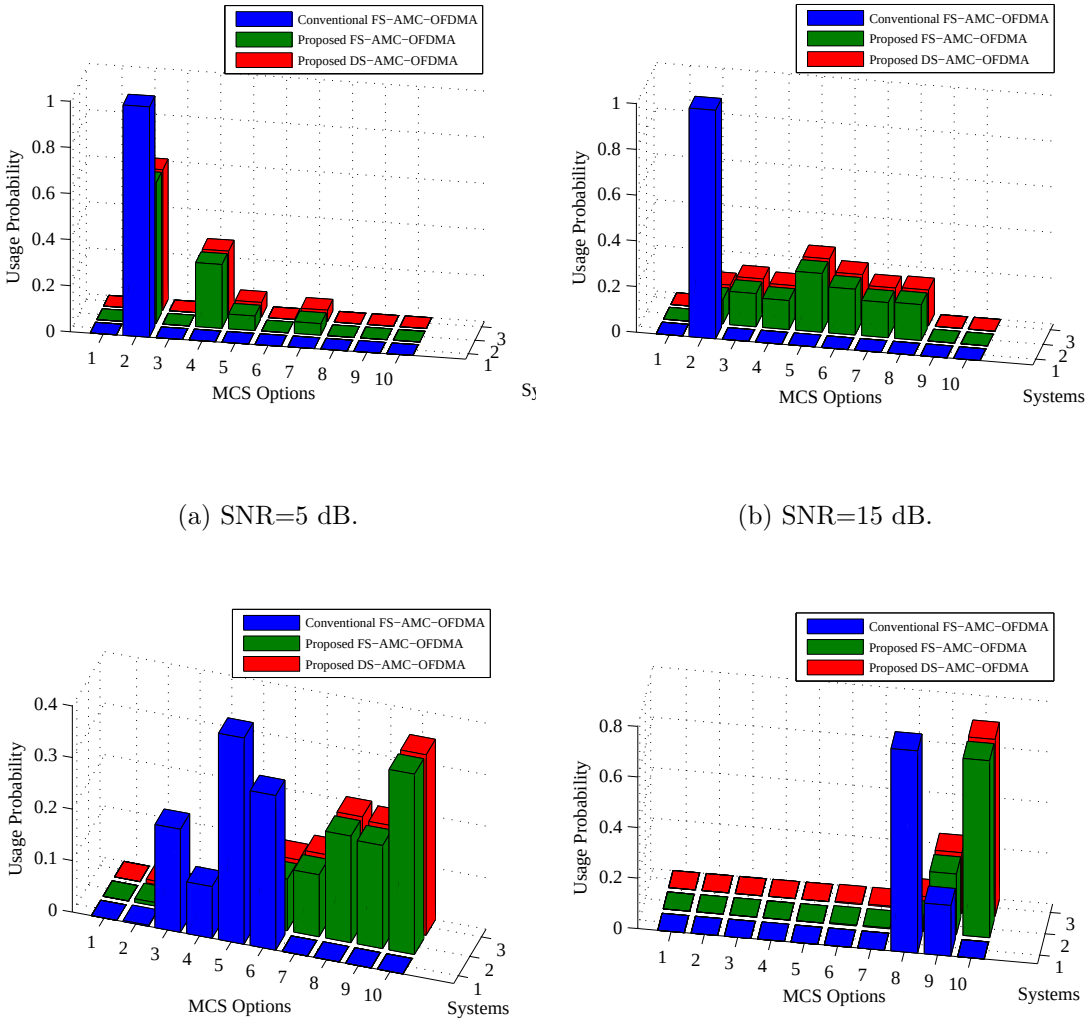

(a) SNR=5 dB.

(b) SNR=15 dB.

(c) SNR=25 dB.

(d) SNR=35 dB.

Figure 2.20: Usage probability of the utilised MCS options for the fixed and dynamic sub-channelling based conventional and proposed convolutional-AMC-OFDMA systems.

dynamic sub-channelling AMC strategy based on a novel pilot adjustment scheme for OFDM was provided. This technique reduced the number of used pilots for channel estimation depending on the measured frequency coherence bandwidth, SNR and the variance of the SNR fluctuation values of each sub-channel, individually. The reduced pilots were replaced with additional data sub-carriers in order to increase the performance of the entitled system in terms of throughput. The fixed and dynamic sub-channelling approaches of the proposed AMC strategy have been expanded to work with the multiuser OFDM systems, called OFDMA. It is important to note that the information of the optimal selection of MCS for each sub-channel and the number of the required pilots was fedback to the transmitter from the receiver through the feedback CSI. The CSI feedback overhead analysis for both OFDM and OFDMA systems was included in this Chapter. The simulation results showed the superior performance of the proposed strategies over the related conventional approaches.

Chapter 3

Resource Allocation Software Algorithms for SISO-AMC-OFDMA systems

The cross-layer resource allocation strategies have been efficiently considered by the research work after 1990s. The term resource includes the available users, transmission power and information bit streams that are distributed optimally, in which the related system constraints and channel conditions can be satisfied. As mentioned earlier, the using of the AMC technology by the OFDMA systems can improve the performance, yet the available channel capacity is not exploited effectively. Therefore, the resource allocation strategies are adopted in order to enhance the performance of the investigated systems in terms of channel capacity, BER, spectral efficiency and throughput. In this Chapter, an improvement in the average system throughput is achieved by proposing a novel cross-layer resource allocation strategy for single-cell downlink SISO based AMC-OFDMA systems. This strategy has been designed based on a developed software engineering life cycle model in order provide it with high scalability, extendibility and portability. The proposed resource allocation strategy can be called as user, bit and power allocation (UBPA). The objective of the UBPA strategy is to maximise the average system throughput by assigning the available users, information bits, and the total transmission power of a base station over the sub-channels, in which the power constraints and the channel conditions are satisfied. The average system throughput is presented as a function of the spectral efficiency and BER for different MCSs within the same transmit-

ted OFDMA frame. Additionally, the approximated BER values for the employed MCS options are evaluated as a function of SNR instead of considering the uncoded adaptive modulation approach presented in [89]. This strategy adopts the presented AMC method and pilot adjustment scheme explained in Chapter 2 and the convolutional coding based MCS scenario. UBPA considers a throughput maximisation problem that has been solved by two approaches. Firstly, the optimised approach that tackles the problem as a one piece with high computational complexity. Secondly, the decoupled approach that divides the complex problem into sub-problems and then solves each of which individually. This approach allocates the available resources with low computational complexity in expense of performance.

It is important to note that the proposed cross-layer resource allocation strategy motivates from the related literatures of [38]-[68] by the following aspects. 1) This strategy aims to maximise the system throughput. Additionally, the throughput maximisation is expressed by a new convex optimisation problem as a function of spectral efficiency and BER subject to power and fair user allocation constraints, whilst most of [38]-[68] research tackled the capacity and power issues. 2) The transmitted OFDMA frame exhibits different MCS options assigned to distinct users using the presented AMC technology in Chapter 2. In contrast, the work in literature so far adopted adaptive modulation without or with fixed error correction coding rate over all the sub-carriers within the same frame. In this work the coding rate is changed for each sub-channel included in the same transmitted OFDMA frame depending on the related channel conditions and resource constraints. 3) The introduced pilot adjustment scheme in Chapter 2 is also considered in order to improve the throughput performance. 4) The proposed strategy is structured based on a developed life cycle model, which is established on the cyclic type of software engineering methodology.

3.1 Developed Life Cycle Model for Resource Allocation Algorithm

A developed evolutionary methodology life cycle model is adopted in the design of the proposed resource allocation strategy [17], [18]. This methodology model is selected as the proposed strategy allocates the available resources in an iterative

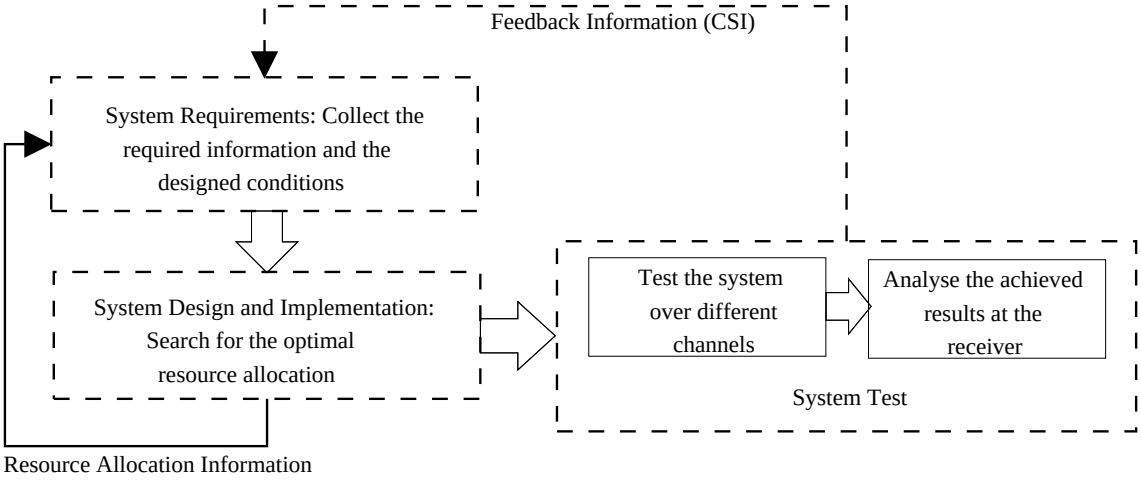

Figure 3.1: Developed life cycle model for the proposed resource allocation algorithm.

way depending on different input variables, such as CSI, transmission power and number of users.

Fig. 3.1 illustrates the developed life cycle model of proposed resource allocation algorithm, that includes three parts. Firstly, *system requirements* that collect the required information of the available resources, CSI, number of users,..., etc. In addition, the requirements for designing a scheme that can satisfy the conditions are also assembled in this part. Secondly, *system design and implementation*, which searches over each transmitted OFDMA frame for the optimal user allocation as well as assigning the suitable power value and MCS option for each user. This is carried out by following an iterative method that is continued until the optimal allocation of the resources is achieved. Finally, system test that exams the implemented system over different channel conditions to verify the validity of such system.

3.2 SISO-AMC-OFDMA System Model

A Mobile WiMAX IEEE 802.16e system with the parameters shown in Table 2.1 is considered. Additionally, the total transmission power is 50 W [92]. The downlink transmission is based on a wireless OFDMA system from a BS to a number of available users, K, which are allocated into M distinct sub-channels, in which there is one user per sub-channel. The pilot and data sub-carriers are initially distributed over the sub-channels equally in a range of $\xi_{p_k}(m) = N_p/M$ and $\xi_{d_k}(m) = N_d/M$ respectively for each sub-channel, where $m = 1, ..., M$ is the sub-channel index and $k = 1, ..., K$, denotes the user index. The assignment of each user to the same

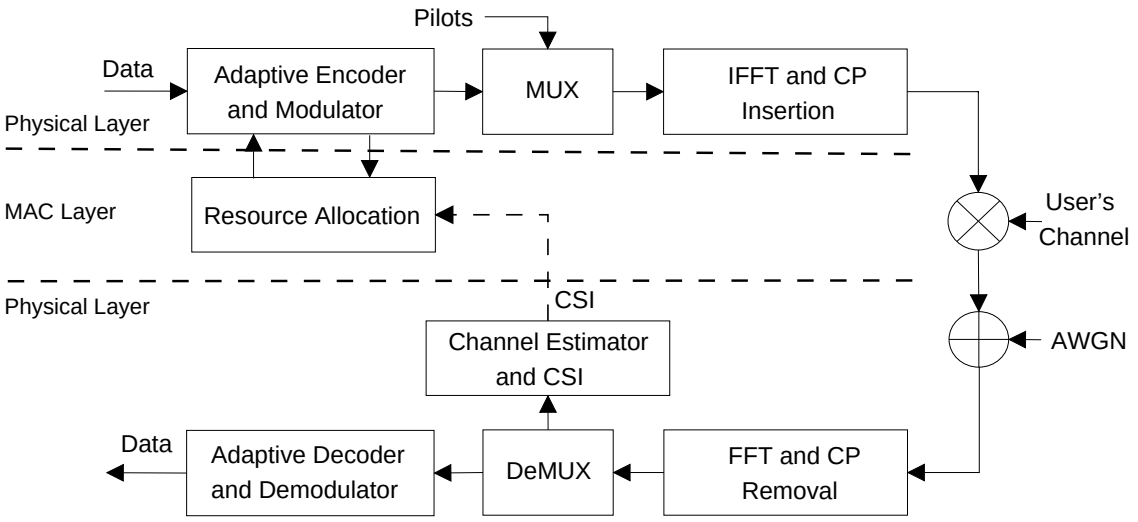

Figure 3.2: Block diagram of the proposed resource allocation strategy for SISO-AMC-OFDMA system.

number of sub-carriers, i.e. sub-channel, can guarantee fair services [67], [70]. It is assumed that there are no interference effects from the neighbouring BSs, i.e. single cell system.

At the physical layer, the function of the first block of the transmitter, shown in Fig. 3.2, is to divide the data of users into groups according to the number of data sub-carriers, $\xi_{d_k}(m)$, within each sub-channel assigned to a user. Subsequently, these groups are encoded and modulated based on the selected MCS options. At the MAC layer, the *Resource Allocation* block implements the proposed UBPA strategy based on the channel conditions of the considered users and the total transmission power. It is important to highlight that the resource allocation information is fed forward to the receivers of the individual users using the downlink control signals [67]. The *MUX* block of the Physical layer mixes the generated pilots with the coded and modulated symbols using the comb-method. The last block of the transmitter implements the IFFT and CP insertion operations.

To test the transmission reliability for the multipath fading channels of the proposed system, the ITU channel profiles expressed in Table 2.4 are considered in this work to present different user categories [102]. The average power values of the channel paths, P_{l_k}, of each user are assumed to be constant across the transmitted OFDMA frame, and are scaled so that $E\{|H_k(n)|^2\} = \sum_{l_k=o}^{L_k-1} P_{l_k} = 1$ [10], where $H_k(n)$ is the frequency response of the simulated channel, L_k refers to the number of paths for each user and $n = 0, ..., N_{FFT} - 1$ denotes the frequency domain index.

At the physical layer of the receiver of each user, the *DeMUX* block shown in Fig.

3.2, extracts the pilots from the assigned sub-channels of the OFDMA frame and feeds them into *Channel Estimator and CSI* block. The latest block estimates the related channel coefficients and implements the proposed pilot adjustment method. These channel coefficients are estimated based on the corresponding pilots by employing a LS method as [10]

$$\hat{H}_{k_p}(m, z_p) = \frac{Y_{k_p}(m, z_p)}{X_{k_p}(m, z_p)}, \tag{3.1}$$

where $X_{k_p}(m, z_p)$, $Y_{k_p}(m, z_p)$ and $z_p \in \{1, \ldots, \xi_{p_k}(m)\}$ represent the transmitted pilots, received pilots and their index of each sub-channel assigned to a user, respectively. The channel coefficients that correspond to the data sub-carriers within m-th sub-channel, $\hat{H}_{k_d}(m, z_d)$, are obtained by implementing 1st order linear interpolation, where $z_d \in \{1, \ldots, \xi_{d_k}(m)\}$ is the index of data sub-carriers of such sub-channel. The channel estimation error, which is caused by the channel estimation and the feedback CSI delay, is considered as additional noise. Thus the received signal in terms of z-th data sub-carriers in the m-th sub-channel assigned to the k-th user can be written in terms of transmitted data sub-carriers, $X_{k,d}(m, z_d)$, the related real and estimated channel coefficients, $H_{k,d}(m, z_d)$, $\hat{H}_{k,d}(m, z_d)$, and the AWGN samples, $W_{k,d}(m, z_d)$, as

$$\begin{aligned} Y_{k_d}(m, z_d) =& X_{k,d}(m, z_d)\hat{H}_{k,d}(m, z_d) \\ &+ X_{k,d}(m, z_d)[H_{k,d}(m, z_d) - \hat{H}_{k,d}(m, z_d)] + W_{k,d}(m, z_d). \end{aligned} \tag{3.2}$$

Therefore, the SNR value of each data sub-carrier for the distinct sub-channels in terms of the channel estimation error is evaluated as a function of sub-carrier power, $P_{s_k}(m)$, estimated channel values, $\hat{H}_{k,d}(m, z_d)$, the variance of square error of the related estimated channel, $\sigma^2_{d,k}(m)$, and the variance of AWGN samples, $\sigma^2_{W_{k,d}(m,z_d)}(m)$, as

$$\gamma_k(m, z_d) = P_{s_k}(m)\frac{|\hat{H}_{k,d}(m, z_d)|^2}{\sigma^2_{d,k}(m)P_{s_k}(m) + \sigma^2_{W_{k,d}(m,z_d)}(m)}, \tag{3.3}$$

In addition, the minimum SNR of each sub-channel is selected to guarantee that the required performance is maintained for each user as

$$\gamma^{*}_{k,\min}(m) = \mu_k(m)\gamma_{k,\min}(m), \tag{3.4a}$$

$$= \mu_k(m)\min\{\gamma_k(m, z_d)\},\ k = 1, \ldots, K, \tag{3.4b}$$

where $\mu_k(m)$ adjusts the required power value for m-th sub-channel assigned to k-th user and its initial value is determined in terms of equal power distribution as $\mu_k(m) = \frac{P_T}{M\xi_{d_k}(m)P_{s_k}(m)}$, where P_T is the total considered power for a BS. The estimated channel coefficients that correspond to data sub-carriers are fed to the final block, which is *Adaptive Decoder and Demodulator*. In this block, the received data symbols are demodulated according to the known selected MCS at the transmitter utilising soft ML demapper [4], [5], [93]. Finally, the data is decoded for each sub-channel, which is assigned to a user, using soft Viterbi decoder [90].

The multiuser channel diversity, which realises the resource allocation, is expected to improve the average system throughput, ψ_{av}, evaluated by computing the average value of the throughput of N_{fr} transmitted OFDMA frames, ψ_g, where $g = 1, ..., N_{fr}$ is the frame index. This enhancement is the results of increasing the average spectral efficiency, $\rho_{av_k}(m) = R_{c_k}(m)\log_2[M_k(m)]$, expressed by (bps/Hz) as a function of the selected coding rate, $R_{c_k}(m) \in \{1/2, 2/3, 3/4\}$, and the modulation order, $M_k(m) \in \{0, 4, 16, 64\}$.

The system throughput for each OFDMA symbol can be mathematically expressed as

$$\psi_g = \sum_{k=1}^{K}\sum_{m=1}^{M} \varphi(k, m)\xi_{d_k}(m)\rho_{av_k}(m)[1 - P_{e_k}(m)], \tag{3.5}$$

where $P_{e_k}(m)$ denotes the approximated BER of each sub-channel, $\varphi(k, m)$ denotes the user allocation matrix, which guarantees fairness in user allocation over the OFDMA frame with dimensions of $K \times M$ [70]. Additionally, the reduction of $P_{e_k}(m)$ based on the selection of the suitable MCS option for each sub-channel leads to an increase in the system throughput, as shown in (3.5). The evaluation of the approximated BER values for different sub-channels assign to distinct users is illustrated in the next Section.

3.3 Approximated BER Evaluation

The BER of each sub-channel is formulated as a function of the minimum sub-channel SNR value, $\gamma^*_{k,\min}(m)$. In order to evaluate the BER for each sub-channel, the users are assumed to be assigned to the considered sub-channels sequentially, while the bit and power are allocated equally.

The approximated BER evaluation is based on the simulation performance of the utilised MCSs, whilst most of the published work so far has considered the upper expected bound of the BER [10], [90], [98]. In order to obtain the suggested BER mathematical expression, the approximated formula for the BER of [89]

$$P_{e_k}(m) = c_{1_k}(m) \exp[-c_{2_k}(m)\gamma^*_{k,\min}(m)], \tag{3.6}$$

has been adopted, where $c_{1_k}(m)$ and $c_{2_k}(m)$ are selected variables for fitting the theoretical BER to practical values for all employed MCS options. The fitting accuracy for these options depends on the proper evaluation of these variables. It can be noted that the BER, expressed by (3.6), is a function of $\gamma^*_{k,\min}(m)$, which is based on $\mu_k(m)$ of each channel. Thus, the evaluated $\mu_k(m)$ affects the BER value of the m-th sub-channel and the throughput function expressed by (3.5). It is important to note that the presented method of the approximated BER evaluation is different from the approach presented in [89] by considering numerous modulation types combined with different convolutional coding rates amongst distinct SNR intervals.

In this work, the value of the $c_{1_k}(m)$ is assumed to be a constant equal to 0.5, whilst the value of $c_{2_k}(m)$ is evaluated based on (3.6) as

$$\ln[P_{e_k}(m)] = \ln[c_{1_k}(m) \exp\{-c_{2_k}(m)\gamma^*_{k,\min}(m)\}], \tag{3.7a}$$

$$= \ln[c_{1_k}(m)] + \ln\{\exp[-c_{2_k}(m)\gamma^*_{k,\min}(m)]\}, \tag{3.7b}$$

$$= \ln[c_{1_k}(m)] - [c_{2_k}(m)\gamma^*_{k,\min}(m)]. \tag{3.7c}$$

From (3.7), $c_{2_k}(m)$ can be evaluated as

$$c_{2_k}(m) = \frac{\ln[c_{1_k}(m)] - \ln[P_{e_k}(m)]}{\gamma^*_{k,\min}(m)}. \tag{3.8}$$

Table 3.1: Approximated values of the $c_{2_k}(m)$ vs. SNR for QPSK and 16-QAM based MCS options

		QPSK			16-QAM		
	$\gamma_{k,\min}(m)$	1/2	2/3	3/4	1/2	2/3	3/4
$c_{2_k}(m)$	< 2	0.911	0.492	0.135	0.494	0.0910	0.094
	$[2, 4)$	0.859	0.707	0.334	0.476	0.164	0.169
	$[4, 6)$	0.927	0.844	0.491	0.476	0.223	0.176
	$[6, 8)$	1.600	1.023	0.706	0.578	0.336	0.204
	$[8, 10)$	1.540	1.082	0.729	0.642	0.451	0.277
	$[10, 12)$	1.322	0.968	0.701	0.609	0.471	0.304
	$[12, 14)$	-	0.778	0.581	0.503	0.419	0.284
	$[14, 16)$	-	595	0.476	0.397	0.339	0.236
	$[16, 18)$	-	-	0.380	0.300	0.271	0.179
	$[18, 20)$	-	-	-	-	0.210	0.140
	≥ 20	-	-	-	-	0.154	0.105

For example, the simulated BER values of different SNR values for each MCS based on modulation types of QPSK and 16-QAM over frequency selective Rayleigh fading channel of [98] are considered to obtain the related $c_{2_k}(m)$ values according to (3.8). Thus, the evaluated $c_{2_k}(m)$ values for the considered MCS options are listed in Table 3.1.

Based on the $c_{1_k}(m)$ and $c_{2_k}(m)$ values and (3.6), the theoretical BER values as a function of the average SNR for different MCSs in terms of QPSK and 16-QAM modulation types are evaluated and compared with the relevant simulated plots as shown in Fig. 3.3. From these figures, it is observed that the theoretical BER plots are almost identical to the relevant simulated curves particularly for high SNR values. Moreover, the slopes of these plots are in agreement with related published work in [98]. It is worth pointing out that these results do not exceeded the upper bounds of the the underlying MCSs in all cases [10], [90], [98].

3.4 Dynamic Sub-Channelling for SISO-AMC-OFDMA

At the physical layer of the receiver, the *Channel Estimator and CSI* block achieves the optimal number of the required pilots for an efficient channel estimation using the

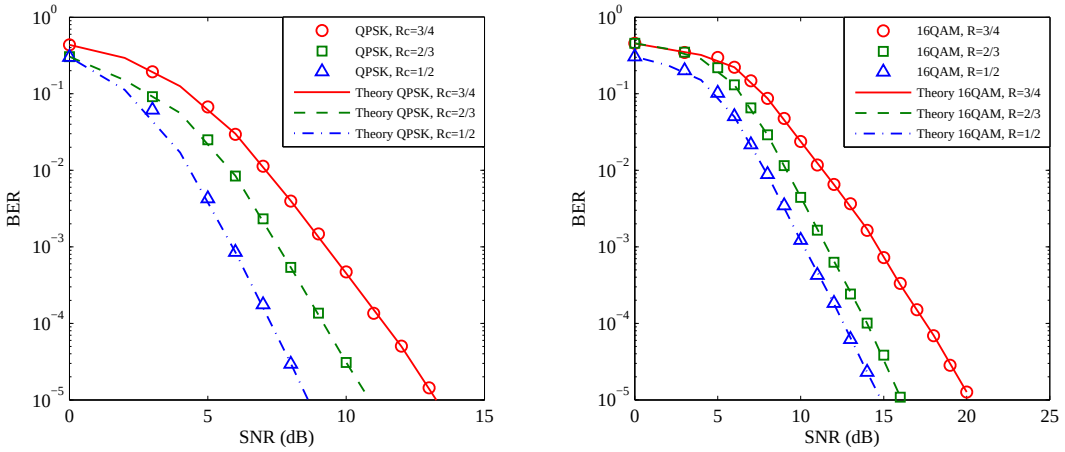

(a) QPSK. (b) 16-QAM.

Figure 3.3: Practical and theoretical BER for different QPSK and 16-QAM based MCSs over Rayleigh fading channel.

proposed pilot adjustment scheme. The same concepts of dynamic sub-channelling explained in Chapter 2 are considered for the investigated SISO-AMC-OFDMA system. Moreover, the presented pilot adjustment scheme has been combined with the proposed resource allocation strategy. The reduction value of required pilots for each user, $\Pi_k(m)$, assigned to a sub-channel is formulated as a function of frequency coherence bandwidth, $B_{k,coh}$, SNR , $\gamma_{k,\min}(m)$, and the variance of SNR fluctuation, $\sigma^2_{k,\Xi_k(m,z)}(m)$ as expressed by (2.33).

It should be noted that the refined number of data and pilot sub-carriers, $\delta_{d_k}(m)$ and $\delta_{d_k}(m)$, respectively are adopted throughout this Chapter.

3.5 Feedback CSI Analysis for SISO-AMC-OFDMA

The information regarding the minimum SNR values and the number of required pilots for each user that can be referred to as feedback CSI is sent to the BS, i.e. the transmitter, after each transmitted OFDMA frame using a TDD uplink in order to overcome the problem of outdated CSI. The feedback CSI is received by the BS with a delay of $T_{k,CSI}(m)$ seconds. In this work, it is assumed that the channel is remaining constant for more than $T_{k,CSI}(m)$. The feedback delay, $T_{k,CSI}(m)$, for the m-th sub-channel of the user $k \in \{1, ..., K\}$ can be computed following (2.29).

The feedback CSI is covered by sending $N_{B,CSI}^{(k)}(m) \approx \{\log_2[\varepsilon_k(m)] + \log_2[\nu_k(m)]\}$ bits, where $\varepsilon_k(m)$ and $\nu_k(m)$ designate the full range of possible SNR values and the number of required pilots respectively. The total effective channel bandwidth, B_{eff}, available for the downlink transmission of all users is evaluated based on (2.44).

3.6 Proposed UBPA Strategy for SISO-AMC-OFDMA

The proposed UBPA distributes the users, total transmission power and information data bits amongst the sub-channels, according to the channel conditions and the power constraints, in order to maximise the average system throughput. As mentioned earlier, this strategy solves a throughput maximisation problem that can be mathematically outlined as

$$\text{Maximise} \quad \psi_g = \sum_{k=1}^{K}\sum_{m=1}^{M} \varphi(k,m)\delta_{d_k}(m)\rho_{av_k}(m)[1 - P_{e_k}(m)], \tag{3.9}$$

subject to :

$$\sum_{k=1}^{K}\sum_{m=1}^{M} \varphi(k,m)\mu_k(m)P_{sc_k}(m) = P_T, \tag{3.10}$$

$$\mu_k(m) \geq 0, \tag{3.11}$$

$$\sum_{k=1}^{K} \varphi(k,m) = 1, \quad m = 1, ..., M, \tag{3.12}$$

$$\sum_{m=1}^{M} \varphi(k,m) = 1, \quad k = 1, ..., K, \tag{3.13}$$

where (3.10) and (3.11) refer to the total power constraints, whilst (3.12) and (3.13) are the users distribution fairness constraints, which guarantee the allocation of one user for each sub-channel following [70]. Moreover, $P_{sc_k}(m) = \delta_{d_k}(m)P_{s_k}(m)$ denotes the sub-channel power as a function of $P_{s_k}(m)$. The term $\mu_k(m)$ refines the power value assigned to each sub-channel as $P^*_{sc_k}(m) = \mu_k(m)P_{sc_k}(m) = \mu_k(m)\delta_{d_k}(m)P_{s_k}(m)$. It is important to note that the constraint of (3.13) controls the number of sub-channels allocated to k-th user. In order to increase the number of the assigned sub-channel to a user, $N_{u_{max}}$, the constraint of (3.13) can be changed to be $\sum_{m=1}^{M} \varphi(k,m) =$

$N_{u_{max}}$. Based on (3.6), the BER of each sub-channel is formulated as a function of $\gamma^*_{k,\min}(m)$. Thus, the evaluated $\mu_k(m)$ affects the BER value of each sub-channel and the objective function expressed by (3.9).

The considered problem expressed in (3.9)-(3.13) have been solved by two approaches utilising the Lagrange multipliers method as follows.

3.6.1 Optimised Approach

The optimised solution of the proposed problem is computed using the Lagrange multipliers optimisation method and the Karush-Kuhn-Tuker (KKT) conditions [62], [104]. In order to formulate the considered problem expressed in (3.9)-(3.13) as a convex optimisation problem that satisfies the Hessian conditions [62], the BER equation of (3.6) can be rewritten as

$$P^*_{e_k}(m) = c_{1_k}(m)\exp[\frac{-\varphi(k,m)c_{2_k}(m)\mu_k(m)\gamma_{k,\min}(m)}{\varphi(k,m)}], \tag{3.14}$$

where $P^*_{e_k}(m) = P_{e_k}(m)$ for all sub-channels that are allocated to distinct users. Thus, the Lagrangian function of the problem expressed in (3.9)-(3.13) is formulated as

$$\begin{aligned} L\Big[\varphi(k,m),\mu_k(m)\Big] =& \sum_{k=1}^{K}\sum_{m=1}^{M}\varphi(k,m)\delta_{d_k}(m)\rho_{av_k}(m) \\ &- \sum_{k=1}^{K}\sum_{m=1}^{M}\big\{\varphi(k,m)\delta_{d_k}(m)\rho_{av_k}(m)c_{1_k}(m) \\ &\cdot\exp[\frac{-\varphi(k,m)c_{2_k}(m)\mu_k(m)\gamma_{k,\min}(m)}{\varphi(k,m)}]\big\} \\ &- \Omega\big[\sum_{k=1}^{K}\sum_{m=1}^{M}\varphi(k,m)\mu_k(m)P_{sc_k}(m) - P_T\big] \\ &- \sum_{k=1}^{K}\eta_m(k)\big[\sum_{m=1}^{M}\varphi(k,m)-1\big] - \sum_{m=1}^{M}\eta_k(m)\big[\sum_{k=1}^{K}\varphi(k,m)-1\big] \end{aligned} \tag{3.15}$$

where Ω, $\eta_k(m)$ and $\eta_m(k)$ are the Lagrange multipliers. It should be noted that the optimal allocation of the k-th user over the m-th sub-channel, expressed by the matrix element of $\varphi(k,m)$, can be achieved within the relaxed continuous domain of the closed interval $[0,1]$ corresponding to each user over M sub-channels. To solve

this problem, the following steps are considered. The first step is done by evaluating a partial derivative of (3.15) in terms of $\varphi(k,m)$ as

$$\begin{aligned}\frac{\partial L\Big[\varphi(k,m),\mu_k(m)\Big]}{\partial\varphi(k,m)} =&\Gamma_A(k,m) - \Bigg[\Big(\varphi(k,m)\Gamma_A(k,m)c_{1_k}(m)\\ &\cdot\exp\{\frac{-\varphi(k,m)c_{2_k}(m)\mu_k(m)\gamma_{k,\min}(m)}{\varphi(k,m)}\}\\ &\cdot\{\frac{-\varphi(k,m)c_{2_k}(m)\mu_k(m)\gamma_{k,\min}(m)}{\varphi(k,m)^2}\\ &+\frac{\varphi(k,m)c_{2_k}(m)\mu_k(m)\gamma_{k,\min}(m)}{\varphi(k,m)^2}\}\Big)\\ &+\Gamma_A(k,m)c_{1_k}(m)\exp\{\frac{-\varphi(k,m)c_{2_k}(m)\mu_k(m)\gamma_{k,\min}(m)}{\varphi(k,m)}\}\Bigg]\\ &-\Omega\mu_k(m)P_{sc_k}(m)-\eta_m(k)\\ -\eta_k(m) =&\begin{cases}>0, & \varphi(k,m)=1,\\ =0, & \varphi(k,m)\in(0,1),\\ <0, & \varphi(k,m)=0,\end{cases}\end{aligned} \tag{3.16}$$

where $\Gamma_A(k,m)=\delta_{d_k}(m)\rho_{av_k}(m)$. From (3.16), it is obtained that

$$\begin{aligned}&\Gamma_A(k,m)-\Gamma_A(k,m)c_{1_k}(m)\exp\{-c_{2_k}(m)\mu_k(m)\gamma_{k,\min}(m)\}\\ &-\Omega\mu_k(m)P_{sc_k}(m)-\eta_m(k)-\eta_k(m)=0.\end{aligned} \tag{3.17}$$

Based on (3.17), $\eta_m(k)$ is the active Lagrange multiplier that controls the user allocation process. Therefore, $\eta_m(k)$ is evaluated as follows

$$\begin{aligned}\eta_m(k) =&\Gamma_A(k,m)-\Gamma_A(k,m)c_{1_k}(m)\exp[-c_{2_k}(m)\mu_k(m)\gamma_{k,\min}(m)]\\ &-\Omega\mu_k(m)P_{sc_k}(m)-\eta_k(m).\end{aligned} \tag{3.18}$$

The $\eta_k(m)$ multiplier, which can be referred to as the allocation value, is used to prevent any selection of the same sub-channel by two or more users. It is initialised by a zero value when the user k has not been allocated to the suitable sub-channel yet. Moreover, $\eta_k(m)$ can be maximised based on (3.18) to be $\eta_k(m)=\Gamma_A(k,m)-$

$\Gamma_A(k,m)c_{1_k}(m)\exp[-c_{2_k}(m)\mu_k(m)\gamma_{k,\min}(m) - \Omega\mu_k(m)P_{sc_k}(m)]$ when the user k is assigned to a suitable sub-channel to achieve $\eta_m(k) = 0$ for the same user over other sub-channels.

In contrast, the second step is performed by obtaining a partial derivative of (3.15) in terms of $\mu_k(m)$ as

$$\begin{aligned}\frac{\partial L\Big[\varphi(k,m),\mu_k(m)\Big]}{\partial\mu_k(m)} =&\varphi(k,m)\Gamma_A(k,m)c_{1_k}(m)c_{2_k}(m)\gamma_{k,\min}(m)\\ &\cdot\exp[-c_{2_k}(m)\mu_k(m)\gamma_{k,\min}(m)]\\ &-\Omega\varphi(k,m)P_{sc_k}(m) = \begin{cases} =0, & \mu_k(m)\in(0,\infty),\\ <0, & \mu_k(m)\in(-\infty,0].\end{cases}\end{aligned} \tag{3.19}$$

If

$$\Gamma_B(k,m) = \Gamma_A(k,m)c_{1_k}(m)\exp[-c_{2_k}(m)\mu_k(m)\gamma_{k,\min}(m)], \tag{3.20}$$

then (3.19) can be rewritten as

$$\begin{aligned}\frac{\partial L\Big[\varphi(k,m),\mu_k(m)\Big]}{\partial\mu_k(m)} =&\varphi(k,m)\Gamma_B(k,m)c_{2_k}(m)\gamma_{k,\min}(m)\\ &-\Omega\varphi(k,m)P_{sc_k}(m) = \begin{cases} =0, & \mu_k(m)\in(0,\infty),\\ <0, & \mu_k(m)\in(-\infty,0].\end{cases}\end{aligned} \tag{3.21}$$

From (3.21), it is obtained that

$$\Gamma_B(k,m) = \frac{\Omega\varphi(k,m)P_{sc_k}(m)}{\varphi(k,m)c_{2_k}(m)\gamma_{k,\min}(m)} = \frac{\Omega P_{sc_k}(m)}{c_{2_k}(m)\gamma_{k,\min}(m)}. \tag{3.22}$$

Based on (3.20) and (3.22), the formula of (3.18) can be rewritten as

$$\eta_m(k) = \Gamma_A(k,m) - \frac{\Omega P_{sc_k}(m)}{c_{2_k}(m)\gamma_{k,\min}(m)} - \Omega\mu_k(m)P_{sc_k}(m) - \eta_k(m). \tag{3.23}$$

The maximum achieved performance of k-th user at m-th sub-channel can be evaluated based on (3.23) as

$$k_{\text{opt}}(m) = \arg\max_k \eta_m(k), \quad k = 1,...,K. \tag{3.24}$$

The user allocation problem is solved in the fixed domain, i.e. $\varphi(k,m) \in \{0,1\}$. Therefore, the m-th sub-channel is allocated to the k-th user with maximum $\eta_m(k)$ based on (3.23), i.e.

$$\varphi(k,i) = \begin{cases} 1, & \text{if } k = k_{\text{opt}}(m), \\ 0, & \text{otherwise.} \end{cases} \quad \forall m = 1, ..., M. \tag{3.25}$$

The Lagrange multiplier Ω, shown in (3.23), can be re-expressed in term of water filling level λ as [70]

$$\Omega = \frac{1}{\lambda \ln 2}. \tag{3.26}$$

Additionally, the desired power value that adjusts the optimal power for m-th sub-channel can be evaluated based on the water filling approach as

$$\mu_k^*(m) = \frac{\Omega - \frac{P_{sc_k}(m)}{\gamma_{k,\min}(m)}}{P_{sc_k}(m)}. \tag{3.27}$$

The optimised approach of the proposed user, bit and power allocation algorithm is illustrated in Algorithm 4. It is observed from this algorithm that the proposed solution of the investigated problem, expressed in (3.9)-(3.13), requires an exhaustive search among all the available options of the utilised MCS levels and the possible power and user assignment for each sub-channel accordingly.

3.6.2 Decoupled approach

The other investigated solution approach decouples the considered problem, expressed in (3.9)-(3.13), into two sub-problems (1. user allocation, 2. Bit and power allocation) based on the decomposition method [62]. This solution avoids the exhaustive search of the optimised approach, presented earlier, which leads to a significant reduction in the computational complexity.

User allocation

The user allocation sub-problem has been tackled here under the assumption of allocating the highest MCS option for all sub-channels and distributing the transmission power equally amongst the involved sub-channels. In other words, the power constraints shown in (3.10) and (3.11) are removed. Thus, the Lagrangian function of

Step 1. MCS initialisation:
Set all bands into highest MCS options
Step 2. $P_{sc_k}(m)$ **initialisation:**
Initialisation:
foreach k **do**
  foreach m **do**
    $P_{sc_k}(m) = \delta_{d_k}(m) P_{s_k}(m)$.
    $\mu_k(m) = \frac{P_T}{M P_{sc_k}(m)}$.
  end
end
Step 3. λ **initialisation:**
initialise $\lambda = 0.001$.
Step 4. Optimal user allocation:
while $\lambda < 10$ **do**
  foreach k **do**
    foreach m **do**
      implementing of (3.23), (3.25) and (3.26)
    end
  end
  Step 5. Power evaluation in terms of λ**:**
  if $\sum_{k=1}^{K} \sum_{m=1}^{M} \varphi(k,m) \mu_k^*(m) P_{sc_k}(m) \neq P_T$ **then**
    $\lambda = \lambda + \frac{\lambda}{2}$, $\mu_k^*(m) = \frac{\Omega - \frac{P_{sc_k}(m)}{\gamma_{k,\min}(m)}}{P_{sc_k}(m)}$.
  end
  else
    λ is the optimal value and $\mu_k^*(m) = \frac{\Omega - \frac{P_{sc_k}(m)}{\gamma_{k,\min}(m)}}{P_{sc_k}(m)}$.
    Go to step 6
  end
end
Reduce the MCS option for the bands with low SNR values. Go to step 2.
Step 6. Adjustment of the optimal power value $P_{sc_k}^*(m)$ **for each sub-channel in terms of** λ**:**
foreach k **do**
  foreach m **do**
    $P_{sc_k}^*(m) = \mu_k^*(m) P_{sc_k}(m)$.
  end
end

Algorithm 4: The proposed algorithm of the optimised UBPA strategy for SISO-AMC-OFDMA system.

the considered problem can be formulated in terms of $P^*_{e_k}(m)$, expressed by (3.14), as

$$\begin{aligned} L[\varphi(k,m)] =& \sum_{k=1}^{K}\sum_{m=1}^{M}\varphi(k,m)\delta_{d_k}(m)\rho_{av_k}(m) \\ & - \sum_{k=1}^{K}\sum_{m=1}^{M}\{\varphi(k,m)\delta_{d_k}(m)\rho_{av_k}(m)c_{1_k}(m) \\ & \cdot \exp[\frac{-\varphi(k,i)c_{2_k}(m)\mu_k(m)\gamma_{k,\min}(m)}{\varphi(k,m)}]\} \\ & - \sum_{k=1}^{K}\eta_m(k)[\sum_{m=1}^{M}\varphi(k,m)-1] \\ & - \sum_{m=1}^{M}\eta_k(m)[\sum_{k=1}^{K}\varphi(k,m)-1]. \end{aligned} \tag{3.28}$$

As highlighted before, the $\varphi(k,m)$ value, which refers to the allocation of the k-th user over the m-th sub-channel, can be achieved within the relaxed continuous domain of the closed interval $[0,1]$ corresponding to each user over M sub-channels. In order to obtain $\varphi(k,i)$, a partial derivative of $L[\varphi(k,m)]$ with respect to $\varphi(k,m)$ is computed as

$$\begin{aligned} \frac{\partial L[\varphi(k,m)]}{\partial\varphi(k,m)} =& \Gamma_A(k,m) - \Bigg[\Big(\varphi(k,m)\Gamma_A(k,m)c_{1_k}(m) \\ & \cdot \exp\{\frac{-\varphi(k,m)c_{2_k}(m)\mu_k(m)\gamma_{k,\min}(m)}{\varphi(k,m)}\} \\ & \cdot \{\frac{-\varphi(k,m)c_{2_k}(m)\mu_k(m)\gamma_{k,\min}(m)}{\varphi(k,m)^2} \\ & + \frac{\varphi(k,m)c_{2_k}(m)\mu_k(m)\gamma_{k,\min}(m)}{\varphi(k,m)^2}\}\Big) \\ & + \Gamma_A(k,m)c_{1_k}(m)\exp\{\frac{-\varphi(k,m)c_{2_k}(m)\mu_k(m)\gamma_{k,\min}(m)}{\varphi(k,m)}\}\Bigg] \\ & - \eta_m(k) - \eta_k(m) = \begin{cases} >0, & \varphi(k,m)=1, \\ =0, & \varphi(k,m)\in(0,1), \\ <0, & \varphi(k,m)=0. \end{cases} \end{aligned} \tag{3.29}$$

Based on (3.29),

$$\Gamma_A(k,m) - \Gamma_A(k,m)c_{1_k}(m)\exp\{-c_{2_k}(m)\mu_k(m)\gamma_{k,\min}(m)\} - \eta_m(k) - \eta_k(m) = 0. \tag{3.30}$$

Based on (3.30), $\eta_m(k)$ is the Lagrange multiplier that manages the user allocation process. Therefore, $\eta_m(k)$ is evaluated as follows

$$\eta_m(k) = \Gamma_A(k,m) - \Gamma_A(k,m)c_{1_k}(m)\exp[-c_{2_k}(m)\mu_k(m)\gamma_{k,\min}(m)] - \eta_k(m). \tag{3.31}$$

In this work, the user allocation problem is solved in the fixed domain, i.e. $\varphi(k,m) \in \{0,1\}$. In this domain, the m-th sub-channel is allocated to the k-th user based on the maximum achieved performance as

$$\varphi(k,m) = \begin{cases} 1, & \text{if } k = k_{\text{opt}}(m), \\ 0, & \text{otherwise,} \end{cases} \quad \forall m = 1, ..., M, \tag{3.32}$$

where

$$k_{\text{opt}}(m) = \arg\max_k \eta_m(k), \quad k = 1, ..., K. \tag{3.33}$$

Algorithm 5 illustrates the proposed user allocation scheme. Initially, all sub-channels of each user are set to the highest MCS level, which is 64-QAM modulation order and 3/4 convolutional coding rate. Subsequently, a zero value is set for all $\eta_k(m)$. The next step is the evaluation of the elements $\varphi(k,m)$ of the user allocation matrix that corresponds to the first user, following (3.32) and (3.33). At the same time, the index of the allocated user, $\eta_k(m)$, is maximised as explained above to prevent choosing the same user over other sub-channels. This process is repeated until all users are allocated.

Bit and Power allocation

The bit and power allocation problem, which is the second sub-problem of the proposed UBPA strategy, is considered after allocating the users across the sub-channels. At this stage, the fairness allocation constraints expressed in (3.12) and (3.13) are removed since the users have already been allocated as shown in (3.32).

Step 1. MCS initialisation:
Set all bands into highest MCS options
Step 2. $P_{sc_k}(m)$ **initialisation:**
Initialisation:
foreach k **do**
  foreach m **do**
    $P_{sc_k}(m) = \delta_{d_k}(m) P_{s_k}(m)$.
    $\mu_k(m) = \frac{P_T}{MP_{sc_k}(m)}$.
  end
end
Step 4. User allocation:
$\eta_k(m) = 0$
foreach k **do**
  foreach m **do**
    Implement (3.31).
    Implement (3.32) and (3.33).
    Maximise $\eta_k(m)$.
  end
end

Algorithm 5: The proposed user allocation algorithm of the decoupled UBPA strategy for SISO-AMC-OFDMA system

The power allocation is expected to minimise the BER for each sub-channel in which the throughput is maximised. To obtain the value of $\mu_k(m)$ that refines the power value of each sub-channel, a Lagrange multipliers method is employed. In addition, the Lagrangian function is formulated as

$$\begin{aligned} L[\mu_k(m)] = & \sum_{k=1}^{K} \sum_{m=1}^{M} \varphi(k,m) \Gamma_A(k,m) [1 - P_{e_k}(m)] \\ & - \Omega \{ [\sum_{k=1}^{K} \sum_{m=1}^{M} \varphi(k,m) \mu_k(m) P_{sc_k}(m)] - P_T \}. \end{aligned} \tag{3.34}$$

The $P_{e_k}(m)$, which is mathematically expressed in (3.6), is substituted into (3.34) as

$$
\begin{aligned}
L[\mu_k(m)] = & \sum_{k=1}^{K}\sum_{m=1}^{M}\varphi(k,m)\Gamma_A(k,m) \\
& - \sum_{k=1}^{K}\sum_{m=1}^{M}\big\{\varphi(k,m)\Gamma_A(k,m)c_{1_k}(m) \\
& \cdot \exp[-c_{2_k}(m)\mu_k(m)\gamma_{k,\min}(m)]\big\} \\
& - \Omega\{[\sum_{k=1}^{K}\sum_{m=1}^{M}\varphi(k,m)\mu_k(m)P_{sc_k}(m)] - P_T\}.
\end{aligned}
\tag{3.35}
$$

To evaluate $\mu_k(m)$, a partial derivative for $L[\mu_k(m)]$ is computed with respect to $\mu_k(m)$ as

$$
\begin{aligned}
\frac{\partial L[\mu_k(m)]}{\partial \mu_k(m)} = & \varphi(k,m)\Gamma_A(k,m)c_{1_k}(m)c_{2_k}(m)\gamma_{k,\min}(m) \\
& \cdot \exp[-c_{2_k}(m)\mu_k(m)\gamma_{k,\min}(m)] \\
& - \Omega\varphi(k,m)P_{sc_k}(m)\begin{cases} = 0, & \mu_k(m) \in (0,\infty), \\ < 0, & \mu_k(m) \in (-\infty, 0], \end{cases}
\end{aligned}
\tag{3.36}
$$

which yields

$$
\begin{aligned}
\ln\Big[\Omega\varphi(k,m)P_{sc_k}(m)\Big] = & \ln\Big[\varphi(k,m)\Gamma_A(k,m)c_{1_k}(m)c_{2_k}(m)\gamma_{k,\min}(m)\Big] \\
& + \ln\Big[\exp\big\{-c_{2_k}(m)\mu_k(m)\gamma_{k,\min}(m)\big\}\Big].
\end{aligned}
\tag{3.37}
$$

Let

$$
\Gamma_B(k,m) = \ln\Big[\varphi(k,m)\Gamma_A(k,m)c_{1_k}(m)c_{2_k}(m)\gamma_{k,\min}(m)\Big], \tag{3.38}
$$

then (3.37) can be rewritten as

$$
\ln\Big[\Omega\varphi(k,m)P_{sc_k}(m)\Big] = \Gamma_B(k,m) + \ln\Big[\exp\big\{-c_{2_k}(m)\mu_k(m)\gamma_{k,\min}(m)\big\}\Big]. \tag{3.39}
$$

By removing the logarithm of the exponential expression, (3.39) can be rewritten as

$$\ln[\Omega\varphi(k,m)P_{sc_k}(m)] = \Gamma_B(k,m) - c_{2_k}(m)\mu_k(m)\gamma_{k,\min}(m), \tag{3.40}$$

which yields,

$$\mu_k(m) = \left(\frac{\Gamma_B(k,m) - \ln(\Omega) - \ln[\varphi(k,m)P_{sc_k}(m)]}{c_2(m)\gamma_{k,\min}(m)}\right)^+, \tag{3.41}$$

where $(b)^+$ indicates $\max(b,0)$. To find Ω, (3.41) is substituted in (3.10) as shown below

$$\begin{aligned}\sum_{k=1}^{K}\sum_{m=1}^{M}\frac{\Gamma_B(k,m)P_{sc_k}(m)\varphi(k,m) - \ln(\Omega)P_{sc_k}(m)\varphi(k,m)}{c_{2_k}(m)\gamma_{k,\min}(m)} \\ -\sum_{k=1}^{K}\sum_{m=1}^{M}\frac{\ln[\varphi(k,m)P_{sc_k}(m)]P_{sc_k}(m)\varphi(k,m)}{c_{2_k}(m)\gamma_{k,\min}(m)} = P_T.\end{aligned} \tag{3.42}$$

By assuming that

$$\Gamma_C(k,m) = P_{sc_k}(m)\varphi(k,m), \tag{3.43}$$

and

$$\Gamma_D(k,m) = \ln[\Gamma_C(k,m)]\Gamma_C(k,m), \tag{3.44}$$

(3.42) can be rewritten as

$$\sum_{k=1}^{K}\sum_{m=1}^{M}\frac{\Gamma_B(k,m)\Gamma_C(k,m) - \ln(\Omega)\Gamma_C(k,m) - \Gamma_D(k,m)}{c_{2_k}(m)\gamma_{k,\min}(m)} = P_T. \tag{3.45}$$

Equivalently, (3.45) is reformulated as

$$\begin{aligned}\ln(\Omega)\sum_{k=1}^{K}\sum_{m=1}^{M}\frac{\Gamma_C(k,m)}{c_{2_k}(m)\gamma_{k,\min}(m)} \\ = \sum_{k=1}^{K}\sum_{m=1}^{M}\frac{\Gamma_B(k,m)\Gamma_C(k,m) - \Gamma_D(k,m)}{c_{2_k}(m)\gamma_{k,\min}(m)} - P_T.\end{aligned} \tag{3.46}$$

From (3.46), $\ln(\Omega)$ is evaluated as

$$\ln(\Omega) = \frac{\Gamma_E(k,m)}{\Gamma_F(k,m)}, \tag{3.47}$$

where

$$\Gamma_E(k,m) = \sum_{k=1}^{K}\sum_{m=1}^{M} \frac{\Gamma_B(k,m)\Gamma_C(k,m) - \Gamma_D(k,m)}{c_{2_k}(m)\gamma_{k,\min}(m)} - P_T, \tag{3.48}$$

and

$$\Gamma_F(k,m) = \sum_{k=1}^{K}\sum_{m=1}^{M} \frac{\Gamma_C(k,m)}{c_{2_k}(m)\gamma_{k,\min}(m)}. \tag{3.49}$$

The power value, $\mu_k(m)$, for each sub-channel assigned to a user is evaluated by substituting (3.47) into (3.41). The Lagrange multiplier, Ω, controls the total transmission power allocation amongst the sub-channels. The distribution criteria depend on the assigned sub-channel gain; for instance, (3.41) allocates more power to the sub-channel with a deep fade, while it reduces the power value for the high SNR sub-channels.

After obtaining the user and power allocation according to (3.32) and (3.41) respectively, the proposed bit allocation algorithm is considered depending on the channel conditions and the power constraints, which are expressed in (3.10) and (3.11). The proposed UBPA strategy avoids any transmission over the sub-channels with SNR value lower than 4 dB due to high BER values for the other MCS levels.

Algorithm 6 explains the proposed bit and power allocation of UBPA strategy. Firstly, the sub-channels are set to the highest MCS order. Secondly, the power is allocated over the utilised sub-channels, which adopt the given MCS options, based on (3.41). Thirdly, the system checks if the power constraints shown in (3.10) and (3.11) are satisfied. A positive response indicates that the two constraints are satisfied, therefore, the transmission is allowed to continue, while a negative response leads to implementing a reduction in the MCS order for the sub-channels that require more power to satisfy the relevant channel conditions. In addition, the option of no transmission is directly chosen for the sub-channels with SNR values less than 4 dB. The sub-carriers of these sub-channels are distributed among the other utilised sub-channels. In other words, the users with SNR values below 4 dB are discarded. Finally, iterative reduction of the MCS options for the selected sub-channels continues until the system conditions are satisfied, or the lowest MCS is reached, which implies no transmission on the corresponding sub-channels.

Step 1. MCS initialisation:
Set all bands into highest MCS options
Step 2. Power evaluation:
Initialisation:
foreach k **do**
  foreach m **do**
    $P_{sc_k}(m) = \delta_{d_k}(m) P_{s_k}(m)$.
    $\mu_k(m) = \left(\frac{\Gamma_B(k,m) - \ln(\Omega) - \ln[\varphi(k,m) P_{sc_k}(m)]}{c_2(m) \gamma_{k,\min}(m)} \right)^+$.
  end
end
Step 3. Power constraints check:
if $\sum_{k=1}^{K} \sum_{m=1}^{M} \varphi(k,m) \mu_k(m) P_{sc_k}(m) = P_T$ *and* $\mu_k(m) \geq 0$ **then**
  Go to step 4.
end
else
  foreach k **do**
    foreach m **do**
      if $\gamma_{k,\min}(m) \leqslant 4$ **then**
        Set this sub-channel to no transmission option.
      end
      else
        Reduce the MCS option levels for the sub-channels with lower $\gamma_{k,\min}(m)$.
        Go to step 2
      end
    end
  end
end
Step 4. Transmission:
Transmit the OFDMA frame.

Algorithm 6: The proposed bit and power allocation algorithm of the decoupled UBPA strategy for SISO-AMC-OFDMA system

3.7 Simulation Results and Discussion

The performance of the investigated SISO-AMC-OFDMA system based on both approaches of the proposed UBPA strategy and pilot adjustment scheme is compared with conventional methods. This system adopts the Mobile WiMAX IEEE 802.16e standard with the parameters listed in Table 2.1. The simulation results are obtained using different ITU channel profiles that represent distinct criteria in terms of mobility speed and channel conditions for $K = 30$ users. The considered SNR values in the simulation results represent the average SNR for all users as

$$\gamma_{av_g} = E\{\gamma^*_{k,\min}(m)\}. \tag{3.50}$$

In the simulation results, eight systems are compared, which divide the OFDMA frame into sub-channels and assign one user per sub-channel as follows:

1. FS-AMC-OFDMA-conventional bit and power allocation (CBPA) system that adopts the bit and power allocation algorithm presented in [38] for convolutional coding rate of 3/4 without considering the ARQ retransmission protocol for fair comparison and with fixed number of pilots.

2. DS-AMC-OFDMA-CBPA system, which utilises the resource allocation algorithm presented in [38] for coding rate of 3/4 with dynamic number of pilots.

3. FS-AMC-OFDMA-optimised user, bit and power allocation (OUBPA) system that considers the optimised approach of the proposed UBPA strategy with fixed number of pilots.

4. DS-AMC-OFDMA-OUBPA system that is based on the optimised approach of the proposed UBPA strategy with dynamic number of pilots.

5. FS-AMC-OFDMA-decoupled user, bit and power allocation (DUBPA) system, which uses the decoupled approach of the proposed UBPA strategy with fixed number of pilots.

6. DS-AMC-OFDMA-DUBPA system that employs the decoupled approach of the proposed UBPA strategy with dynamic number of pilots.

7. FS-AMC-OFDMA, which uses the proposed AMC strategy explained in Chapter 2 with full-use of pilots.

8. DS-AMC-OFDMA that employs the proposed dynamic sub-channelling AMC strategy presented in Chapter 2.

It is important to note that the systems, which consider the fixed number of pilots, use the full number of the available pilots. Moreover, the proposed pilots adjusting technique is utilised by the schemes, which adopt the dynamic number of pilots.

Fig. 3.4 demonstrates the average throughput performance of the eight systems under investigation. The simulated average system throughput is evaluated for $N_{fr} = 1 \times 10^6$ transmitted OFDMA frames, with respect to the effective bandwidth, B_{eff}, based on (2.45). It is important to note that the effective bandwidth, B_{eff}, is based on the number of data sub-carriers, $\delta_{d_k}(m)$, revised by the proposed pilot adjustment scheme, within each transmitted frame as shown in (2.44).

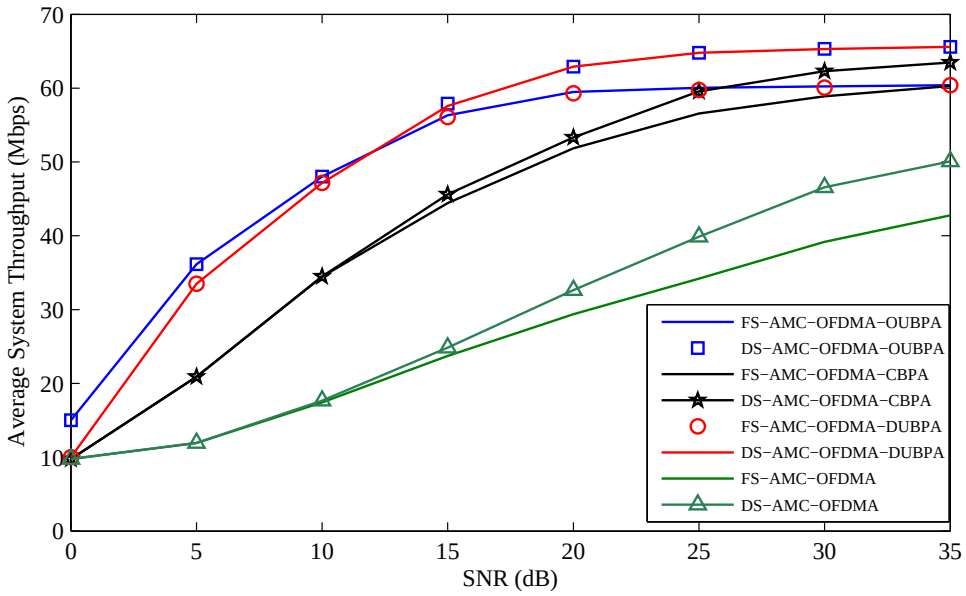

Figure 3.4: Average system throughput for the investigated SISO-AMC-OFDMA systems.

From Fig. 3.4, it is evident that the DS-AMC-OFDMA-OUBPA system outperforms the other investigated schemes that adopt the proposed pilot adjustment scheme, while the FS-AMC-OFDMA-OUBPA shows a superior performance in comparison with the systems, which consider the fixed number of pilots. Additionally, performance of the FS-AMC-OFDMA-DUBPA and DS-AMC-OFDMA-DUBPA is significantly improved in comparison to FS-AMC-OFDMA-CBPA and DS-AMC-OFDMA-CBPA, respectively. Furthermore, the systems adopted the proposed pilot adjustment scheme outperform such related schemes that consider the full-use

of pilot sub-carriers. In contrast, the performance of the systems of FS-AMC-OFDMA-DUBPA, DS-AMC-OFDMA-DUBPA, FS-AMC-OFDMA-CBPA and DS-AMC-OFDMA-CBPA is better than both FS-AMC-OFDMA and DS-AMC-OFDMA due to the utilisation of different resource allocation strategies.

The enhancement in the performance of both investigated schemes based on UBPA strategy for fixed and dynamic number of pilots is due to the behaviour of the adopted resource allocation strategy. This strategy exploits the multiuser channel diversity to allocate the users amongst the sub-channels of the transmitted OFDMA frame rather than using sequential assignment as in [38]. Additionally, the transmission power value is utilised to counteract the channel fading effects on the sub-carriers in the presence of sufficient MCS options. Moreover, the proposed bit allocation algorithm of the UBPA strategy selects higher MCS orders for most of the sub-channels in order to guarantee successful high transmission rate of the data with the lowest number of errors in comparison with method of [38]. In addition, the proposed strategy provides a low power value for the high SNR sub-channels and more power for the deep fade channel to increase the resilience and reliability of the involved sub-carriers against channel fading. The UBPA can decide to avoid transmission over sub-channels with worst conditions in order to save more power for other sub-channels. On the other hand, the systems that adopts the proposed pilot adjustment scheme outperform the related schemes with fixed number of pilot since this technique increases the transmission data rate and throughput by adding additional data sub-carriers instead of the unused pilots.

It should be noted that the performance of the AMC-OFDMA-OUBPA systems that employ the optimised approach of UBPA strategy for both fixed and dynamic number of pilots is improved compared to AMC-OFDMA-DUBPA due to the optimal solution of the presented optimisation problem. In other words, the decoupling of the problem into sub-problems considered by AMC-OFDMA-DUBPA systems affects the optimal solution particularly for low SNR values. The major drawback of the optimised approach is the computational complexity that comes from exhaustive search for the optimal solution in terms of user, bit and power allocation amongst the utilised sub-channels that assigned to different users. On the other hand, the decoupled approach produces a low computational complexity solution since it divides the complex optimisation problem into sub-problems and solves each one individually under the assumption of perfect tackling for others. It is evident from Fig.

3.4 that the optimised and decoupled approaches of the proposed UBPA strategy provide the same performance after SNR value of 15 dB.

Fig. 3.5 presents a comparison of the throughput outage probability, P_{out}, obtained with the investigated systems. Note that P_{out} is evaluated based on (2.46). It is worthy to note that Fig. 3.5 shows the superior performance of AMC-OFDMA-OUBPA system for both fixed and dynamic pilots in comparison with the other approaches. Additionally, both approaches of the proposed strategy can achieve the lowest outage probability at SNR values in comparison with the other approaches. At the other hand, the AMC-OFDMA-DUBPA with both pilot assignment methods shows a low throughput outage probability in comparison with the conventional approaches due to the utilisation of the proposed decoupled approach of UBPA.

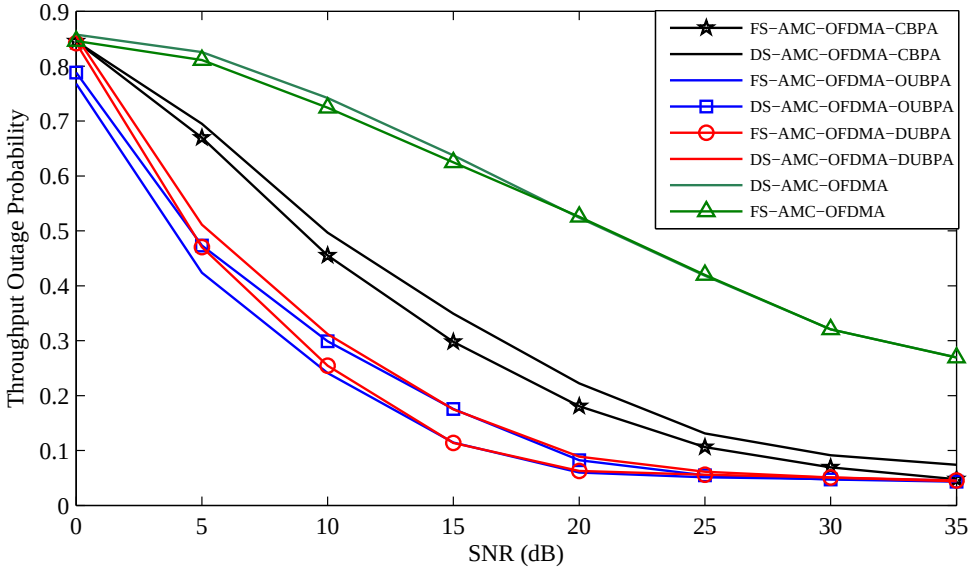

Figure 3.5: Throughput outage probability for the investigated SISO-AMC-OFDMA systems.

Fig. 3.6 illustrates the average throughput performance of the considered system in terms of the number of users at the assigned BS for average SNR value of 5, 15, 25 and 35 dB. This figure is presented to test the performance efficiency of the underlying systems for different numbers of users. Although the performance of the AMC-OFDMA-OUBPA and AMC-OFDMA-DUBPA systems for both fixed and dynamic number of pilots is increased accordingly with the number of users, it remains the same after 30 users. Moreover, the enhancement in the throughput of the FS-AMC-OFDMA-CBPA, DS-AMC-OFDMA-CBPA, FS-AMC-OFDMA and DS-AMC-OFDMA is restricted to be the same after 30 users. This is due to reach-

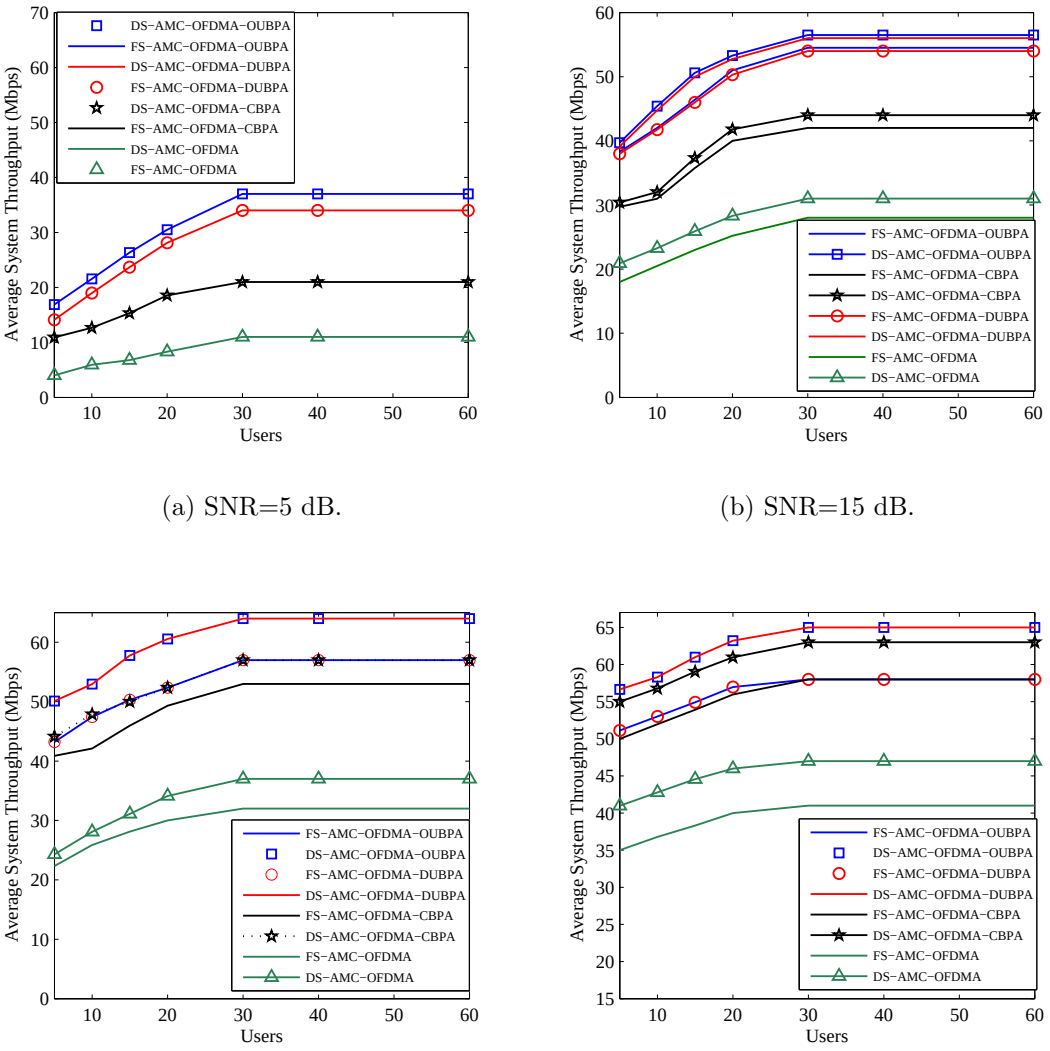

(a) SNR=5 dB.

(b) SNR=15 dB.

(c) SNR=25 dB.

(d) SNR=35 dB.

Figure 3.6: Average system throughput vs. number of users for the investigated SISO-AMC-OFDMA systems.

ing the saturation of the channel diversity. The improvement in the performance of the investigated systems with the increase of user's number is the results of the multiuser channel diversity. This diversity allows the proposed UBPA strategy to select different MCS options for distinct users in the same transmitted OFDMA frame. In contrast, the performance of the fixed and dynamic sub-channelling systems is identical for SNR value of 5 dB as shown in Fig. 3.6(a) due to the restriction of implementing the proposed pilot adjustment scheme for SNR lower than 10 dB. In addition, the performance of the systems that utilise both approaches of the proposed UBPA strategy is identical for fixed and dynamic sub-channelling methods in high SNR values as illustrated in Fig 3.6(c) and 3.6(d).

Fig. 3.7 demonstrates the effect of the pilot reduction on the channel estimation. It is shown that the effects of pilot reduction on the channel estimation MSE is noted after SNR value of 10 dB. The same performance of Fig. 2.15 has been achieved, which proves that the proposed pilot adjustment scheme can efficiently work with different systems and environments.

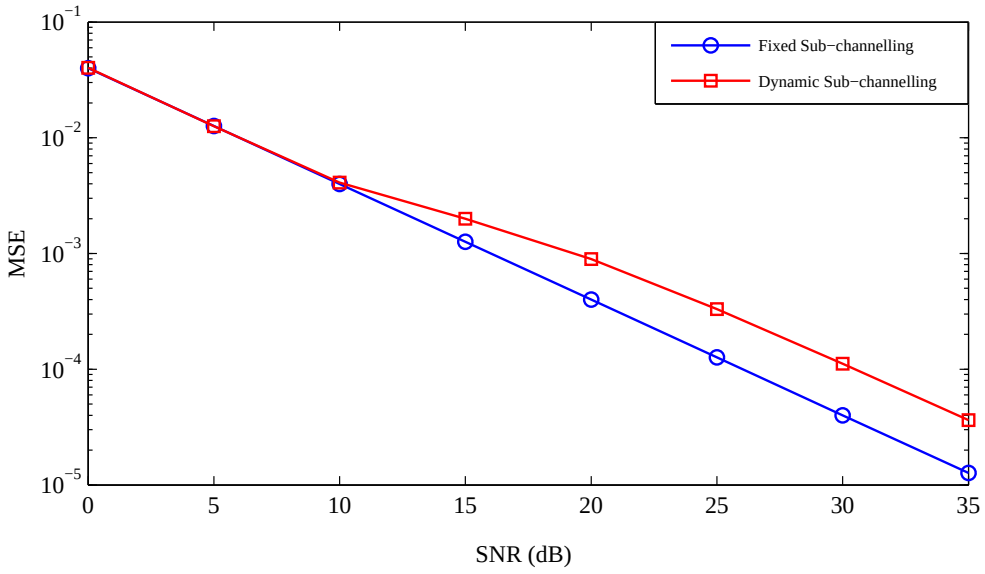

Figure 3.7: MSE of the channel estimation for fixed and dynamic sub-channelling SISO-AMC-OFDMA.

In order to study the systems employing each MCS, a statistical analysis in terms of usage ratio is performed. Fig. 3.8 illustrates the usage ratio, which is computed for a transmission time of 1.7 min, i.e. 1×10^6 OFDMA frame, of the MCSs for distinct SNR levels of 5, 15, 23 and 35 dB, respectively. In these plots, the ten convolutional based MCSs are sorted from the lowest to the highest level as explained in Fig. 2.16. It is observed from Fig. 3.8(a) and Fig. 3.8(b) that the MCS options of 2-7 are widely chosen by most systems. In contrast, the AMC-OFDMA-OUBPA scheme adopts the highest transmission level of 64-QAM combined with 3/4 convolutional coding rate throughout the simulations due to the use of the proposed strategy, which distributes the power optimally to increase the resilience of the sub-channels to the corresponding fading values. Additionally, the AMC-OFDMA-DUBPA system considers the MCS option 10 more often than AMC-OFDMA-CBPA scheme. The improved performance of AMC-OFDMA-OUBPA and AMC-OFDMA-DUBPA is the result of employing the proposed UBPA strategy. This strategy aims to increase the total throughput by selecting the higher MCS options and distributing the power

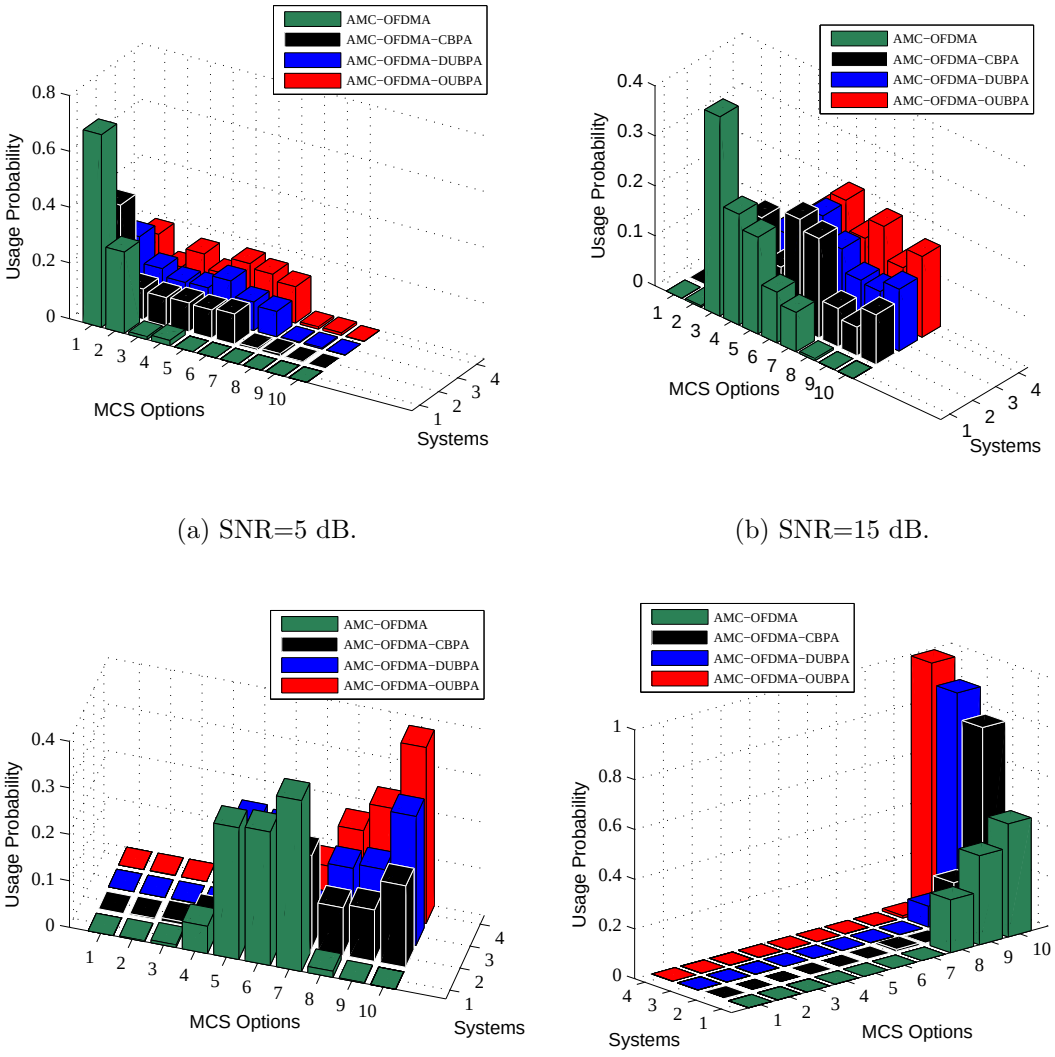

(a) SNR=5 dB.

(b) SNR=15 dB.

(c) SNR=25 dB.

(d) SNR=35 dB.

Figure 3.8: Usage probability of the utilised MCS options for the investigated SISO-AMC-OFDMA systems.

optimally amongst the sub-channels assigned to users, in which the power constraints of the maximisation problem are satisfied. On the other hand, Fig. 3.8(c) and Fig. 3.8(d) illustrate that AMC-OFDMA-OUBPA, AMC-OFDMA-DUBPA, AMC-OFDMA-CBPA and AMC-OFDMA systems select the highest MCS with a high usage ratio, while the remainder distributed over the other options. It is important to note that the fixed and dynamic sub-channelling techniques for each system are combined together due to the same achieved performance.

3.8 Chapter Summary

The focus of this Chapter was on the proposed resource allocation strategies, which were designed based on a developed software engineering life cycle model, for SISO based AMC-OFDMA systems. The resource allocation strategy, called UBPA, for SISO-AMC-OFDMA system has been firstly presented as a throughput maximisation problem. Then, the solution of this problem is introduced by two approaches, optimised and decoupled. The optimised approach provided the optimal solution for the investigated problem with a huge computational complexity. In contrast, the decoupled approach presented a low complexity solution on the cost of performance particularly at low SNR values. This was carried out by dividing the main problem into two sub-problems based on the decomposition method. The proposed UBPA strategy has been combined with the pilot adjustment scheme to produce two types of systems based on fixed and dynamic sub-channelling methods. The simulation results discussed the performance of the proposed strategies for distinct systems.

Chapter 4

Resource Allocation Software Algorithms for MIMO-AMC-OFDMA systems

A resource allocation (RA) strategy, called UBPA, for SISO-AMC-OFDMA system expressed in Chapter 3 has been expanded to work with single-cell spatial multiplexing MIMO technique based downlink AMC-OFDMA systems. This strategy is also designed based on cyclic type of software engineering life cycle model. In this Chapter, two RA strategies for MIMO-OFDMA system are presented. The first strategy allocates the available resources amongst the sub-carriers included in individual sub-channels based on the best SISO link between each transmit antenna and the related received antennas. In contrast, the second strategy employs the eigen mode transmission to distribute the resources optimally over the sub-channels.

4.1 Developed Life Cycle Model for MIMO Based Resource Allocation Algorithm

As mentioned earlier, the software engineering life cycle models are utilised in designing the proposed strategies. This is to produce strategies with more flexibility in dealing with the communication traffic problem and the updated system models.

In this Chapter, the same developed life cycle model of resource allocation algorithm for SISO-AMC-OFDMA, expressed in Fig. 3.1 of Chapter 3, is adopted. The only difference is the number if transmit and receive antennas.

4.2 RA for MIMO-AMC-OFDMA

This strategy aims to maximise the average system throughput by allocating the users, related bit streams and total transmission power among the considered sub-channels at each transmit antenna based on the best channel between such antenna and the receive antennas. It has not considered the interference, caused by the transmitted signals from other transmit antennas, at each received antenna. Additionally, RA strategy exploits the different transmission domains as well as the multiuser and channel diversities in order to achieve the optimal allocation for the available resources. The average system throughput is formulated as a trade-off criterion between the spectral efficiency and BER based on selected MCS levels. The MCS scenario based on convolutional coding method with ten options is employed. It is important to note that the fixed sub-channelling method has been adopted for MIMO based systems with a perfect channel knowledge at both transmitter and receivers.

4.2.1 MIMO-AMC-OFDMA System Model

A single-cell MIMO downlink channel to transmit a wireless OFDMA signal from an assigned BS into K mobile users is adopted. The BS is equipped with N_t transmit antennas, whilst each user has N_r receive antennas, where $N_t \geq N_r$. The transmitted OFDMA frame at each transmit antenna is divided into M sub-channels and each sub-channel has been assigned to a user. Moreover, the utilised N_d data sub-carriers are distributed uniformly over M sub-channels that assigned to K users at t-th transmit antenna in terms of r-th receive antenna in a range of $\xi_k^{(t,r)}(m) = N_d/M$. Therefore, the considered channel between the BS and k-th user, $\mathbf{H_k}$, is characterised to be of $N_t \times N_r \times \xi_k^{(t,r)}(m)$ corresponding to the data sub–carriers. Moreover, $m \in \{1, ..., M\}$, $k \in \{1, ..., K\}$, $t \in \{1, ..., N_t\}$ and $r \in \{1, ..., N_r\}$ are the index of utilised sub-channels, users, transmit antennas and receive antennas, respectively. As highlighted earlier, the CSI further to resource allocation information (RAI) are assumed to be perfectly known at the transceivers of both BS and mobile users.

Fig. 4.1 illustrates the block digram of the investigated MIMO-AMC-OFDMA system based on the proposed RA strategy. From this figure, the transmitter encodes and modulates the assigned information of M sub-channels at each transmit antenna according to the selected MCS options, which satisfy the total transmission

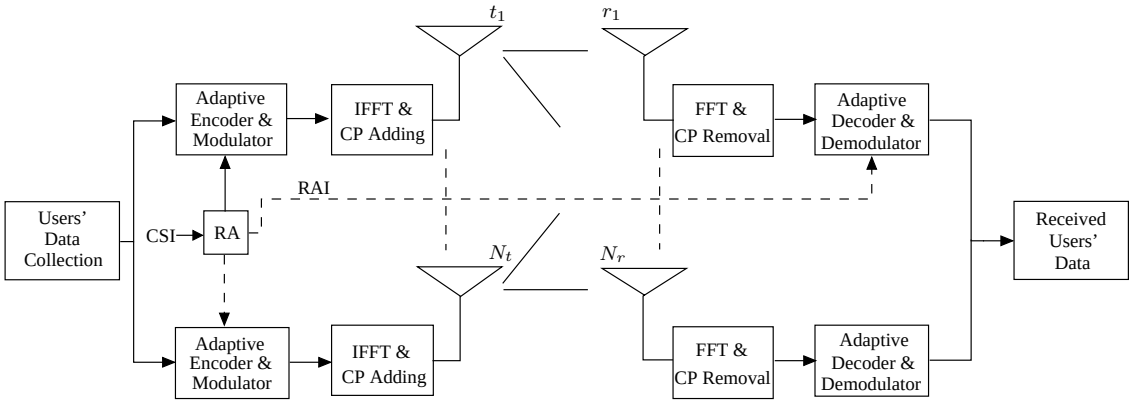

Figure 4.1: Block diagram of the proposed RA strategy based MIMO-AMC-OFDMA system.

power constraints and corresponding channel conditions. The *RA* block allocates the users among the utilised sub-channels and selects the suitable MCS for them at each transmit antenna individually by implementing the proposed strategy. It also distributes the total transmission power over the sub-channels of all transmit antennas. The block, *IFFT and CP Adding*, performs the IFFT operation and CP adding.

Different ITU channel profiles, explained in Chapter 2, are considered to generate distinct time varying MIMO multipath fading channels that realise the physical location of each user with different mobility speed [102]. The utilised channel between the k-th user and the assigned BS in terms of the transmit and receive antennas for the m-th sub-channel and the d-th data sub-carrier can be mathematically expressed as

$$\mathbf{H_k^{(m,d)}} = \begin{bmatrix} H_{k_{1,1}}^{m,d} & H_{k_{1,2}}^{m,d} & ... & H_{k_{1,N_r}}^{m,d} \\ H_{k_{2,1}}^{m,d} & H_{k_{2,2}}^{m,d} & ... & H_{k_{2,N_r}}^{m,d} \\ . & . & ... & . \\ . & . & ... & . \\ . & . & ... & . \\ H_{k_{N_t,1}}^{m,d} & H_{k_{N_t,2}}^{m,d} & ... & H_{k_{N_t,N_r}}^{m,d} \end{bmatrix}, \tag{4.1}$$

where $d = 1, ..., \xi_k^{(t,r)}(m)$ is the data sub-carrier index for the sub-channel m that assigned to the user k at the transmit antenna t.

After the FFT operation and CP removal, the received signal for the k-th user in terms of the d-th data sub-carrier at the m-th sub-channel can be formulated as

$$\mathbf{Y}_k^{(m,d)} = \mathbf{X}_k^{(m,d)}[\mathbf{H}_k^{(m,d)}]^T + \mathbf{W}_k^{(m,d)}, \tag{4.2}$$

where $\mathbf{Y}_k^{(m,d)}$, $\mathbf{X}_k^{(m,d)}$ and $\mathbf{W}_k^{(m,d)}$ denotes the received $N_r \times 1$ signal, the transmitted $N_t \times 1$ signal and the related AWGN $N_r \times 1$ sample vectors respectively. Furthermore, the received signal at antenna r for user k, $Y_{k_r}^{m,d}$, is a combination of all transmitted signals from N_t antenna as shown below

$$Y_{k_r}^{m,d} = \sum_{t=1}^{N_t} X_{k_{t,r}}^{(m,d)} H_{k_{t,r}}^{(m,d)} + W_{k_{t,r}}^{(m,d)}, \tag{4.3}$$

where $X_{k_{t,r}}^{m,d}$, $H_{k_{t,r}}^{m,d}$ and $W_{k_{t,r}}^{m,d}$ are the transmitted data sub-carriers, related channel coefficients and AWGN samples, respectively. Additionally, the zero forcing (ZF) receiver is utilised to detect the assigned data for the k-th user and to cancel the interferences, caused by other transmitted signal from different transmit antennas, [11]. The received data sub-carriers are demodulated and decoded according to the known selected MCS of each sub-channel utilising soft ML demapper and Viterbi decoder, respectively [90].

The throughput of the investigated MIMO-AMC-OFDMA system in terms of the g-th OFDMA block that includes the transmitted OFDMA frames from the transmit antennas can be formulated as

$$\psi_g = \sum_{k=1}^{K} \sum_{t=1}^{N_t} \sum_{r=1}^{N_r} \sum_{m=1}^{M} \varphi_{t,r}(k,m) \xi_k^{(t,r)}(m) \rho_k^{(t,r)}(m)[1 - P_{e_k}^{(t,r)}(m)], \tag{4.4}$$

where $\varphi_{t,r}(k,m)$ is an element in the user allocation matrix that assigns the user k at the transmit antenna t to the sub-channel m in terms of the receive antenna r [70]. Moreover, $\rho_k^{(t,r)}(m)$ denotes the spectral efficiency of the user k over the sub-channel m from the transmit antenna t to receive antenna r. Furthermore, $P_{e_k}^{(t,r)}(m)$ is the BER of the transmitted k-th user signal over the m-th sub-channel from the t-th transmit antenna to the r-th receive antenna. It should be noted the formula of (4.4) represents the approximated system throughput evaluation as a combination of numerous SISO transmissions. This is an approximated value since the interference between the transmitted signal from the t-th antenna with the transmitted signals from other antennas has not been considered.

4.2.2 Proposed RA Strategy for MIMO-AMC-OFDMA

The objective of the proposed RA strategy is to maximise the throughput of the investigated MIMO-AMC-OFDMA system. It is important to note that the RA strategy allocates the available resources based on the best SISO link between each transmit antenna and N_r receive antennas. In addition, it provides a solution to an optimisation problem that can be mathematically formulated as

$$\text{Maximise} \quad \psi_g = \sum_{k=1}^{K}\sum_{t=1}^{N_t}\sum_{r=1}^{N_r}\sum_{m=1}^{M}\varphi_{t,r}(k,m)\xi_k^{(t,r)}(m)\rho_k^{(t,r)}(m)[1-P_{e_k}^{(t,r)}(m)], \tag{4.5}$$

subject to :

$$\sum_{k=1}^{K}\sum_{t=1}^{N_t}\sum_{r=1}^{N_r}\sum_{m=1}^{M}\varphi_{t,r}(k,m)\mu_k^{(t,r)}(m)P_{sc_k}^{(t,r)}(m) = P_T, \tag{4.6}$$

$$\mu_k^{(t,r)}(m) \geq 0, \tag{4.7}$$

$$\sum_{r=1}^{N_r}\sum_{k=1}^{K}\varphi_{t,r}(k,m) = 1, \quad \begin{matrix} m = 1,...,M, \\ t = 1,...,N_t, \end{matrix} \tag{4.8}$$

$$\sum_{r=1}^{N_r}\sum_{m=1}^{M}\varphi_{t,r}(k,m) = 1, \quad \begin{matrix} k = 1,...,K, \\ t = 1,...,N_t, \end{matrix} \tag{4.9}$$

where $P_{sc_k}^{(t,r)}(m) = \xi_k^{(t,r)}(m)P_{s_k}^{(t,r)}(m)$ is the power value of the m-th sub-channel that assigned to the k-th user and transmitted from the t-th transmit antenna to the r-th receive antenna in terms of the related coded and modulated symbol power, $P_{s_k}^{(t,r)}(m)$. Additionally, (4.6) and (4.7) are the power constraints, while (4.8) and (4.9) denote the fairness user allocation constraints, which guarantee the allocation of one user per sub-channel at the transmit antenna t. Moreover, $\mu_k^{(t,r)}(m)$ is a power value that optimises the required power value for each sub-channel. Finally, P_T is the total transmission power of the corresponding BS.

From (4.5), the throughput evaluation is based on the related BER values. Therefore, $P_{e_k}^{(t,r)}(m)$ can be obtained utilising the general approximated BER formula following (3.6) as

$$P_{e_k}^{(t,r)}(m) = c_{1_k}^{(t,r)}(m) \exp[-c_{2_k}^{(t,r)}(m)\gamma_{k,\min}^{*(t,r)}(m)], \tag{4.10}$$

It is important to note that the same method of evaluating $c_{1_k}^{(t,r)}(m)$ and $c_{2_k}^{(t,r)}(m)$ values as used in SISO systems, presented in Chapter 3, is adopted here. Furthermore, $\gamma_{k,\min}^{(t,r)}(m)$, which is the minimum SNR value for the data sub-carriers within each sub-channel, can be evaluated based on (3.4) as

$$\gamma_{k,\min}^{*(t,r)}(m) = \mu_k^{(t,r)}(m)\gamma_{k,\min}^{(t,r)}(m) = \min\{\mu_k^{(t,r)}(m)\gamma_k^{(t,r)}(m,d)\}, \tag{4.11}$$

where $\gamma_k^{(t,r)}(m,d)$ is the SNR value for the d-th data sub-carriers in the m-th sub-channel assigned to the k-th user transmitted from the t-th transmit antenna to the r-th receive antenna. In order to achieve a practical solution to the investigated complex problem expressed in (4.5)-(4.9), the problem has been decoupled into two sub-problems and an algorithm is proposed to solve each one individually. These proposed algorithm are combined together in the RA strategy.

User allocation

In this Section, the user allocation sub-problem is presented and solved by a proposed algorithm. It is assumed that the information bits are allocated to highest MCS level. Additionally, the total transmission power of the BS are distributed equally over the transmit antennas and the power value of each antenna is allocated equally over the corresponding sub-channels. Therefore, the power constraints expressed in (4.6) and (4.7) are removed. Furthermore, the objective function shown in (4.5) is reformulated to satisfy the Hessian matrix conditions [62] by rewriting (4.10) based on (3.14) as

$$P_{e_k}^{*(t,r)}(m) = c_{1_k}^{(t,r)}(m) \exp[\frac{-\varphi_{t,r}(k,m)c_{2_k}^{(t,r)}(m)\gamma_{k,\min}^{*(t,r)}(m)}{\varphi_{t,r}(k,m)}]. \tag{4.12}$$

The user allocation sub-problem expressed in (4.5), (mimocon3) and (4.9) can be solved by applying the Lagrange optimisation method [62]. Therefore, the La-

grangian function is written as

$$\begin{aligned} L\Big[\varphi_{t,r}(k,m)\Big] =& \sum_{k=1}^{K}\sum_{t=1}^{N_t}\sum_{r=1}^{N_r}\sum_{m=1}^{M}[\varphi_{t,r}(k,m)\xi_k^{(t,r)}(m)\rho_k^{(t,r)}(m)] \\ & - \sum_{k=1}^{K}\sum_{t=1}^{N_t}\sum_{r=1}^{N_r}\sum_{m=1}^{M}\Big\{\varphi_{t,r}(k,b)\xi_k^{(t,r)}(m)\rho_k^{(t,r)}(m) \\ & \cdot c_{1_k}^{(t,r)}(m)\exp[\frac{-\varphi_{t,r}(k,m)c_{2_k}^{(t,r)}(m)\mu_k^{(t,r)}(m)\gamma_{k,\min}^{(t,r)}(m)}{\varphi_{t,r}(k,m)}]\Big\} \\ & - \sum_{t=1}^{N_t}\sum_{m=1}^{M}\eta_{r,k}(t,m)[\sum_{r=1}^{N_r}\sum_{k=1}^{K}\varphi_{t,r}(k,m)-1] \\ & - \sum_{t=1}^{N_t}\sum_{k=1}^{K}\eta_{r,m}(t,k)[\sum_{r=1}^{N_r}\sum_{m=1}^{M}\varphi_{t,r}(k,m)-1], \end{aligned} \tag{4.13}$$

where $\eta_{r,k}(t,m)$ and $\eta_{r,m}(t,k)$ are the Lagrange multipliers. Following the same derivative procedure of the user allocation of the decoupled UBPA strategy for SISO-AMC-OFDMA system expressed in Chapter 3, the $\varphi_{t,r}(k,m)$ values can be evaluated as

$$\begin{aligned} \varphi_{t,r}(k,m) = \left\{ \begin{array}{ll} 1, & \text{if } k = k_{\text{opt}}^{(t,r)}(m), \\ 0, & \text{otherwise,} \end{array} \right\}, \ \forall \ m = 1,...,M, \\ \forall \ t = 1,...,N_t, \\ \forall \ r = 1,...,N_r, \end{aligned} \tag{4.14}$$

where

$$\begin{aligned} k_{\text{opt}}^{(t,r)}(m) = \arg\max_k\{\eta_{r,m}(t,k)\}, \ k = 1,...,K, \\ t = 1,...,N_t \\ r = 1,...,N_r, \end{aligned} \tag{4.15}$$

$$\begin{aligned} \eta_{r,m}(t,k) =& \Gamma_{A_{t,r}}(k,m) - \Gamma_{A_{t,r}}(k,m)c_{1_k}^{(t,r)}(m) \\ & \cdot \exp[-c_{2_k}^{(t,r)}(m)\mu_k^{(t,r)}(m)\gamma_{k,\min}^{(t,r)}(m)] - \eta_{r,k}(t,m), \end{aligned} \tag{4.16}$$

and

$$\Gamma_{A_{t,r}}(k,m) = \xi_k^{(t,r)}(m)\rho_k^{(t,r)}(m). \tag{4.17}$$

Algorithm 7 illustrates the proposed user allocation algorithm. From this algorithm, all sub-channels of the available users at the considered transmit antenna are set to the modulation order of 64-QAM and coding rate of 3/4. Then, $\eta_{r,k}(t,m)$ for all users are initialised by zero. After obtaining the performance of all users among the sub-channels using (4.16), the $\varphi_{t,r}(k,m)$ value for the k-th user is evaluated following (4.14) and (4.15). In addition, in order to prevent choosing the same user over other sub-channels, the $\eta_{r,k}(t,m)$ for the selected user is maximised to be

$$\eta_{r,k}(t,m) = \Gamma_{A_{t,r}}(k,m) - \beta_{A_{t,r}}(k,m)c_{1_k}(m)\exp[-c_{2_k}^{(t,r)}(m)\mu_k^{(t,r)}(m)\gamma_{k,\min}^{(t,r)}(m)]. \tag{4.18}$$

The repetition of the algorithm is continued until allocating all users.

Bit and Power Allocation

The proposed bit and power allocation algorithm that tackles the second investigated sub-problem is presented. Under the assumption of achieving the user allocation, the fairness user allocation constraints of (4.8) and (4.9) are removed. In order to solve this optimisation problem by calculating $\mu_k^{(t,r)}(m)$, a Lagrange optimisation method is employed. Therefore, the Lagrangian function can be written in terms of (4.10) as

$$\begin{aligned} L\left[\mu_k^{(t,r)}(m)\right] =& \sum_{k=1}^{K}\sum_{t=1}^{N_t}\sum_{r=1}^{N_r}\sum_{m=1}^{M}\varphi_{t,r}(k,m)\Gamma_{A_{t,r}}(k,m) \\ &- \sum_{k=1}^{K}\sum_{t=1}^{N_t}\sum_{r=1}^{N_r}\sum_{m=1}^{M}\big\{\varphi_{t,r}(k,m)\Gamma_{A_{t,r}}(k,m)c_{1_k}^{(t,r)}(m) \\ &\cdot \exp[-c_{2_k}^{(t,r)}(m)\mu_k^{(t,r)}(m)\gamma_{k,\min}^{(t,r)}(m)]\big\} \\ &- \Omega\big[\sum_{k=1}^{K}\sum_{t=1}^{N_t}\sum_{r=1}^{N_r}\sum_{m=1}^{M}\varphi_{t,r}(k,m)\mu_k^{(t,r)}(m)P_{sc_k}^{(t,r)}(M)\big] - P_T. \end{aligned} \tag{4.19}$$

Step 1. MCS initialisation:
Set all sub-channels at the transmit antennas into highest MCS option
Step 2. $P_{sc_k}^{(t,r)}(m)$ **initialisation:**
Initialisation:
foreach k **do**
  foreach t **do**
    foreach r **do**
      foreach m **do**
        $P_{sc_k}^{(t,r)}(m) = \xi_k^{(t,r)}(m) P_{s_k}^{(t,r)}(m)$.
        $\mu_k^{(t,r)}(m) = \frac{P_T}{N_t M P_{sc_k}^{(t,r)}(m)}$.
        $\eta_{r,k}(t,m) = 0$
      end
    end
  end
end
Step 4. User allocation:
foreach k **do**
  foreach t **do**
    foreach r **do**
      foreach m **do**
        Implement (4.16) and (4.15).
        Implement (4.14).
        Implement (4.18)
      end
    end
  end
end

Algorithm 7: The proposed user allocation algorithm of the RA strategy for MIMO-AMC-OFDMA system

where Ω is a Lagrange multiplier that controls the desired power values for the sub-channels. The $\mu_k^{(t,r)}(m)$ values for different sub-channel are obtained from (4.19) by implementing the partial derivative of $L\left[\mu_k^{(t,r)}(m)\right]$ in terms of $\mu_k^{(t,r)}(m)$ as

$$\mu_k^{(t,r)}(m) = \left(\frac{\Gamma_{B_{t,r}}(k,m) - \ln(\Omega) - \ln[\varphi_{t,r}(k,m) P_{sc_k}^{(t,r)}(m)]}{c_{2_k}^{(t,r)}(m)\gamma_{k,\min}^{(t,r)}(m)} \right)^+. \tag{4.20}$$

After some mathematical operations, $\ln(\Omega)$ can be formulated as

$$\ln(\Omega) = \frac{\Gamma_{E_{t,r}}(k,m)}{\Gamma_{F_{t,r}}(k,m)}, \tag{4.21}$$

where

$$\Gamma_{E_{t,r}}(k,m) = \sum_{k=1}^{K}\sum_{t=1}^{N_t}\sum_{r=1}^{N_r}\sum_{m=1}^{M}[\frac{\Gamma_{B_{t,r}}(k,m)\Gamma_{C_{t,r}}(k,m) - \Gamma_{D_{t,r}}(k,m)}{c_{2_k}^{(t,r)}(m)\gamma_{k,\min}^{(t,r)}(m)}] - P_T, \tag{4.22}$$

$$\Gamma_{F_{t,r}}(k,m) = \sum_{k=1}^{K}\sum_{t=1}^{N_t}\sum_{r=1}^{N_r}\sum_{m=1}^{M}\frac{\Gamma_{C_{t,r}}(k,m)}{c_{2_k}^{(t,r)}(m)\gamma_{k,\min}^{(t,r)}(m)}, \tag{4.23}$$

$$\Gamma_{B_{t,r}}(k,m) = \ln[\varphi_{t,r}(k,m)\Gamma_{A_{t,r}}(k,m)c_{1_k}^{(t,r)}(m)c_{2_k}^{(t,r)}(m)\gamma_{k,\min}^{(t,r)}(m)], \tag{4.24}$$

$$\Gamma_{C_{t,r}}(k,m) = \varphi_{t,r}(k,m)P_{sc_k}^{(t,r)}(m), \tag{4.25}$$

and

$$\Gamma_{D_{t,r}}(k,m) = \ln[\Gamma_{C_{t,r}}(k,m)]\Gamma_{C_{t,r}}(k,m). \tag{4.26}$$

Based on the achieved power distribution formula of (4.20), the bit allocation of the information bit streams over the utilised sub-channels at each transmit antenna can be achieved in an iterative way as shown in Algorithm 8. This algorithm follows the same work steps of Algorithm 6 that explains the bit and power allocation algorithm of the proposed decoupled UBPA strategy.

Step 1. MCS initialisation:
Set all bands into highest MCS options
Step 2. Power evaluation:
Initialisation:
foreach k **do**
  foreach t **do**
    foreach r **do**
      foreach m **do**
        $P_{sc_k}^{(t,r)}(m) = \xi_k^{(t,r)}(m) P_{s_k}^{(t,r)}(m)$.
        $\mu_k^{(t,r)}(m) = \left(\frac{\Gamma_{B_{t,r}}(k,m) - \ln(\Omega) - \ln[\varphi_{t,r}(k,m) P_{sc_k}^{(t,r)}(m)]}{c_{2_k}^{(t,r)}(m) \gamma_{k,\min}^{(t,r)}(m)} \right)^+$.
      end
    end
  end
end
Step 3. Power constraints check:
if $\sum_{k=1}^{K} \sum_{t=1}^{N_t} \sum_{r=1}^{N_r} \sum_{m=1}^{M} \varphi_{t,r}(k,M) \mu_k^{(t,r)}(m) P_{sc_k}^{(t,r)}(m)] = P_T$ *and* $\mu_k^{(t,r)}(m) \geq 0$ **then**
  Go to step 4.
end
else
  foreach k **do**
    foreach t **do**
      foreach r **do**
        foreach m **do**
          if $\gamma_{k,\min}^{(t,r)}(m) \leqslant 4$ **then**
            Set this sub-channel to no transmission option.
          end
          else
            Reduce the MCS option levels for the sub-channels with lower $\gamma_{k,\min}^{(t,r)}(m)$.
            Go to step 2
          end
        end
      end
    end
  end
end
Step 4. Transmission:
Transmit the OFDMA frame.

Algorithm 8: The proposed bit and power allocation algorithm of RA strategy for the MIMO-AMC-OFDMA

4.2.3 Simulation Results and Discussion

The performance of the investigated MIMO-AMC-OFDMA system based on the proposed RA and conventional strategies has been studied. This system considers the parameters of Table 2.1. The number of users, $k = 15$, and a spatial multiplexing MIMO system equipped with different numbers of transmit and receive antennas are considered. Most of the results are achieved in terms of the average SNR values of all users, γ_{av}, as a function of the average SNR of g-th transmitted OFDMA block, $\gamma_{av_g} = E\{\gamma_{k,\min}^{*(t,r)}(m)\}$. The presented results compare the performance of three systems as follows:

1. MIMO-OFDMA-conventional resource allocation (CRA) system that adopts the bit and power allocation algorithm of [38], where this algorithm has been developed to work with MIMO systems based on combining coding rate of 3/4 with QPSK, 16-QAM and 64-QAM modulation types.

2. MIMO-OFDMA-proposed resource allocation (PRA), which uses the proposed bit and power allocation algorithms of the RA strategy.

3. MIMO-OFDMA-RA system, which considers the proposed user, bit and power allocation of the RA strategy.

The average throughput performance of the investigated MIMO systems for different number of transmit and receive antennas is compared in Fig. 4.2. The achieved average system throughput for $N_{fr} = 1000$ transmitted OFDMA block from all transmit antennas are computed based on (2.45).

From Fig. 4.2, it is evident that the MIMO-OFDMA-RA system outperforms the other MIMO schemes throughout the included sub-figures. In addition, the MIMO-OFDMA-PRA system throughput is improved in comparison with the MIMO-OFDMA-CRA scheme. The enhancement in the performance of the proposed MIMO-OFDMA-RA scheme over other systems is due to the exploiting of the MIMO channel and user diversities by the employed RA strategy. Additionally, the proposed user allocation algorithm assigns the optimal sub-channel to each user at transmit antenna t based on the best SISO link with the N_r receive antennas rather than the sequential users distribution. The proposed power allocation algorithm distributes the total BS transmission power over the utilised sub-channels of all transmit antennas optimally to increase the resilience of them against the channel fade effects. Furthermore, the

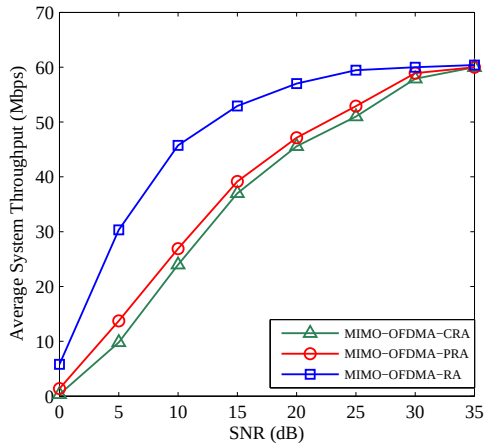

(a) $N_t = 1$, $N_r = 1$.

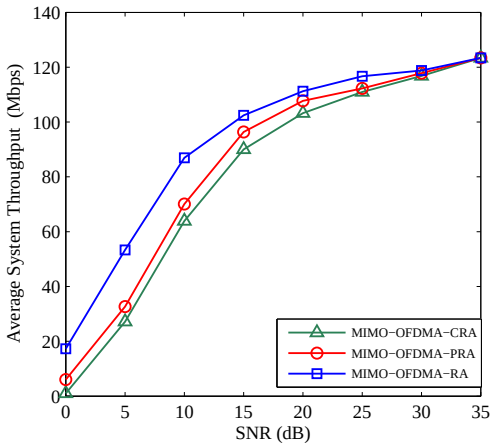

(b) $N_t = 2$, $N_r = 2$.

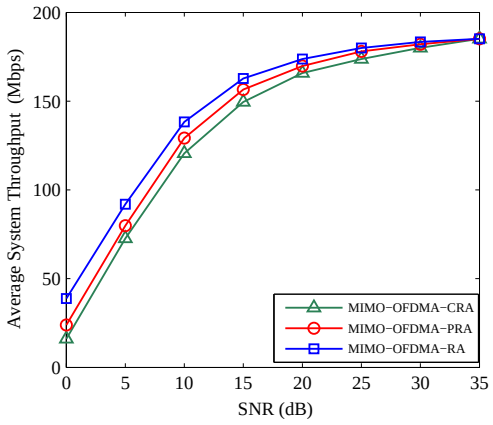

(c) $N_t = 3$, $N_r = 3$.

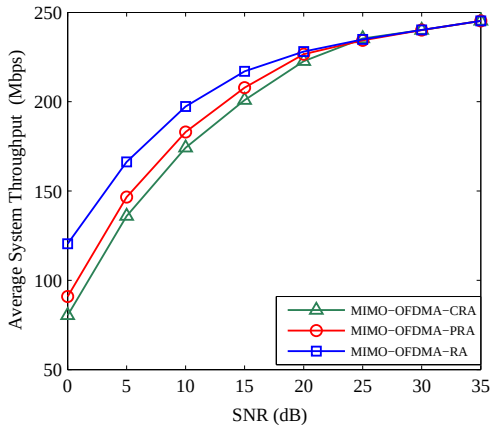

(d) $N_t = 4$, $N_r = 4$.

Figure 4.2: Average system throughput for the investigated MIMO-AMC-OFDMA systems.

bit allocation algorithm of the proposed RA strategy raises the selected MCS levels for each sub-channel assigned to a user, in which the related channel conditions and the power constraints are satisfied. Otherwise, the MIMO-AMC-OFDMA-RA system prevents any transmission over the sub-channels with worst conditions and distributes the assigned sub-carriers across other sub-channels. Moreover, the improvement of the MIMO-OFDMA-PRA over MIMO-OFDMA-CRA is the results of the utilising of the proposed bit and power allocation algorithms of the RA strategy.

Fig. 4.3 demonstrates the performance of the average spectral efficiency, ρ_{av}, expressed in (bps/Hz) for the considered MIMO systems. In addition, ρ_{av} can be evaluated in terms of the spectral efficiency of the m-th sub-channel that assigned to the k-th user from the t-th transmit antenna to the r-th receive antenna, $\rho_k^{(t,r)}(m)$, for N_{fr} blocks as

$$\begin{aligned}\rho_{av} &= \frac{1}{N_{fr}} \sum_{g=1}^{N_{fr}} \rho_{av_g} \\ &= \frac{1}{N_{fr}} \sum_{g=1}^{N_{fr}} \frac{1}{K} \sum_{k=1}^{K} \sum_{t=1}^{N_t} \sum_{r=1}^{N_r} \sum_{m=1}^{M} \varphi_{t,r}(k,m) \rho_k^{(t,r)}(m).\end{aligned} \tag{4.27}$$

where ρ_{av_g} is the average spectral efficiency for each block transmitted from N_t transmit antennas. From this figure, the performance of MIMO-OFDMA-RA system is shown to exceed other compared schemes. Furthermore, the performance of the MIMO-OFDMA-PRA is significantly increased over the conventional approach. It is important to note that the enhancement of the proposed MIMO-OFDMA-RA over other schemes is the result of exploiting the MIMO channel and multiuser diversities, which allows the transmitter to select high MCS levels for the sub-channels over the considered SNR values. Additionally, the throughput increasing of the MIMO-OFDMA-PRA over the last approach is due to the optimal power distribution that allows the sub-channels with worst conditions to select medium and high MCS levels.

The throughput outage probability as a function of the average system throughput and the upper throughput bound, $\psi_{MIMO,UB}$, for the investigated approaches is presented in Fig. (4.4). The throughput outage probability is evaluated following (2.46). Additionally, $\psi_{MIMO,UB}$ can be evaluated as

$$\psi_{MIMO,UB} = N_t B_{eff} \rho_{max}. \tag{4.28}$$

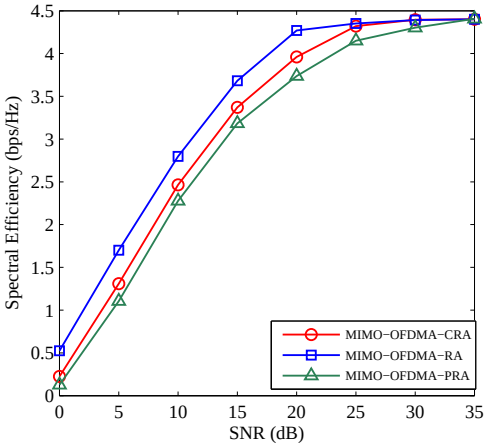

(a) $N_t = 1$, $N_r = 1$.

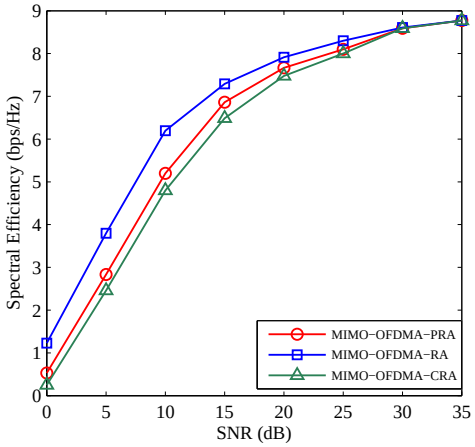

(b) $N_t = 2$, $N_r = 2$.

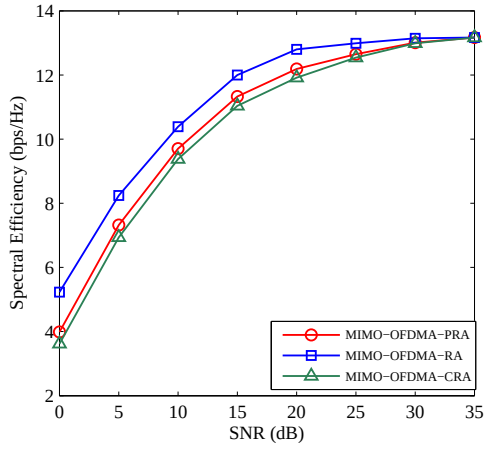

(c) $N_t = 3$, $N_r = 3$.

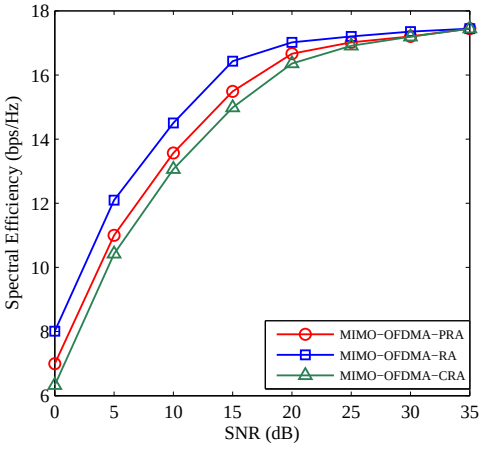

(d) $N_t = 4$, $N_r = 4$.

Figure 4.3: Spectral efficiency for the investigated MIMO-AMC-OFDMA systems.

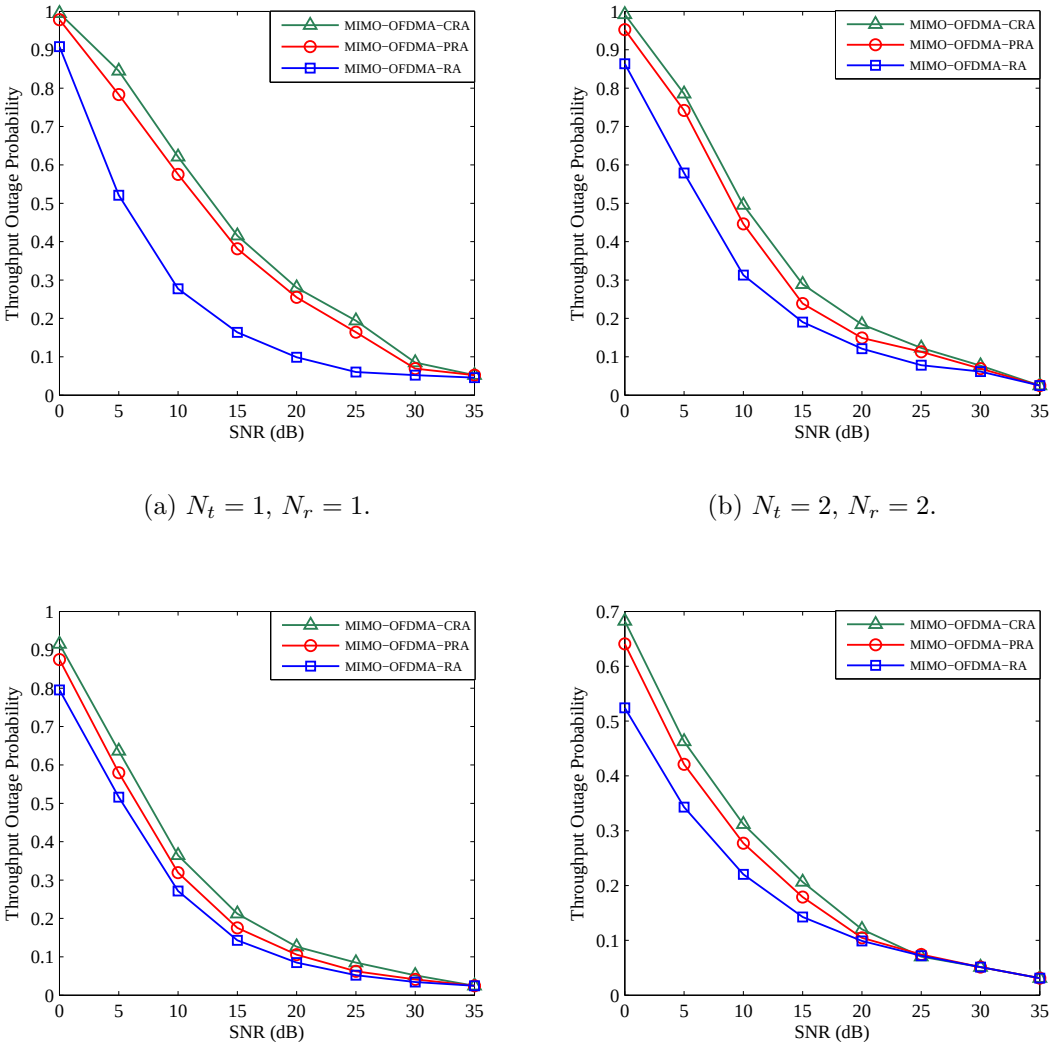

(a) $N_t = 1$, $N_r = 1$.

(b) $N_t = 2$, $N_r = 2$.

(c) $N_t = 3$, $N_r = 3$.

(d) $N_t = 4$, $N_r = 4$.

Figure 4.4: Throughput outage probability for the investigated MIMO-AMC-OFDMA systems.

This figure illustrates that the proposed RA strategy of the MIMO-OFDMA-RA system achieves low outage probability in comparison with the other two schemes. It is evident that the increasing in the number of transmit and receive antennas can improve the performance for all investigated systems significantly.

4.3 RA for SVD Based MIMO-AMC-OFDMA

The introduced RA strategy for spatial multiplexing MIMO-AMC-OFDMA system, expressed in the previous Section, has been modified to accommodate the eigen mode or a singular value decomposition (SVD) transmission. In spatial mul-

tiplexing MIMO technique, the SVD transmission provides an accurate information regarding the spacial mode channels in comparison with the selection of the best channel profiles in each transmit antenna due to the consideration of the antenna interferences. As mentioned earlier, the proposed RA strategy aims to maximise the average system throughput as a function of spectral efficiency and BER.

4.3.1 SVD-MIMO-AMC-OFDMA System Model

SVD based MIMO downlink channel between an assigned BS to K mobile users has been considered [70]. The system parameters of Table 2.1 are considered. Additionally, the system block diagram, shown in Fig. 4.1, of the downlink MIMO-AMC-OFDMA with the same functions of the included blocks is also considered.

In terms of the utilised channel profiles, the ITU channels are considered to generate i.i.d time varying MIMO multipath fading channels [102]. The utilised MIMO channel between k-th user and the assigned BS in terms of the d-th sub-carrier within the m-th sub-channel is mathematically expressed by (4.1). The considered channel can be formulated in terms of SVD as

$$\mathbf{H} = \mathbf{U}\mathbf{\Sigma}\mathbf{V}^{H}, \tag{4.29}$$

where $\mathbf{\Sigma}$ is a $\Psi \times \Psi$ diagonal matrix containing the singular values $\varsigma_1, \varsigma_1, ..., \varsigma_\Psi$ as diagonal elements, and Ψ is the number of obtained eigen values. The terms $\mathbf{U}$ and $\mathbf{V}$ denote $N_r \times \Psi$ and $N_t \times \Psi$ complex unitary matrices, respectively. The columns of these matrices are called the left and right singular vectors, respectively. Additionally, both $\mathbf{U}$ and $\mathbf{V}$ contain orthogonal columns, i.e. $\mathbf{U}^H\mathbf{U} = \mathbf{I}$ and $\mathbf{V}^H\mathbf{V} = \mathbf{I}$, where $\mathbf{I}$ is an identity matrix with dimensions $\Psi \times \Psi$ and $(.)^H$ is the Hermitian operation. Based on SVD transmission concepts and Fig. 4.5, the transmitted signal vector is reformulated as [3]

$$\mathbf{X} = \mathbf{V}\mathbf{X}. \tag{4.30}$$

Based on (4.30), the received signal can be mathematically written as

$$\mathbf{Y} = \mathbf{H}\mathbf{X} + \mathbf{W} = \mathbf{H}\mathbf{V}\mathbf{X} + \mathbf{W}. \tag{4.31}$$

At the receiver side, the received signal vector is processed with $\mathbf{U}^H$, which yields

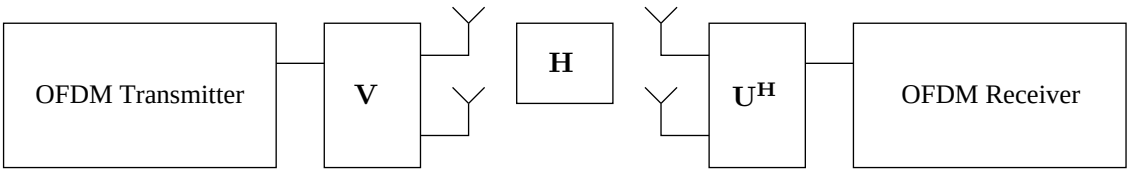

Figure 4.5: SVD approach of MIMO system.

to obtain the transmitted signal vector as

$$\begin{aligned}
\mathbf{X} &= \mathbf{U}^H\mathbf{Y}, && (4.32a)\\
&= \mathbf{U}^H\mathbf{H}\mathbf{V}\mathbf{X} + \mathbf{U}^H\mathbf{W}, && (4.32b)\\
&= \mathbf{U}^H\mathbf{U}\mathbf{\Sigma}\mathbf{V}^H\mathbf{V}\mathbf{X} + \mathbf{\Sigma}\mathbf{U}^H\mathbf{W}, && (4.32c)\\
&= \mathbf{\Sigma}\mathbf{X} + \mathbf{U}^H\mathbf{W}. && (4.32d)
\end{aligned}$$

It is important to note that the number of spatial channels, N_c, for each sub-carrier in the m-th sub-channel is bounded by $\min(N_t, N_r)$. In other words, $\mathbf{H}_k^{(m,d)}$ is a full rank matrix, i.e. $N_c = \min(N_t, N_r)$ for $k \in \{1, .., K\}$ users and $m \in \{1, .., M\}$ sub-channels for a rich scattering environment.

The MIMO channel diversity and the implementation of the proposed resource allocation are expected to improve the throughput performance of the MIMO-AMC-OFDMA system. The throughput of g-th OFDMA block, which includes different transmitted OFDMA frames from N_t antennas over N_c channels can be formulated as

$$\begin{aligned}
\psi_g = &\sum_{k=1}^{K}\sum_{m=1}^{M}\varphi(k,m)\sum_{r=1}^{N_c}\xi_k^{(r)}(m)\rho_k^{(r)}(m)\\
&-\sum_{k=1}^{K}\sum_{m=1}^{M}\varphi(k,b)\sum_{r=1}^{N_c}\xi_k^{(r)}(m)\rho_k^{(r)}(m)P_{e_k}^{(r)}(m),
\end{aligned} \tag{4.33}$$

where $\varphi(k,m) \in \{0,1\}$ is the value of the user allocation matrix that assigns the user k to the sub-channel m [70]. The term $\xi_k^{(r)}(m)$ denotes the number of data sub-carriers of the sub-channel m assigned to the user k propagated over the spatial channel r. Moreover, $\rho_k^{(r)}(m)$ denotes the related spectral efficiency. Furthermore, the BER, $P_{e_k}^{(r)}(m)$, is approximately evaluated based on (3.6) as

$$P_{e_k}^{(r)}(m) = c_{1_k}^{(r)}(m) \exp[-c_{2_k}^{(r)}(m)\gamma_{k,\min}^{*(r)}(m)], \tag{4.34}$$

where $\gamma_{k,\min}^{*(r)}(m)$ is the minimum SNR value that can be computed as

$$\gamma_{k,\min}^{*(r)}(m) = \mu_k^{(r)}(m)\gamma_{k,\min}^{(r)}(m) = \mu_k^{(r)}(m) \min[\gamma_{s_k}^{(r)}(m,d)], \tag{4.35}$$

where $\gamma_{s_k}^{(r)}(m,d)$ is the average SNR value for the d-th data sub-carriers of the m-th sub-channel and $d \in \{1,...,\xi_k^{(r)}(m)\}$ denotes the data sub-carrier index. In addition, $\gamma_{s_k}^{(r)}(m,d)$ is evaluated as

$$\gamma_{s_k}^{(r)}(m,d) = E\{|X_{k_r}^{(m,d)}|^2\} \frac{\alpha_{k_r}^{(m,d)}}{E\{|W_{k_r}^{(m,d)}|^2\}}, \tag{4.36a}$$

$$= P_{s_k}^{(r)}(m) \frac{\alpha_{k_r}^{(m,d)}}{\sigma^2_{W_{k_r}^{(m,d)}}(m)}, \tag{4.36b}$$

where $P_{s_k}^{(r)}(m) = E\{|X_{k_r}^{(m,d)}|^2\}$ is the average power value of the modulated and coded symbols for each sub-channel. Additionally, $\sigma^2_{W_{k_r}^{(m,d)}}(m) = E\{|W_{k_r}^{(m,d)}|^2\}$ is the variance of the AWGN coefficients. The term $[\alpha_{k_r}^{(m,d)}]_{r\in\{1,...,N_c\}}$ denotes the r-th eigenvalue of $[\mathbf{H}_k^{(m,d)}\big(\mathbf{H}_k^{(m,d)}\big)^H]$.

4.3.2 Proposed RA Strategy for SVD-MIMO-AMC-OFDMA

The throughput maximisation problem for MIMO-AMC-OFDMA system, expressed in (4.5)-(4.9), can be rewritten in terms of eigen mode transmission as

$$\begin{aligned} \text{Maximise } \psi_g = &\sum_{k=1}^{K}\sum_{m=1}^{M} \varphi(k,m) \sum_{r=1}^{N_c} \xi_k^{(r)}(m)\rho_k^{(r)}(m) \\ &- \sum_{k=1}^{K}\sum_{m=1}^{M} \varphi(k,b) \sum_{r=1}^{N_c} \xi_k^{(r)}(m)\rho_k^{(r)}(m)P_{e_k}^{(r)}(m), \end{aligned} \tag{4.37}$$

subject to:

$$\sum_{k=1}^{K}\sum_{m=1}^{M} \varphi(k,m) \sum_{r=1}^{N_c} \mu_k^{(r)}(m)P_{sc_k}^{(r)}(m) = P_T, \tag{4.38}$$

$$\mu_k^{(r)}(m) \geq 0, \tag{4.39}$$

$$\sum_{k=1}^{K} \varphi(k,m) = 1, \quad m = 1, ..., M, \tag{4.40}$$

$$\sum_{m=1}^{M} \varphi(k,m) = 1, \quad k = 1, ..., K. \tag{4.41}$$

In contrast, two approaches have been introduced to solve the investigated maximisation problem of (4.37)-(4.41) as below.

Optimised Approach

The optimised approach provides an optimal solution of the throughput maximisation problem using the Lagrange multiplier method and KKT conditions [62]. The Lagrangian function of the investigated problem can be written as

$$\begin{aligned} L\Big[\varphi(k,m), \mu_k^{(r)}(m)\Big] = & \sum_{k=1}^{K}\sum_{m=1}^{M}\sum_{r=1}^{N_c} \varphi(k,m)\xi_k^{(r)}(m)\rho_k^{(r)}(m) \\ & - \sum_{k=1}^{K}\sum_{m=1}^{M}\sum_{r=1}^{N_c} \big\{\varphi(k,m)\xi_k^{(r)}(m)\rho_k^{(r)}(m)c_{1_k}^{(r)}(m) \\ & \cdot \exp[\frac{-\varphi(k,m)c_{2_k}^{(r)}(m)\mu_k^{(r)}(m)\gamma_{k,\min}^{(r)}(m)}{\varphi(k,m)}]\big\} \\ & - \Omega\big[\sum_{k=1}^{K}\sum_{m=1}^{M}\sum_{r=1}^{N_c} \varphi(k,m)\mu_k^{(r)}(m)P_{sc_k}^{(r)}(m) - P_T\big] \\ & - \sum_{k=1}^{K} \eta_m(k)\big[\sum_{m=1}^{M} \varphi(k,m) - 1\big] \\ & - \sum_{m=1}^{M} \eta_k(m)\big[\sum_{k=1}^{K} \varphi(k,m) - 1\big], \end{aligned} \tag{4.42}$$

where the BER formula of (4.34) is rewritten based on (4.12) as

$$P_{e_k}^{*(r)}(m) = c_{1_k}^{(r)}(m)\exp[\frac{-\varphi(k,m)c_{2_k}^{(r)}(m)\gamma_{k,\min}^{(r)}(m)}{\varphi(k,m)}]. \tag{4.43}$$

The solution steps of the optimised approach of UBPA strategy for SISO-AMC - OFDMA system are followed to achieve the optimal user, bit and power allocation. Therefore, the Lagrange multiplier $\eta_m(k)$ is obtained from (4.42) as

$$\eta_m(k) = \sum_{r=1}^{N_c} \Gamma_{A_r}(k,m) - \Omega \sum_{r=1}^{N_c} \frac{P_{sc_k}^{(r)}(m)}{c_{2_k}^{(r)}(m)\gamma_{k,\min}^{(r)}(m)} - \Omega \sum_{r=1}^{N_c} \mu_k^{(r)}(m) P_{sc_k}^{(r)}(m) - \eta_k(m), \tag{4.44}$$

where $\Gamma_{A_r}(k,m) = \xi_k^{(r)}(m)\rho_k^{(r)}(m)$. Additionally, the optimal user for each sub-channel that maximise the system throughput is obtained as

$$k_{\text{opt}}(m) = \arg\max_k \eta_m(k), \quad k \in \{1, ..., K\}. \tag{4.45}$$

Based on (4.45), the user allocation value $\varphi(k,m)$ is evaluated as

$$\varphi(k,m) = \begin{cases} 1, & \text{if } k = k_{\text{opt}}(m), \\ 0, & \text{otherwise,} \end{cases} \quad \forall m \in \{1, ..., M\}. \tag{4.46}$$

Based on water filling level λ, the Lagrange multiplier Ω can be computed as

$$\Omega = \frac{1}{\lambda \ln 2}, \tag{4.47}$$

thus, the desired power value that adjusts the optimal power for m-th sub-channel can be evaluated as

$$\mu_k^{*(r)}(m) = \frac{\Omega - \frac{P_{sc_k}^{(r)}(m)}{\gamma_{k,\min}^{(r)}(m)}}{P_{sc_k}^{(r)}(m)}. \tag{4.48}$$

The proposed user and power allocation algorithm is illustrated in algorithm 9.

Decoupled Approach

As highlighted earlier, the decoupled approach can reduce the computational complexity of the optimised one significantly. Thus, a practical solution to the investigated complex problem expressed in (4.37)-(4.41) is introduced by decoupling the problem into two sub-problems and propose an algorithm to solve each one based on decomposition method as follows [62].

User allocation: The user allocation sub-problem is presented and solved by a proposed algorithm. It is assumed that the information bits are allocated to highest MCS option. Additionally, the total transmission power of the BS are distributed equally over the employed M sub-channels that assigned to K users. Therefore,

Step 1. MCS initialisation:
Set all sub-channels into highest MCS option
Step 2. $P_{sc_k}^{(r)}(m)$ **initialisation:**
Initialisation:
foreach k **do**
  foreach m **do**
    foreach r **do**
      $P_{sc_k}^{(r)}(m) = \xi_k^{(r)}(m) P_{s_k}^{(r)}(m)$.
      $\mu_k^{(r)}(m) = \frac{P_T}{N_c M P_{sc_k}^{(r)}(m)}$.
    end
  end
end
Step 3. λ **initialisation:**
initialise $\lambda = 0.001$.
Step 4. Optimal user allocation:
while $\lambda < 10$ **do**
  foreach k **do**
    foreach m **do**
      implementing of (4.45) (4.46) and (4.47).
    end
  end
  Step 5. Power evaluation in terms of λ**:**
  if $\sum_{k=1}^{K} \sum_{m=1}^{M} \varphi(k,m) \mu_k^{*(r)}(m) P_{sc_k}^{(r)}(m) \neq P_T$ **then**
    $\lambda = \lambda + \frac{\lambda}{2}$, $\mu_k^{*(r)}(m) = \frac{\Omega - \frac{P_{sc_k}^{(r)}(m)}{\gamma_{k,\min}^{(r)}(m)}}{P_{sc_k}^{(r)}(m)}$.
  end
  else
    λ is the optimal value and $\mu_k^{*(r)}(m) = \frac{\Omega - \frac{P_{sc_k}^{(r)}(m)}{\gamma_{k,\min}^{(r)}(m)}}{P_{sc_k}^{(r)}(m)}$. Go to step 6
  end
end
Reduce the MCS option level for the bands with minimum SNR values. Go to step 2.
Step 6. Adjustment of the optimal power value $P_{sc_k}^{*(r)}(m)$ **for each sub-channel in terms of** λ**:**
foreach k **do**
  foreach m **do**
    foreach r **do**
      $P_{sc_k}^{*(r)}(m) = \mu_k^{*(r)}(m) P_{sc_k}^{(r)}(m)$.
    end
  end
end

Algorithm 9: The proposed algorithm of the optimised RA strategy for SVD based MIMO-AMC-OFDMA system

the power constraints expressed in (4.38) and (4.39) are removed. In contrast, the Lagrangian function is written as

$$\begin{aligned} L[\vartheta(k,b)] = & \sum_{k=1}^{K}\sum_{m=1}^{M}\vartheta(k,m)\sum_{r=1}^{N_c}\xi_k^{(r)}(m)\rho_k^{(r)}(m) \\ & - \sum_{k=1}^{K}\sum_{m=1}^{M}\vartheta(k,m)\sum_{r=1}^{N_c}\Bigg\{\xi_k^{(r)}(m)\rho_k^{(r)}(m) \\ & \cdot c_{1_k}^{(r)}(m)\exp\Big[\frac{-\varphi(k,m)c_{2_k}^{(r)}(m)\mu_k^{(r)}(m)\gamma_{k,\min}^{(r)}(m)}{\varphi(k,m)}\Big]\Bigg\} \\ & - \sum_{m=1}^{M}\eta_k(m)\Big[\sum_{k=1}^{K}\varphi(k,m)-1\Big] \\ & - \sum_{k=1}^{K}\eta_m(k)\Big[\sum_{m=1}^{M}\varphi(k,m)-1\Big], \end{aligned} \tag{4.49}$$

where $\eta_k(m)$ and $\eta_m(k)$ are the Lagrange multipliers. It should be noted that the best allocation $\varphi(k,m)$ of the k-th user over the m-th sub-channel can be achieved within the relaxed continuous domain of the closed interval $[0,1]$. Based on the mathematical processes of the decoupled approach of UBPA strategy for the SISO-AMC-ODMA system, the active Lagrange multiplier can be obtained as

$$\begin{aligned} \eta_m(k) = & \sum_{r=1}^{N_c}\Gamma_{A_r}(k,m) - \sum_{r=1}^{N_c}\Gamma_{A_r}(k,m)\{c_{1_k}^{(r)}(m) \\ & \cdot\exp[-c_{2_k}^{(r)}(m)\mu_k^{(r)}(m)\gamma_{k,\min}^{(r)}(m)]\} - \eta_k(m). \end{aligned} \tag{4.50}$$

Additionally, $\eta_k(m)$, which is also called as *user allocation value*, has been set to zero when the user k has not assigned to sub-channel m yet. Then, the user allocation value is maximised to prevent the selection of the same sub-channel by another user.

In this work, the user allocation problem is solved in the discrete domain, i.e. $\vartheta(k,m)\in\{0,1\}$. In this domain, the m-th sub-channel is allocated to the k-th user with maximum $\eta_k(m)$ value. The maximum value amongst $\eta_k(m)$, $k_{\text{opt}}(m)$, can be evaluated as

$$k_{\text{opt}}(m) = \underset{k}{\arg\max}\{\eta_m(k)\},\ \ k \in \{1, ..., K\}. \tag{4.51}$$

Based on (4.51), the $\varphi(k, m)$ values are evaluated as

$$\varphi(k, m) = \left\{ \begin{array}{ll} 1, & \text{if } k = k_{\text{opt}}(m) \\ 0, & \text{otherwise} \end{array} \right\},\ \forall\ \ m \in \{1, ..., M\}. \tag{4.52}$$

Step 1. MCS initialisation:
Set all sub-channels at the transmit antennas into highest MCS options
Step 2. $P_{sc_k}^{(r)}(m)$ **initialisation:**
Initialisation:
foreach k **do**
  foreach r **do**
    foreach m **do**
      $P_{sc_k}^{(t)}(m) = \xi_k^{(r)}(m) P_{s_k}^{(r)}(m)$.
      $\mu_k^{(r)}(m) = \frac{P_T}{N_c M P_{sc_k}^{(r)}(m)}$.
      $\eta_k(m) = 0$
    end
  end
end
Step 4. User allocation:
foreach k **do**
  foreach r **do**
    foreach m **do**
      Implement (4.50) and (4.51).
      Implement (4.52).
      Maximise $\eta_k(m)$.
    end
  end
end

Algorithm 10: The proposed user allocation algorithm of the decoupled RA strategy for SVD based MIMO-AMC-OFDMA system.

The proposed user allocation algorithm allocates the users over the sub-channels for N_c channels by evaluating $\varphi(k, m)$ values in an iterative way. Algorithm 10 illustrates the proposed user allocation algorithm. It is important to note that the steps of the user allocation algorithm of the RA strategy for MIMO-AMC-OFDMA, expressed in Algorithm 7, are considered with the required modifications.

Bit and power allocation: The proposed power allocation algorithm that tackles the second investigated sub-problem is presented here. Under the assumption of achieving the user allocation and the highest MCS option is selected, the user allocation constraints of (4.40) and (4.41) are removed. Based on Lagrange multiplier method, the Lagrangian function can be written as

$$\begin{aligned} L[\mu_k^{(r)}(m)] = & \sum_{k=1}^{K}\sum_{m=1}^{M}\varphi(k,m)\sum_{r=1}^{N_c}\Gamma_{A_r}(k,m) \\ & - \sum_{k=1}^{K}\sum_{m=1}^{M}\varphi(k,m)\sum_{r=1}^{N_c}\{\Gamma_{A_r}(k,m)c_{1_k}^{(r)}(m) \\ & \cdot \exp[-c_{2_k}^{(r)}(m)\mu_k^{(r)}(m)\gamma_{k,\min}^{(r)}(m)]\} \\ & - \Omega\big[\sum_{k=1}^{K}\sum_{m=1}^{M}\vartheta(k,m)\sum_{r=1}^{N_c}\mu_k^{(r)}(m)P_{sc_k}^{(r)}(m)\big] - P_T. \end{aligned} \tag{4.53}$$

where Ω is a Lagrange multiplier that controls the required power values for the sub-channels. Additionally, $\mu_k^{(r)}(m)$ can be evaluated as

$$\mu_k^{(r)}(m) = \left(\frac{\Gamma_{B_r}(k,m) - \ln(\Omega) - \ln[\varphi(k,m)P_{sc_k}^{(r)}(m)]}{c_{2_k}^{(r)}(m)\gamma_{k,\min}^{(r)}(m)}\right)^{+}, \tag{4.54}$$

where

$$\Gamma_{B_r}(k,m) = \ln[\varphi(k,m)\Gamma_{A_r}(k,m)c_{1_k}^{(r)}(m)c_{2_k}^{(r)}(m)\gamma_{k,\min}^{(r)}(m)]. \tag{4.55}$$

The value of $\ln(\Omega)$ is computed as

$$\ln(\Omega) = \frac{\Gamma_{E_r}(k,m)}{\Gamma_{F_r}(k,m)}, \tag{4.56}$$

where

$$\begin{aligned} \Gamma_{E_r}(k,m) = & \sum_{k=1}^{K}\sum_{m=1}^{M}\sum_{r=1}^{N_c}[\frac{\Gamma_{B_r}(k,m)\Gamma_{C_r}(k,m)}{c_{2_k}^{(r)}(m)\gamma_{k,\min}^{(r)}(m)}] \\ & - \sum_{k=1}^{K}\sum_{m=1}^{M}\sum_{r=1}^{N_c}[\frac{\Gamma_{D_r}(k,m)}{c_{2_k}^{(r)}(m)\gamma_{k,\min}^{(r)}(m)}] - P_T, \end{aligned} \tag{4.57}$$

$$\Gamma_{F_r}(k,m) = \sum_{k=1}^{K}\sum_{m=1}^{M}\sum_{r=1}^{N_c}\frac{\Gamma_{C_r}(k,m)}{c_{2_k}^{(r)}(m)\gamma_{k,\min}^{(r)}(m)}, \tag{4.58}$$

$$\Gamma_{C_r}(k,m) = \varphi(k,m)P_{sc_k}^{(r)}(m), \tag{4.59}$$

and

$$\Gamma_{D_r}(k,m) = \ln[\Gamma_{C_r}(k,m)]\Gamma_{C_r}(k,m). \tag{4.60}$$

On the other hand, the bit allocation for each sub-channel at a spatial channel r can be performed by selecting the suitable MCS level from the employed ten options, in which the related power constraints and channel conditions are satisfied. Algorithm 11 illustrates the proposed bit and power allocation algorithm following the aspects of Algorithm 8.

4.3.3 Simulation Results and Discussion

The behaviour of the investigated SVD based spatial multiplexing MIMO-AMC-OFDMA system that adopts the proposed RA strategy is investigated. The system parameters listed in Table 2.1 have been considered for each transmitted OFDMA frame from the t-th antenna. In contrast, distinct ITU channel profiles shown in Table 2.4 are adopted to generate a rich scattering MIMO multiuser environment. The obtained results are based on $k = 15$, as well as different number of the transmit and receive antennas. The considered SNR values in the simulation results represent the average SNR of all users evaluated based on (3.50). The presented results compare the performance of the following systems:

1. MIMO-OFDMA-optimised resource allocation (ORA) that adopts the optimised approach of the proposed SVD based RA strategy.

2. MIMO-AMC-decoupled resource allocation (DRA), which considers the decoupled approach of the proposed SVD based RA strategy.

3. MIMO-OFDMA-conventional resource allocation (CRA) that utilises the bit and power allocation algorithm of [38] as explained in the previous Section.

4. MIMO-OFDMA-proposed resource allocation (PRA), which employs the proposed bit and power allocation algorithm of the decoupled approach of SVD

Step 1. MCS initialisation:
Set all bands into highest MCS options
Step 2. Power evaluation:
Initialisation:
foreach k **do**
  foreach m **do**
    foreach r **do**
      $P_{sc_k}^{(r)}(m) = \xi_k^{(r)}(m) P_{s_k}^{(r)}(m)$.
      $\mu_k^{(r)}(m) = \left(\frac{\Gamma_{B_r}(k,m) - \ln(\Omega) - \ln[\varphi(k,m) P_{sc_k}^{(r)}(m)]}{c_{2_k}^{(r)}(m) \gamma_{k,\min}^{(r)}(m)} \right)^+$.
    end
  end
end
Step 3. Power constraints check:
if $\sum_{k=1}^{K} \sum_{m=1}^{M} \sum_{r=1}^{N_c} \varphi(k,m) \mu_k^{(r)}(m) P_{sc_k}^{(r)}(m)] = P_T$ *and* $\mu_k^{(r)}(m) \geq 0$ **then**
  Go to step 4.
end
else
  foreach k **do**
    foreach m **do**
      foreach r **do**
        if $\gamma_{k,\min}^{(r)}(m) \leqslant 4$ **then**
          Set this sub-channel to no transmission option.
        end
        else
          Reduce the MCS option levels for the sub-channels with lower $\gamma_{k,\min}^{(r)}(m)$.
          Go to step 2
        end
      end
    end
  end
end
Step 4. Transmission:
Transmit the OFDMA frame.

Algorithm 11: The proposed bit and power allocation algorithm of the decoupled RA strategy for SVD based MIMO-AMC-OFDMA system.

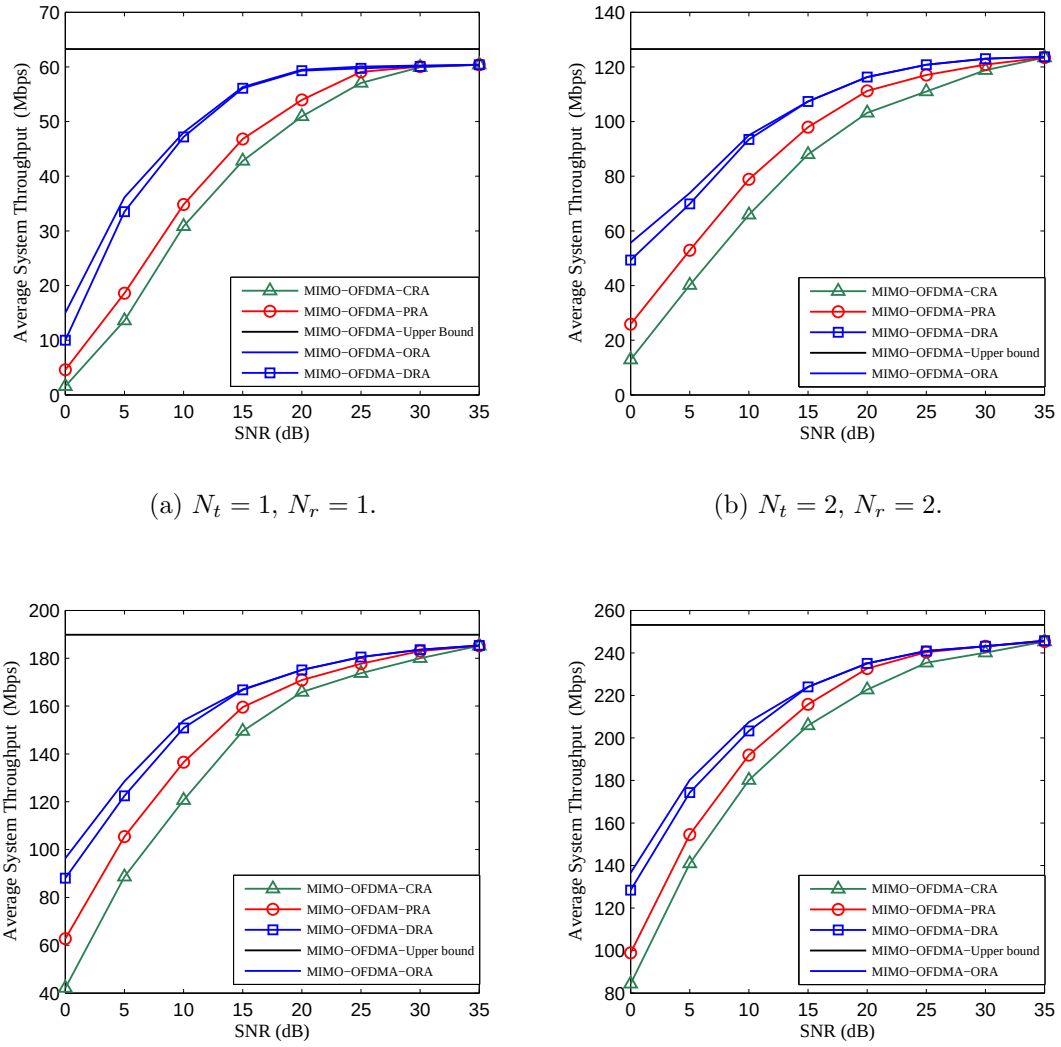

(a) $N_t = 1$, $N_r = 1$.

(b) $N_t = 2$, $N_r = 2$.

(c) $N_t = 3$, $N_r = 3$.

(d) $N_t = 4$, $N_r = 4$.

Figure 4.6: Average system throughput for the investigated SVD-MIMO-AMC-OFDMA systems.

based RA strategy.

Fig. 4.6 shows the performance of the investigated system in terms of the average system throughput for different number of $N_t = N_r$. The achieved average system throughputs for $N_{fr} = 1000$ transmitted OFDMA block are achieved based on (2.45).

From Fig. 4.6, the performance of the MIMO-OFDMA-ORA system is shown to exceed the other schemes for different number of transmit and receive antennas. The upper-bound throughput shown in the figure represents the maximum expected value that the proposed strategy aimed to reach. This value can be evaluated based on (4.28). It is noted that the performance of both approaches of the proposed

strategy becomes closer to the upper throughput bound more than other compared approaches over medium and high SNR values.

The achieved improvement in the performance of the MIMO-OFDMA-ORA and MIMO-OFDMA-DRA schemes over other systems is due to the use of the proposed RA strategy that exploits the available channel diversity and resources efficiently. In contrast, the MIMO-OFDMA-PRA system outperforms the MIMO-OFDMA-CRA as it considers different convolutional coding rates in addition to the employed modulation types. This can yield a high flexibility of choosing the suitable MCS. It is important to note that the eigen mode transmission adopted by the SVD based MIMO systems can improve the throughput performance of these systems in comparison with the performance of the MIMO schemes that adopt the previous approach as shown in Fig. 4.6 and Fig. 4.2. The reason behind this enhancement is the consideration of the multi transmit antennas interference by eigen mode transmission in the process of allocating the available resources rather than adopting the best SISO link between a transmit antenna and receive antennas.

Fig. 4.7 shows the throughput performance of the MIMO-OFDMA-ORA, MIMO-OFDMA-DRA, MIMO-OFDMA-PRA and MIMO-OFDMA-CRA systems for $N_t = 2, 3$, while the N_r is set with different numbers. It is noted that the increasing in the number of receive antennas can improve the performance of the investigated system due to the MIMO channel diversity that has been exploited to increase the spectral efficiency and decrease the BER. The spectral efficiency is improved by selecting higher MCS options. These figures explain the superior of the MIMO-OFDMA-ORA system over other approaches since it employs the proposed RA strategy. Furthermore, the performance of this system is closer to the upper bound, which is evaluated based on (4.28), than other schemes particularly for high number of receive antennas N_r.

The throughput outage probability is presented in Fig. 4.8 for different $N_t = N_r$ numbers. The MIMO-OFDMA-ORA and MIMO-OFDMA-DRA achieve lowest throughput outage probability. At the same time, the MIMO-OFDMA-PRA scheme obtains lower outage probability than the MIMO-OFDMA-CRA. It is important to note that the performance of the SVD based MIMO-OFDMA systems shown in this figure is improved significantly in comparison with the performance of the MIMO-OFDMA schemes expressed in Fig. 4.4. This is because of the adopting of eigen mode transmission, which considers the interference of the multiple antennas signals.

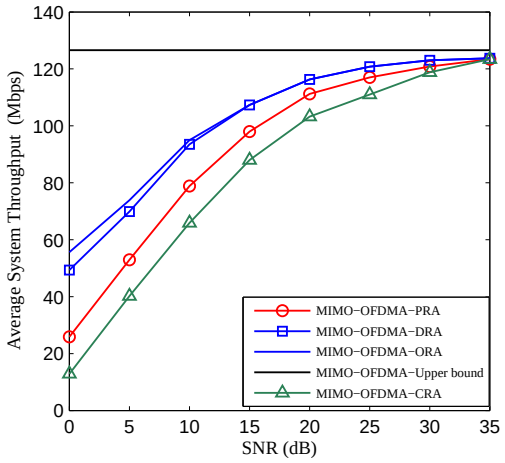

(a) $N_t = 2$, $N_r = 2$.

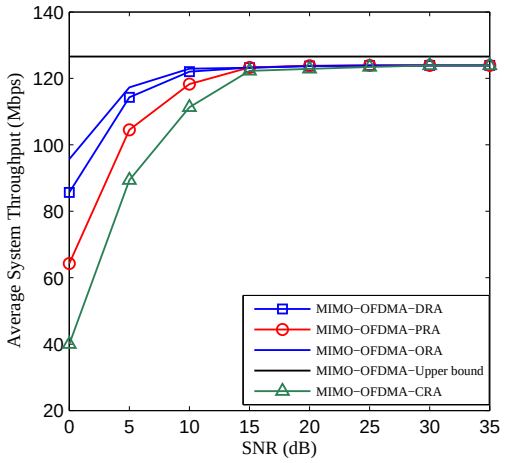

(b) $N_t = 2$, $N_r = 4$.

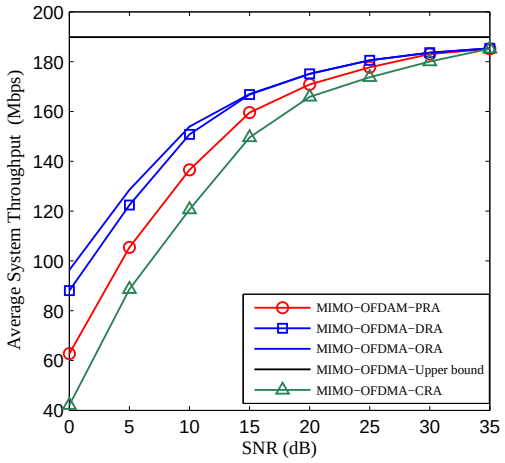

(c) $N_t = 3$, $N_r = 3$.

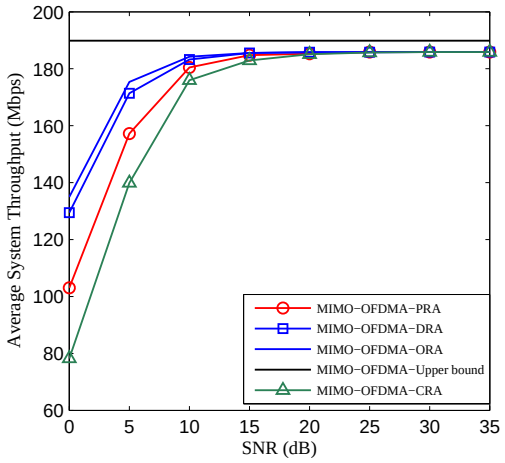

(d) $N_t = 3$, $N_r = 5$.

Figure 4.7: Average system throughput for the investigated SVD-MIMO-AMC-OFDMA systems in terms of different number of receive antennas.

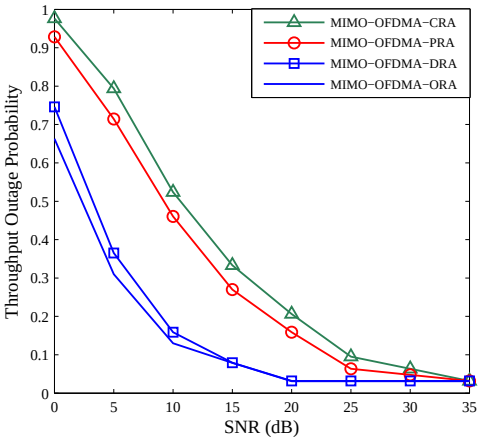

(a) $N_t = 1$, $N_r = 1$.

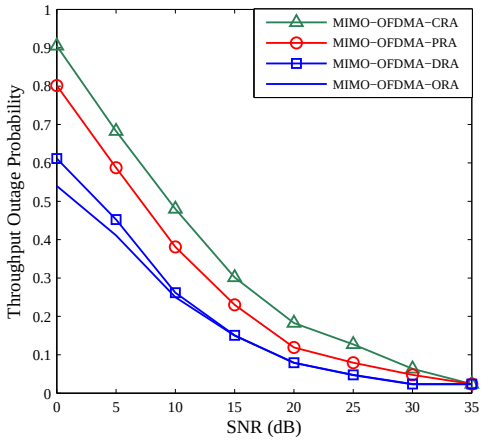

(b) $N_t = 2$, $N_r = 2$.

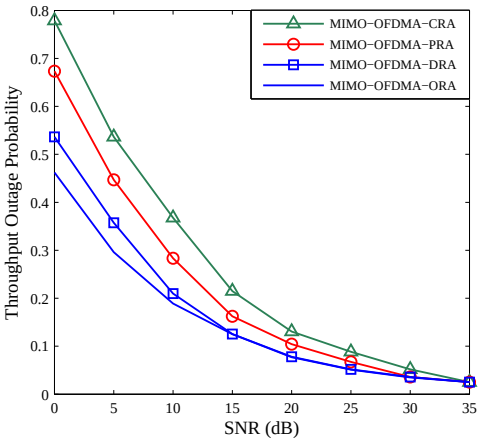

(c) $N_t = 3$, $N_r = 3$.

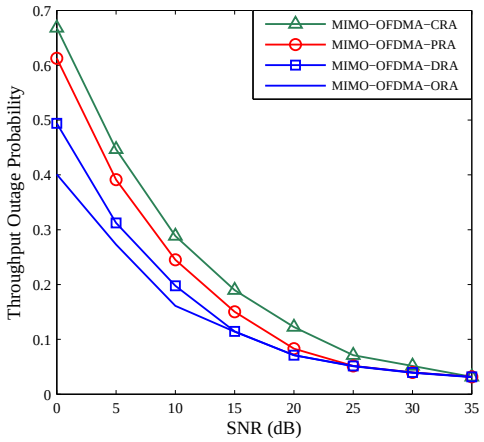

(d) $N_t = 4$, $N_r = 4$.

Figure 4.8: Outage probability of the average system throughput for the investigated SVD-MIMO-AMC-OFDMA systems .

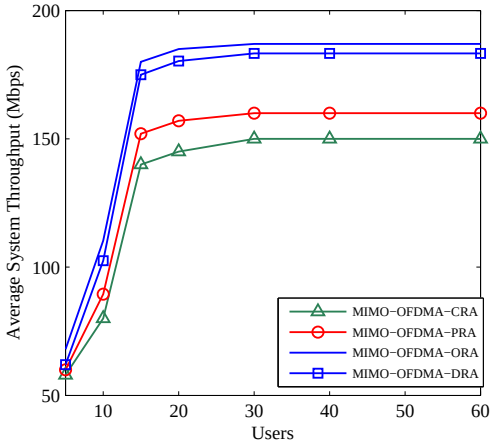

(a) 5 dB.

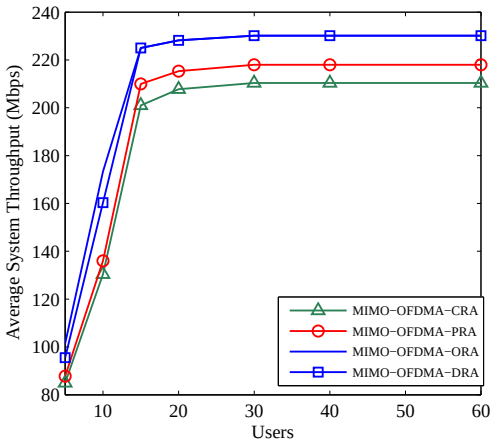

(b) 15 dB.

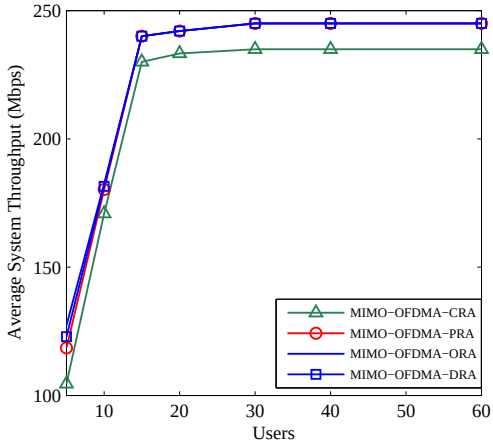

(c) 25 dB.

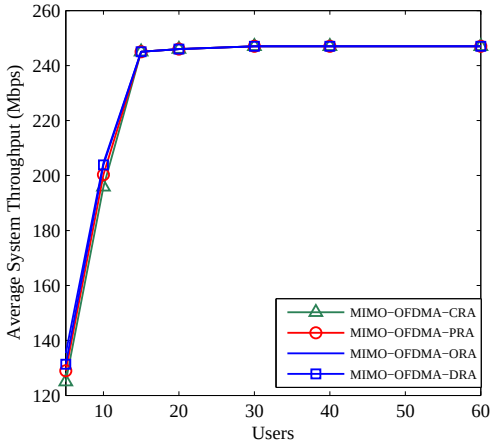

(d) 35 dB.

Figure 4.9: Average System throughput v.s. number of users for the investigated $N_t = N_r = 4$ SVD-MIMO-AMC-OFDMA systems.

Fig. 4.9 illustrates the average system throughput of the four MIMO approaches in terms of the number of users for average SNR values of 5, 15, 25 and 35 dB, as well as $N_t = N_r = 4$. It is apparent that the performance of the investigated systems is improved significantly with the increasing in the number of users due to multiuser diversities. Furthermore, the proposed RA strategy exploits the channel diversity more than other approaches. It is also highlighted that the throughput of the MIMO-OFDMA-PRA system can exceeds the conventional approach because of using the proposed bit and power allocation algorithms. In contrast, the same throughput performance of the investigated systems is achieved after 30 users because of reaching the multiuser diversity saturation.

4.4 Chapter Summary

This Chapter explained the expansion of the proposed UBPA strategy, presented in Chapter 3, to work with spatial multiplexing based MIMO systems. The same software engineering life cycle model, used for designing resource allocation strategy of SISO-AMC-OFDMA system, has been adopted to build the structure of the MIMO based resource allocation strategies. Two resource allocation strategies were proposed for MIMO systems. The first one allocated the available resources at each individual transmit antenna based on the best SISO channel profile between such antenna and the involved receive antennas without any consideration to received signal interferences. The second strategy allocated the information bits and the transmission power amongst the sub-channels assigned to different users based on SVD method, i.e. the eigen mode transmission. The latest strategy provided an accurate evaluation as it considered the interferences between the received signal at each receive antenna. The proposed RA strategies for MIMO systems were established on the known channel profiles and fixed sub-channelling method. The simulation results discussed the performance of the proposed strategies for distinct systems.

Chapter 5

User Scheduling Software Algorithms for SISO-AMC-OFDMA Systems

Multi-carrier-multiple-access systems that work across open system interconnection (OSI) layers, such as OFDMA, have been adopted by most mobile networks to increase data rates and average system throughput. The OSI layers manage the information transmission between the assigned BS and mobile terminals, i.e. users, using efficient protocols. Moreover, each layer is designed to achieve a specific target, such as scheduling and resource allocation in addition to the AMC techniques, which utilise different MCS options.

In this Chapter, a cross-layer scheduling and resource allocation (SRA) strategy for SISO-AMC-OFDMA system has been presented based on a developed software engineering life cycle model. This strategy adopts the proposed UBPA for SISO-AMC-OFDMA systems introduced in Chapter 3 as well as AMC and pilot adjustment schemes presented in Chapter 2. It aims to maximise the average system throughput as a function of the BER and spectral efficiency by considering different combinations of modulation types and coding rates within each transmitted OFDMA frame, in addition to the priority of the included users. SRA sorts the users into queues based on their priorities and then selects the optimal user that can maximise the system throughput in each queue to guarantee fair services for all users in different priority levels. It also fills the empty queues with the higher priority users to offer more bandwidth for these users. Furthermore, SRA allocates the

available resources amongst sub-channels depending on the related CSI and the total transmission power constraints. In this work, the performance of the proposed SRA is compared with the conventional first in first out (FIFO) queuing based scheduling and resource allocation strategies used for an SISO-AMC-OFDMA system. The simulation results show that the investigated SISO-AMC-OFDMA system based on the proposed SRA strategy outperforms the conventional approaches.

5.1 Developed Life Cycle Model for User Scheduling and Resource Allocation Algorithm

The proposed user scheduling algorithm is combined with the introduced resource allocation. Thus, a two levels life cycle model is designed based on evolutionary methodology as shown in Fig. 5.1 [17], [18]. The *System Requirement* block of the first level collects the required information, which includes CSI and user priority, to implement the designed algorithm. The design requirements of the user scheduling algorithm is passed to the next block, i.e. *System Design and Implementation*. In this block, the user are sorted in queues depending on the priority and then the optimal user that can maximise the average system throughput in each queue is selected.

The scheduled users have been forwarded to the first block of the second level, which is *System Requirements*. This block collects the CSI and the available resources for the scheduled users and passes the design requirements to the second block, i.e. *System Design and Implementation*. The distribution of the user, information bits and power amongst the sub-channels is obtained in this block. After the allocation of the resources, the algorithm is tested over different channel profiles. In addition, the achieved results are analysed in the last blocks.

5.2 SRA-SISO-AMC-OFDMA System Model

A Mobile WiMAX IEEE 802.16e system is considered with the parameters listed in Table 2.1. Fig. 5.2 shows the block diagram of the SRA strategy for a single-cell downlink SISO-AMC-OFDMA system. Following the design of the OSI layers, the system structure is divided into three layers, as described below.

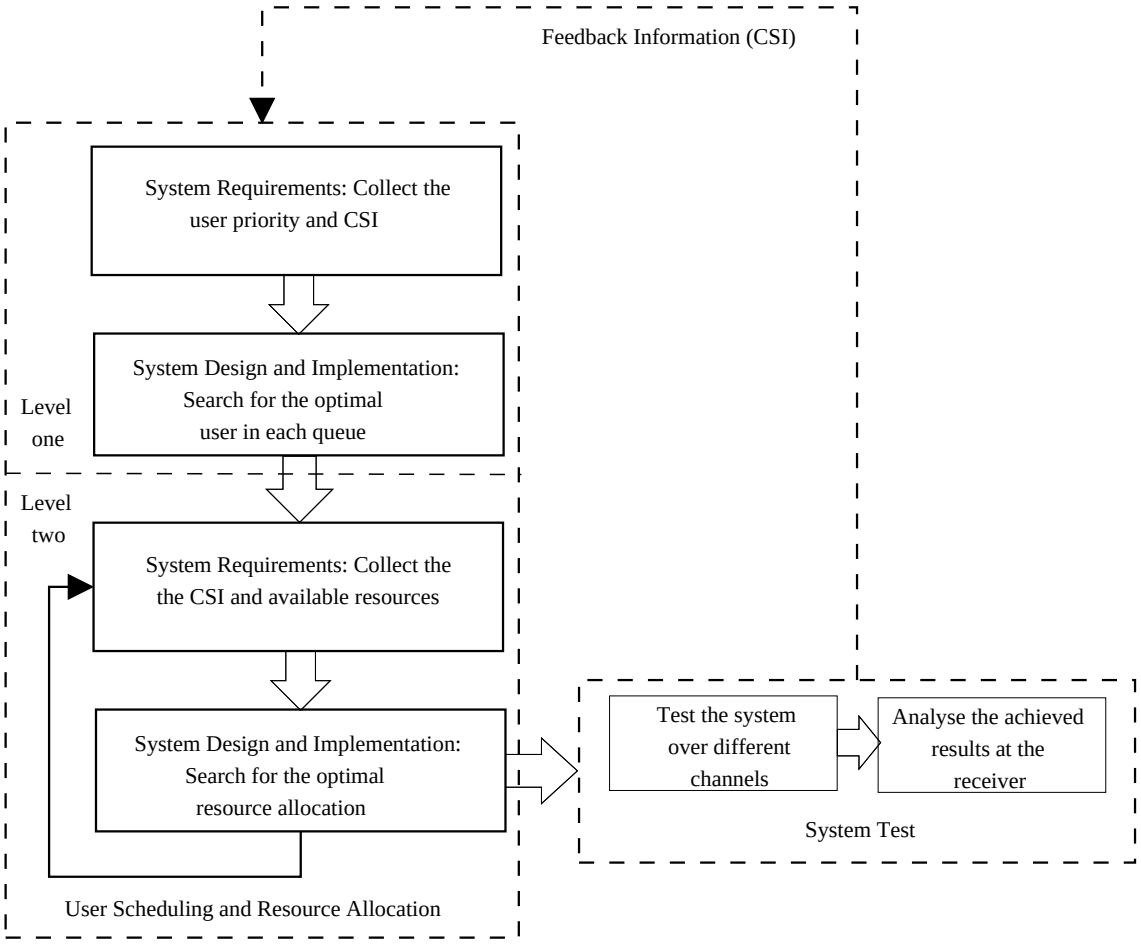

Figure 5.1: Developed life cycle model for the proposed user scheduling algorithm.

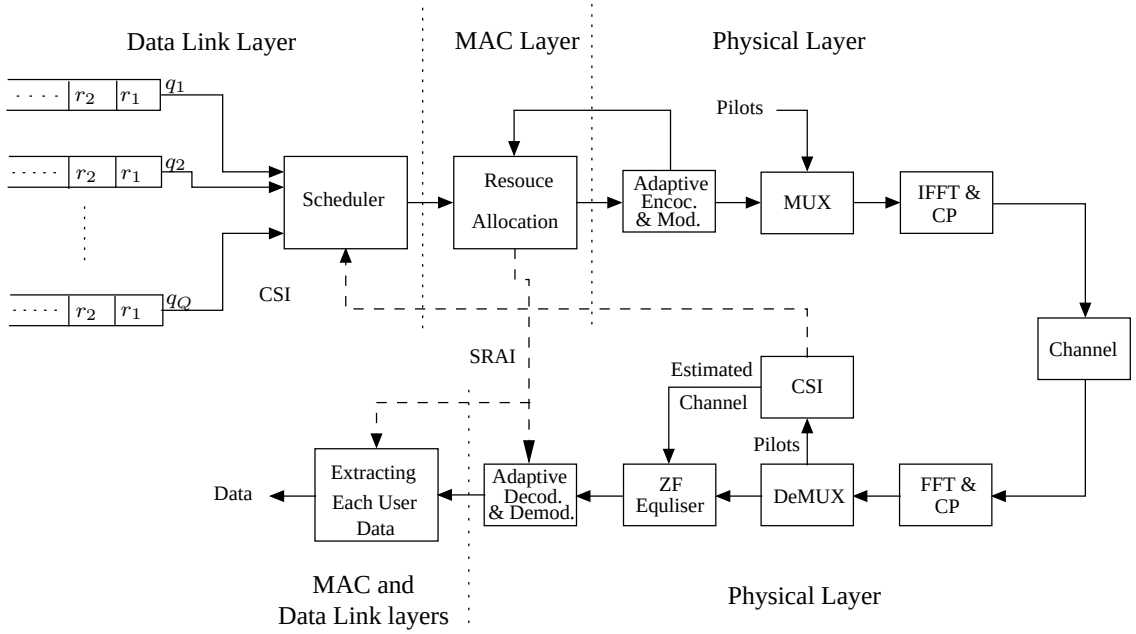

Figure 5.2: Block diagram of the cross-layer SRA strategy based SISO-AMC-OFDMA system.

5.2.1 Data link layer

In this layer, the data and related CSI of all users are collected. In Fig. 5.2, the *scheduler* block implements the scheduling algorithm of the proposed SRA strategy that arranges the users in Q queues according to their priority. Moreover, each queue is assumed to have unlimited capacity and contains $R(q)$ users with an index of $r = 1, ..., R(q)$, where $q = 1, ..., Q$ is the queue index. The other function of the proposed scheduling algorithm is the selection of a user that can maximise the average system throughput in each queue.

It should be noted that the proposed user scheduling strategy concentrates on arranging the data of all users at the same time rather than managing the data packets of each user individually as expressed in the literature of [77]-[88]. In these research papers, the service waiting time, length of the data packets and the queue conditions were considered and expressed in mathematical formulas. These formulas sorted the problem of outdated data and long waiting time for serving each user. However, these methods ignored the serving of different users with distinct conditions, such as priority, at the same time. In this work, the users of all priority levels are served simultaneously and more bandwidth is allocated for users with high priority by filling the empty queues. In other words, the benefit of priority is considered and also different users from different priority level have been served depending on

their channel conditions. The empty queues are the results of designing the system with a sufficient number of priority queues, in which these queues are practically not filled. On the other hand, the fair service concept is adopted in the proposed user scheduling strategy. In this work, the fair service means that the SRA strategy serves different users from all priority levels at the same time as shown in Fig. 5.2. Additionally, there is a preference for high priority users by assigning more bandwidth for them using the empty queues. It is also important to mention that the only drawback of the proposed method is the long serving waiting time for users with worst channel. This drawback is recommended to be solved in future work.

In contrast, it is assumed that at the transmit instant, T, one data packet of the selected user in each queue is served. Additionally, the queue state information (QSI) of each queue that includes the number of users and the related information expiry time is changed every T by updating the number of new and served users, as well as their time statues. Although queuing delay has not been considered in this work, the expiry time for each user is utilised to prevent sending any outdated information and save the system bandwidth for other mobile terminals. The scheduler passes the scheduled users to the next layer, which is the MAC layer.

5.2.2 MAC layer

The proposed resource allocation algorithm is implemented in this layer by the *Resource Allocation* block, as shown in Fig. 5.2. The CSI and the information of the scheduled users are fed into this block to allocate the user, bit and power amongst the sub-channels of the transmitted OFDMA frame according to the related CSI and the power constraints. The proposed resource allocation algorithm controls the selection of the suitable MCS for each scheduled user that can be assigned to a sub-channel in the physical layer using an iterative method until the constraints and the channel conditions are satisfied. It is important to note that the scheduled users after this layer can be indexed by q, since the number of scheduled users is equal to the number of utilised queues.

5.2.3 Physical layer

In this work, a downlink transmission of a wireless OFDMA system from an assigned BS to corresponding mobile users scheduled from Q queues is considered. The sched-

uled Q users are allocated into M distinct sub-channels with index $m = 1, ..., M$, in which there is one user per sub-channel. The sub-carriers of the AMC-OFDMA system are divided into $N_d = 1440$ data sub-carriers, $N_p = 240$ pilot sub-carriers and $N_g = 368$ guard sub-carriers. The data and pilot sub-carriers are initially distributed over the sub-channels equally in a range of $\xi_{q_d}(r, m) = N_d/M$ and $\xi_{q_p}(r, m) = N_p/M$, respectively, for each sub-channel that is assigned to the selected r-th user of the q-th queue.

As shown in Fig. 5.2, the physical layer of the transmitter contains three main blocks. The function of the first block is to encode and modulate the information bit streams depending on the selected MCS option for each sub-channel. The second block mixes the pilots with the coded and modulated symbols. Finally, the last block of the transmitter implements the IFFT and CP insertion operations.

Different mobile vehicular ITU channel profiles are considered in order to generate different time varying channels for distinct users to simulate the random physical measurements of users around the assigned BS [11]. As highlighted in the previous Chapters, each ITU channel profile expressed by Table 2.4 has been considered by different user category.

In this Chapter, the scheduling and the resource allocation information (SRAI) for distinct sub-channels is assumed to be sent to the receiver of each user using downlink control signals [67]. The CP is removed and the FFT operation is applied to the entire OFDMA frame at the receiver of a user. Following the FFT operation, the related channel coefficients are estimated in *CSI* block utilising LS method as [10]

$$\hat{H}_{q_p}^{(r)}(m, z_p) = \frac{Y_{q_p}^{(r)}(m, z_p)}{X_{q_p}^{(r)}(m, z_p)}, \tag{5.1}$$

where $X_{q_p}^{(r)}(m, z_p)$ are the transmitted pilots assigned for the r-th user in the q-th queue over the m-th sub-channel, while $Y_{q_p}^{(r)}(m, z_p)$ are the related received pilots and $z_p \in \{1, \ldots, \xi_{q_p}(r, m)\}$ represents the pilot index. The first order linear interpolation method is adopted to obtain the channel fading values that correspond to the data sub-carriers, $\hat{H}_{q_d}(m, z_d)$, where $z_d \in \{1, \ldots, \xi_{q_d}(r, m)\}$ is the index of data sub-carriers of the m-th sub-channel. In this work, the channel estimation error, caused by the channel estimation is also considered as additional noise to the received signal. Therefore, the received signal at each user can be represented in terms of transmitted

data sub-carriers, $X_{q_d}^{(r)}(m, z_d)$, and the AWGN samples, $W_{q_d}^{(r)}(m, z_d)$, following (3.2) as

$$\begin{aligned} Y_{q_d}^{(r)}(m, z_d) =& X_{q_d}^{(r)}(m, z_d)\hat{H}_{q_d}^{(r)}(m, z_d) + X_{q_d}^{(r)}(m, z_d) \\ & \cdot [H_{q_d}^{(r)}(m, z_d) - \hat{H}_{q_d}^{(r)}(m, z_d)] + W_{q_d}^{(r)}(m, z_d). \end{aligned} \tag{5.2}$$

Based on (5.2), the SNR value of each received data sub-carrier can be computed as

$$\gamma_q^{(r)}(m, z_d) = P_{s_q}(r, m)\frac{|H_{d_q}^{(r)}(m, z_d)|^2}{\sigma_{q_d}^2(r, m)P_{s_q}(r, m) + \sigma^2_{W_{d_q}^{(r)}(m,z_d)}(r, m)}, \tag{5.3}$$

where, $P_{s_q}(r, m) = E\{|X_{d_q}^{(r)}(m, z_d)|^2\}$ is the average coded and modulated symbol power, $\sigma_{q_d}^2(r, m)$ is the variance of square error of the channel and $\sigma^2_{W_{d_q}^{(r)}(m,z_d)}(r, m)$ is the variance of the AWGN samples. The minimum SNR among the sub-carriers within each sub-channel is selected to be the sub-channel SNR value based on (3.4) as

$$\gamma_{q,\min}(r, m) = \min\{\gamma_q^{(r)}(m, z_d)\},\ q = 1, \ldots, Q. \tag{5.4}$$

As the aim of this work is to maximise the average system throughput by allocating the transmission power over the transmitted sub-channels, the SNR value is affected by the power adjustment value, $\mu_q(r, m)$, as

$$\gamma^*_{q,\min}(r, m) = \mu_q(r, m)\gamma_{q,\min}(r, m). \tag{5.5}$$

It is important to note that the $\mu_q(r, m)$ refines the power value for the m-th sub-channel. As highlighted in Chapter 3, $\mu_q(r, m) = \frac{P_T}{M\xi_{q_d}(r,m)P_{s_q}(r,m)}$, for the equal power distribution, where P_T is the total considered power for a BS. The estimated channel coefficients that correspond to data sub-carriers are entered in the *ZF Equliser* block and then to the *Adaptive Decod. and Demod.* block. In this block, the received data symbols for each sub-channel are demodulated and decoded according to the selected MCS, which is included in the SRAI. At the same time, the generated CSI is sent back to the transmitter using TDD uplink.

The average system throughput, ψ_{av}, is the average value of N_{fr} transmitted OFDMA frame throughputs, ψ_g, where $g = 1, ..., N_{fr}$ is the frame index. The system throughput for each OFDMA symbol can be written as

$$\psi_g = \sum_{q=1}^{Q} \sum_{r=1}^{R(q)} \sum_{m=1}^{M} \beta(q,r)\varphi(q,m)\xi_{q_d}(r,m)\rho_{av_q}(r,m)[1 - P_{e_q}(r,m)], \tag{5.6}$$

where $P_{e_q}(r,m)$ denotes the average BER of each sub-channel assigned to the r-th user from the q-th queue. Additionally, the user scheduling matrix elements, $\beta(q,r)$, set '1' for the selected r-th user in the q-th queue and '0' for others. Whereas $\varphi(q,m)$ denote the elements of the scheduled user allocation matrix. Each element is set to '1' for the m-th sub-channel assigned to the scheduled q-th user and '0' for the other sub-channels in order to achieve fairness in user allocation over the OFDMA frame. The average spectral efficiency, $\rho_{av_q}(r,m)$, expressed in (bps/Hz) as a function of the coding rate, $R_{c_q}(r,m)$, and the number of modulation states, $M_q(r,m)$, is obtained from $\rho_{av_q}(r,m) = R_{c_q}(r,m)\log_2[M_q(r,m)]$.

5.3 Approximated BER Evaluation

The BER is computed using the proposed method, expressed in Chapter 3, that starts from the approximated BER formula of

$$P_{e_q}(r,m) = c_{1_q}(r,m)\exp[-c_{2_q}(r,m)\gamma_{q,\min}(r,m)], \tag{5.7}$$

where $c_{1_q}(r,m)$ and $c_{2_q}(r,m)$ are selected variables for fitting the theoretical BER to practical values. The fitting accuracy depends mainly on the proper evaluation of these variables for different MCS options.

5.4 Dynamic Sub-Channelling for SRA-SISO-AMC-OFDMA

At the physical layer of the receiver, the *CSI* block applies the proposed pilot adjustment scheme that optimises the required number of pilots for the channel estimation in each sub-channel. The combination of the pilot adjustment scheme and the proposed scheduling and resource allocation strategy is adopted following the procedure

concepts of the dynamic sub-channelling for SISO-AMC-OFDMA system. Therefore, the refined number of data and pilot sub-carriers can be written in terms of the reduction value of required pilots for each user, $\Pi_q(r,m)$, based on (2.33)-(2.35) as

$$\delta_{q_p}(r,m) = \xi_{q_p}(r,m) - \Pi_q(r,m), \tag{5.8}$$

$$\delta_{q_d}(r,m) = \xi_{q_d}(r,m) + \Pi_q(r,m), \tag{5.9}$$

where

$$\Pi_q(r,m) = \zeta_q(r,m)\frac{B_{q,coh}\gamma_{q,\min}(r,m)}{\sigma^2_{q,\Xi_q(m,z)}(r,m)}, \tag{5.10}$$

and $\zeta_q(r,m)$ is a constant value that guarantees the equal distribution of the new number of data and pilot sub-carriers amongst the sub-channels. Additionally, $B_{q,coh}$ and $\sigma^2_{q,\Xi_q(m,z)}(r,m)$ refer to the detected coherence bandwidth of the scheduled user in the q-th queue and the variance of the SNR fluctuation values, respectively. The adjusted number of data and pilot sub-carriers, $\delta_{q_d}(r,m)$ and $\delta_{q_d}(r,m)$, are adopted throughout the mathematical formulas of this Chapter.

5.5 Feedback CSI Analysis for SRA-SISO-AMC-OFDMA

The same feedback CSI overhead analysis of SISO-AMC-OFDMA presented in Chapter 3 system is considered in this Chapter. The only difference is the $R(q)$-th dimension of the users in the Q queues. Thus, the feedback delay, $T_{q,CSI}(r,m)$, for the m-th sub-channel of the user r in the q-th queue can be expressed following (2.29) as

$$T_{q,CSI}(r,m) = \frac{N^{(q)}_{B,CSI}(r,m)}{R_{b,q}(r,m)}, \tag{5.11}$$

where $R_{b,q}(r,m)$ is the bit rate of the corresponding feedback link and $N^{(q)}_{B,CSI}(r,m)$ refers to the number of bits that are required to convey the feedback CSI associated with sub-channel m. These two metrics are evaluated as shown in Chapter 3.

The real effective total channel bandwidth B_{eff} available for the downlink trans-

mission of all users is mathematically expressed in terms of total channel bandwidth, B_T, and the total bandwidth used by the feedback CSI, B_{CSI}, following (2.44) as

$$B_{eff} = \left[\frac{\sum_{q=1}^{Q}\sum_{r=1}^{R(q)}\sum_{m=1}^{M}\beta(q,r)\varphi(q,m)\delta_{q_d}(r,m)}{N_{FFT}}\right]\left[B_T - B_{CSI}\right], \tag{5.12}$$

It can be shown that this bandwidth B_{CSI} can be expressed as a function of the feedback delays $T_{q,CSI}(r,m)$ based on (2.30) as

$$B_{CSI} = \sum_{q=1}^{Q}\sum_{r=1}^{R(q)}\sum_{m=1}^{M}\frac{\beta(q,r)\varphi(q,m)}{T_{q,CSI}(r,m)}. \tag{5.13}$$

5.6 Proposed SRA strategy for SISO-AMC-OFDMA

The complex throughput optimisation problem, which can be solved by the proposed SRA strategy, is mathematically expressed as

$$\text{Maximise} \quad \psi_g = \sum_{q=1}^{Q}\sum_{r=1}^{R(q)}\sum_{m=1}^{M}\beta(q,r)\varphi(q,m)\delta_{q_d}(r,m)\rho_{av_q}(r,m)[1-P_{e_q}(r,m)], \tag{5.14}$$

Subject to:

$$\sum_{q=1}^{Q}\sum_{r=1}^{R(q)}\sum_{m=1}^{M}\beta(q,r)\varphi(q,m)\mu_q(r,m)P_{sc_q}(r,m) = P_T, \tag{5.15}$$

$$\mu_q(r,m) \geq 0, \tag{5.16}$$

$$\sum_{r=1}^{R(q)}\beta(q,r) = 1, \quad q = 1,...,Q, \tag{5.17}$$

$$\sum_{q=1}^{Q}\varphi(q,m) = 1, \quad m = 1,...,M, \tag{5.18}$$

$$\sum_{m=1}^{M}\varphi(q,m) = 1, \quad q = 1,...,Q, \tag{5.19}$$

where (5.15) and (5.16) refer to the total power constraints, (5.17) denotes the scheduling constraint that selects one user for each utilised queue, whilst (5.18) and (5.19) are the fairness constraints that guarantee the allocation of one user per sub-channel. Additionally, $P_{sc_q}(r,m) = \delta_{q_d}(r,m)P_{s_q}(r,m)$ denotes the average power of the sub-channel that is assigned to the r-th user of the q-th queue as a function of the average coded and modulated symbol power, $P_{s_q}(r,m)$. It is apparent that the problem expressed in (5.14)-(5.19) is convex and there are significant difficulties for it to be determined analytically due to mathematical complexity. Therefore, this problem is decoupled into two main sub-problems based on the decomposition method to obtain a practical solution. These sub-problems can be solved by proposing two algorithms, i.e. scheduling and resource allocation.

5.6.1 User Scheduling

In this work, the user scheduling is adopted rather than the data packets of each user [82],[77], [80], [78]. In order to achieve the best scheduling of the users, equal power allocation amongst the entitled sub-channels of users and sequential user assignment are assumed, i.e. the power and user fairness allocation constraints of (5.15), (5.16), (5.18) and (5.19) are removed. In this case, the user allocation matrix, $\varphi(q,m)$, is also removed.

In order to obtain the $\beta(q,r)$ values, which select the optimal user in each queue, the Lagrange multiplier optimisation method is utilised. Based on (5.7), (5.14) and (5.17), the Lagrangian function, $L[\beta(q,r)]$, can be written as a function of $\beta(q,r)$ as

$$\begin{aligned} L[\beta(q,r)] = & \sum_{q=1}^{Q}\sum_{r=1}^{R(q)}\sum_{m=1}^{M}\beta(q,r)\delta_{q_d}(r,m)\rho_{av_q}(r,m) \\ & - \sum_{q=1}^{Q}\sum_{r=1}^{R(q)}\sum_{m=1}^{M}\Big\{\beta(q,r)\delta_{q_d}(r,m)\rho_{av_q}(r,m)c_{1_q}(r,m) \\ & \cdot \exp[\frac{-\beta(q,r)c_{2_q}(r,m)\mu_q(r,m)\gamma_{q,\min}(r,m)}{\beta(q,r)}]\Big\} - \sum_{q=1}^{Q}\phi_r(q)\sum_{r=1}^{R(q)}\beta(q,r), \end{aligned} \tag{5.20}$$

where $\phi_r(q)$ is a Lagrange multiplier, and the $P_{e_q}(r,m)$, expressed in (5.7), has been mathematically reformulated in terms of $\beta(q,r)$ as

$$P^{*}_{e_q}(r,m) = c_{1_q}(r,m)\exp[\frac{-\beta(q,r)c_{2_q}(r,m)\gamma_{q,\min}(r,m)}{\beta(q,r)}]. \tag{5.21}$$

For more mathematical expression simplicity, it is assumed that

$$\Gamma_A(q,r,m) = \delta_{q_d}(r,m)\rho_{av_q}(r,m). \tag{5.22}$$

To evaluate the scheduling matrix elements, $\beta(q,r)$, a partial derivative has been taken to $L[\beta(q,r)]$ in terms of $\beta(q,r)$. It should be noted that the continuous domain of the closed interval $[0,1]$ of $\beta(q,r)$ is adopted instead of fixed values of '0' or '1' in order to avoid the partial derivative operation on constants. Thus $\beta(q,r)$ values can be achieved as

$$\beta(q,r) = \begin{cases} 1, & \text{if } r = r_{\text{opt}}(q), \\ 0, & \text{otherwise}, \end{cases} \quad \forall q = 1,...,Q. \tag{5.23}$$

where the optimal user of each queue, $r_{\text{opt}}(q)$, is selected utilising

$$r_{\text{opt}}(q) = \arg\max_{r} \phi_r(q), \quad q = 1,...,Q, \tag{5.24}$$

and

$$\begin{aligned} \phi_r(q) = \sum_{m=1}^{M}[\Gamma_A(q,r,m)] - \sum_{m=1}^{M} \big\{ & \Gamma_A(q,r,m)c_{1_q}(r,m) \\ & \cdot \exp[-c_{2_q}(r,m)\mu_q(r,m)\gamma_{q,\min}(r,m)] \big\}. \end{aligned} \tag{5.25}$$

It is apparent from (5.25) that the performance evaluation of each user in a queue is obtained from the summation of the corresponding sub-channels.

Algorithm 12 illustrates the proposed user scheduling algorithm. In this algorithm, the CSI and the data of the users at a BS are collected by the data link layer. The scheduler, shown in Fig. 5.2, arranges the users into queues according to their priorities. At this stage, the proposed algorithm searches for empty queues, in order to fill them with users from higher priority levels. This is to allocate more bandwidth for the users with high priority levels and also to avoid ignoring the priority benefits in the proposed algorithm. Then, the proposed user scheduling algorithm selects the optimal user of each queue utilising (5.23). It should be noted that the proposed algorithm ensures a fair service for users with different priority levels instead

of serving users with higher priority at the cost of ignoring the rest. As mentioned earlier, the fairness means that the proposed algorithm can serve users from different priority levels with high consideration to the preference of users' priorities. The last conditional threshold checks that all queues are covered in order to pass the scheduled users to the MAC layer.

Step 1. Information collection:
Collect the data, related CSI and priority of the users.
Step 2. User assignment:
Assign the users into different queues depending on their priority levels.
Step 3. Queue checking:
if *there is an empty queue* **then**
  Assign users from higher priority queues.
  Go to step 2.
end
Step 4. MCS initialisation:
Set all sub-channels of users across different queues to the highest MCS option.
Step 5. $P_{sc_q}(m)$ **initialisation:**
foreach q **do**
  foreach r **do**
    foreach m **do**
      $P_{sc_q}(r,m) = \delta_{q_d}(r,m) P_{s_q}(r,m)$.
      $\mu_q(r,m) = \frac{P_T}{MP_{sc_q}(r,m)}$.
    end
  end
end
Step 6. User Scheduling:
foreach q **do**
  foreach r **do**
    Implement (5.23).
  end
end
Step 7. User scheduling checking:
if *there is a queue that still needs a service* **then**
  Go to step 4.
end
Step 8. Scheduled user pass:
Pass the scheduled users to MAC layer.

Algorithm 12: The proposed user scheduling algorithm of the SRA strategy

5.6.2 Resource Allocation

The proposed resource allocation UPBA strategy for SISO-AMC-OFDMA system, expressed in Chapter 3, is combined with the user scheduling algorithm to realise

three main functions. Firstly, it allocates the scheduled users amongst the sub-channels optimally and with fairness distribution, i.e. one user per sub-channel. Secondly, the proposed algorithm distributes the available transmission power over the utilised sub-channels based on the related channel conditions. Finally, it assigns the data bit streams into the OFDMA frame data sub-carriers using the utilised MCS options.

The optimised and decoupled approaches of UBPA are adopted, in order to produce a comprehensive investigation of the proposed user scheduling and resource allocation strategy. Since the users are scheduled based on (5.23), the scheduling constraint of (5.17) has been removed.

Optimised Approach

As mentioned in Chapter 3, the optimised approach provides an optimal solution to the considered throughput maximisation problem. Following the procedure steps of the optimised approach of UBPA strategy and based on the Lagrange multiplier method with KKT conditions [62], The Lagrangian function is mathematically expressed as

$$
\begin{aligned}
L\Big[\varphi(q,m),\mu_q(r,m)\Big] = & \sum_{q=1}^{Q}\sum_{r=1}^{R(q)}\sum_{m=1}^{M}\beta(q,r)\varphi(q,m)\delta_{q_d}(r,m)\rho_{av_q}(r,m) \\
& - \sum_{q=1}^{Q}\sum_{r=1}^{R(q)}\sum_{m=1}^{M}\big\{\beta(q,r)\varphi(q,m)\delta_{q_d}(r,m)\rho_{av_q}(r,m)c_{1_q}(r,m) \\
& \cdot \exp[\frac{-\varphi(q,m)c_{2_q}(r,m)\mu_q(r,m)\gamma_{q,\min}(r,m)}{\varphi(q,m)}]\big\} \\
& - \Omega\big[\sum_{q=1}^{Q}\sum_{r=1}^{R(q)}\sum_{m=1}^{M}\beta(q,r)\varphi(q,m)\mu_q(r,m)P_{sc_q}(r,m) - P_T\big] \\
& - \sum_{q=1}^{Q}\eta_m(q)\big[\sum_{m=1}^{M}\varphi(q,m) - 1\big] \\
& - \sum_{m=1}^{M}\eta_q(m)\Big[\sum_{q=1}^{Q}\varphi(q,m) - 1\big],
\end{aligned}
\tag{5.26}
$$

where the Lagrange multiplier Ω can be expressed as a function of water filling level, λ, as $\Omega = \frac{1}{\lambda \ln 2}$. In contrast, the Lagrange multiplier, $\eta_m(q)$, that controls the

scheduled user allocation is obtained as

$$\eta_m(q) = \sum_{r=1}^{R(q)} \beta(q,r)\Gamma_A(q,r,m) - \Omega \sum_{r=1}^{R(q)} \frac{\beta(q,r)P_{sc_q}(r,m)}{c_{2_q}(r,m)\gamma_{q,\min}(r,m)} - \Omega \sum_{r=1}^{R(q)} \left[\beta(q,r)\mu_q(r,m)P_{sc_q}(r,m)\right] - \eta_q(m). \tag{5.27}$$

For each sub-channel, the optimal scheduled user that maximise the average system throughput is selected based on (3.24) as

$$q_{\text{opt}}(m) = \arg\max_q \eta_m(q), \quad q \in \{1,...,Q\}. \tag{5.28}$$

Based on (5.28), the user allocation matrix elements, $\varphi(q,m)$, are evaluated as

$$\varphi(q,m) = \begin{cases} 1, & \text{if } q = q_{\text{opt}}(m), \\ 0, & \text{otherwise,} \end{cases} \quad \forall m \in \{1,...,M\}. \tag{5.29}$$

Algorithm 13 demonstrates the proposed algorithm of the optimised approach of SRA strategy. This algorithm is built based on the same steps of Algorithm 4.

Decoupled Approach

The investigated problem, expressed by (5.14)-(5.19), has been decoupled into two main sub-problems.

User allocation: At this stage, the values of the scheduling matrix elements, $\beta(q,r)$, are achieved. Moreover, the bits are assumed to be allocated over all sub-channels using the highest MCS option, i.e. the combination of 64-QAM and convolutional coding rate of 3/4. At the same time, the power is distributed equally amongst the entire sub-channels. Therefore, the power and scheduling constraints shown in (5.15), (5.16) and (5.17) are removed. To achieve the user allocation over distinct sub-channels of the transmitted OFDMA, a Lagrange multiplier optimisation method is utilised. The Lagrangian function can be formulated as

Step 1. MCS initialisation:
Set all sub-channels to the highest MCS option
Step 2. $P_{s_q}(r,m)$ **initialisation:**
Initialisation:
foreach q **do**
  foreach m **do**
    foreach r **do**
      $P_{sc_q}(r,m) = \delta_{q_d}(r,m)P_{s_q}(r,m)$.
      $\mu_q(r,m) = \frac{P_T}{MP_{sc_q}(r,m)}$.
    end
  end
end
Step 3. λ **initialisation:**
initialise $\lambda = 0.001$.
Step 4. Optimal user allocation:
while $\lambda < 10$ **do**
  foreach q **do**
    foreach m **do**
      Implementing of (5.28) and (5.29).
    end
  end
  Step 5. Power evaluation in terms of λ**:**
  if $\sum_{q=1}^{Q}\sum_{r=1}^{R(q)}\sum_{m=1}^{M}\beta(q,r)\varphi(q,m)\mu_q^*(r,m)P_{sc_q}(r,m) \neq P_T$ **then**
    $\lambda = \lambda + \frac{\lambda}{2}$, $\mu_q^*(r,m) = \frac{\Omega - \frac{P_{sc_q}(r,m)}{\gamma_{q,\min}(r,m)}}{P_{sc_q}(r,m)}$.
  end
  else
    λ is the optimal value and $\mu_q^*(r,m) = \frac{\Omega - \frac{P_{sc_q}(r,m)}{\gamma_{q,\min}(r,m)}}{P_{sc_q}(r,m)}$. Go to step 6
  end
end
Reduce the MCS option level for the bands with minimum SNR values. Go to step 2.
Step 6. Adjustment of the optimal power value $P_{sc_q}^*(r,m)$ **for each sub-channel in terms of** λ**:**
foreach q **do**
  foreach r **do**
    foreach m **do**
      $P_{sc_q}(r,m) = \mu_q^*(r,m)P_{sc_q}(r,m)$.
    end
  end
end

Algorithm 13: The proposed algorithm of the optimised approach of SRA strategy

$$
\begin{aligned}
L[\varphi(q,m)] = & \sum_{q=1}^{Q}\sum_{r=1}^{R(q)}\sum_{m=1}^{M}\beta(q,r)\varphi(q,m)\delta_{q_d}(r,m)\rho_{av_q}(r,m) \\
& - \sum_{q=1}^{Q}\sum_{r=1}^{R(q)}\sum_{m=1}^{M}\Big\{\beta(q,r)\varphi(q,m)\delta_{q_d}(r,m)\rho_{av_q}(r,m)c_{1_q}(r,m) \\
& \cdot \exp[\frac{-\varphi(q,m)c_{2_q}(r,m)\mu_q(r,m)\gamma_{q,\min}(r,m)}{\varphi(q,m)}]\Big\} - \sum_{q=1}^{Q}\eta_m(q)\sum_{m=1}^{M}\varphi(q,m) \\
& - \sum_{m=1}^{M}\eta_q(m)\sum_{q=1}^{Q}\varphi(q,m),
\end{aligned}
\tag{5.30}
$$

where $\eta_q(m)$ and $\eta_m(q)$ are the Lagrange multipliers. A partial derivative of $L[\varphi(q,m)]$ is obtained in terms of $\varphi(q,m)$. Therefore, $\varphi(q,m)$ can be expressed as

$$
\varphi(q,m) = \begin{cases} 1, & \text{if } q = q_{\text{opt}}(m), \\ 0, & \text{otherwise,} \end{cases} \quad \forall m = 1, ..., M, \tag{5.31}
$$

where the optimal user allocation, $q_{\text{opt}}(m)$, is achieved as

$$
q_{\text{opt}}(m) = \arg\max_{q}\eta_m(q), \quad q = 1, ..., Q. \tag{5.32}
$$

and

$$
\begin{aligned}
\eta_m(q) = & \sum_{r=1}^{R(q)}\beta(q,r)\Gamma_A(q,r,m) - \sum_{r=1}^{R(q)}\beta(q,r)\Gamma_A(q,r,m)c_{1_q}(r,m) \\
& \cdot \exp[-c_{2_q}(r,m)\mu_q(r,m)\gamma_{q,\min}(r,m)] - \eta_q(m).
\end{aligned}
\tag{5.33}
$$

As highlighted before, the allocation value, $\eta_q(m)$, is used to reduce the throughput value of the assigned user over other sub-channels in order to prevent assigning the same user to other sub-channels.

Algorithm 14 illustrates the user allocation algorithm that tackles the user allocation sub-problem. It is observed from this algorithm that the same steps of the user allocation algorithm of the decoupled approach in UBPA strategy have been adopted with the required modifications to the employed mathematical formulas.

Bit and power allocation: For the bit and power allocation, the fairness con-

straints, expressed in (5.18) and (5.19), and the scheduling constraint of (5.17) are removed. In order to obtain the value of the power adjustment, $\mu_q(r,m)$, for each sub-channel, a Lagrange multiplier optimisation approach is employed. The Lagrange function is formulated as

$$\begin{aligned} L[\mu_q(r,m)] = &\sum_{q=1}^{Q}\sum_{r=1}^{R(q)}\sum_{m=1}^{M}\beta(q,r)\varphi(q,m)\Gamma_A(q,r,m) \\ &- \sum_{q=1}^{Q}\sum_{r=1}^{R(q)}\sum_{m=1}^{M}\big\{\beta(q,r)\varphi(q,m)\Gamma_A(q,r,m) \\ &\cdot c_{1_q}(r,m)\exp[-c_{2_q}(r,m)\mu_q(r,m)\gamma_{q,\min}(r,m)]\big\} \\ &- \Omega\big\{[\sum_{q=1}^{Q}\sum_{r=1}^{R(q)}\sum_{m=1}^{M}\beta(q,r)\varphi(q,m) \\ &\cdot \mu_q(r,m)P_{sc_q}(r,m)] - P_T\big\}, \end{aligned} \tag{5.34}$$

where Ω denotes the Lagrange multiplier. To evaluate $\mu_q(r,m)$, a partial derivative for $L[\mu_q(r,m)]$ is computed with respect to $\mu_q(r,m)$. Thus, $\mu_q(r,m)$ can be evaluated as

$$\mu_q(r,m) = \left(\frac{\Gamma_B(q,r,m) - \ln(\Omega) - \ln[\beta(q,r)\varphi(q,m)P_{sc_q}(m)]}{c_{2_q}(r,m)\gamma_{q,\min}(r,m)}\right)^{+}, \tag{5.35}$$

where $\Gamma_B(q,r,m) = \ln[\beta(q,r)\varphi(q,m)\Gamma_A(q,r,m)c_{1_q}(r,m)c_{2_q}(r,m)\gamma_{q,\min}(r,m)]$. To find Ω, (5.35) is substituted in (5.15) and by assuming that

$$\Gamma_C(q,r,m) = P_{sc_q}(r,m)\beta(q,r)\varphi(q,m), \tag{5.36}$$

and

$$\Gamma_D(q,r,m) = \ln[\Gamma_C(q,r,m)]\Gamma_C(q,r,m), \tag{5.37}$$

The multiplier Ω can be calculated as

$$\ln(\Omega) = \frac{\Gamma_E(q,r,m)}{\Gamma_F(q,r,m)}, \tag{5.38}$$

where

$$\Gamma_E(q,r,m) = \sum_{q=1}^{Q}\sum_{r=1}^{R(q)}\sum_{m=1}^{M}\frac{\Gamma_B(q,r,m)\Gamma_C(q,r,m) - \Gamma_D(q,r,m)}{c_{2_q}(r,m)\gamma_{q,\min}(r,m)} - P_T, \tag{5.39}$$

and

$$\Gamma_F(q,r,m) = \sum_{q=1}^{Q}\sum_{r=1}^{R(q)}\sum_{m=1}^{M}\frac{\Gamma_C(q,r,m)}{c_{2_q}(r,m)\gamma_{q,\min}(r,m)}. \tag{5.40}$$

The data bit streams are allocated over the data sub-carriers utilising one of the MCS options based on the related channel conditions and power constraints. The bit allocation algorithm avoids any transmission over sub-channels with SNR value lower than 4 dB due to high BER values for all utilised MCS levels as shown in Fig. 3.3.

Step 1. MCS initialisation:
Set all sub-channel to the highest MCS option.
Step 2. $P_{sc_q}(r,m)$ **initialisation:**
foreach q **do**
  foreach r **do**
    foreach m **do**
      $P_{sc_q}(r,m) = \delta_{q_d}(r,m)P_{s_q}(r,m)$.
      $\mu_q(r,m) = \frac{P_T}{MP_{sc_q}(r,m)}$.
      $\eta_q(m) = 0$.
    end
  end
end
Step 4. User allocation:
foreach q **do**
  foreach r **do**
    foreach m **do**
      Implement (5.32) and (5.33).
      Implement (5.31).
      Maximise $\eta_q(m)$.
    end
  end
end

Algorithm 14: The proposed user allocation algorithm of the decoupled SRA strategy.

Algorithm 15 explains the steps of bit and power allocation of the decoupled approach. The bit and power allocation is achieved in multi processing levels as follows. Firstly, a high MCS order is selected for all sub-channels that are assigned to a scheduled user. Secondly, the power allocation of (5.35) is implemented for given MCS options, as well as the related BER and SNR values. Thirdly, this stage checks the state of both power constraints shown in (5.15) and (5.16). If they are satisfied, the system allows the transmission to continue. Otherwise, a reduction in the MCS level for the sub-channels that require more power to satisfy the relevant

channel conditions is performed. In addition, the option of no transmission is directly selected for the sub-channels with SNR values less than 4 dB. Finally, iterative reduction of the MCS levels for the selected sub-channels continues until the system conditions are satisfied or the lowest MCS level is reached.

Step 1. MCS initialisation:
Set all sub-channels to the highest MCS option.
Step 2. Power evaluation:
foreach q **do**
  foreach r **do**
    foreach m **do**
      $P_{sc_q}(r,m) = \delta_{q_d}(r,m) P_{s_q}(r,m)$.
      $\mu_q(r,m) = \left(\frac{\Gamma_B(q,r,m) - \ln(\Omega) - \ln[\beta(q,r)\varphi(q,m)P_{sc_q}(m)]}{c_2(r,m)\gamma_{q,\min}(r,m)} \right)^+$.
    end
  end
end
Step 3. Power constraints check:
if $\sum_{q=1}^{Q} \sum_{r=1}^{R(q)} \sum_{m=1}^{M} \beta(q,r)\varphi(q,m)\mu_q(r,m)P_{sc_q}(r,m) = P_T$ *and* $\mu_q(r,m) \geq 0$ **then**
  Go to step 4.
end
else
  foreach q **do**
    foreach r **do**
      foreach m **do**
        if $\gamma_{q,\min}(r,m) \leqslant 4$ **then**
          Set this sub-channel to no transmission option.
        end
        else
          Reduce the MCS option levels for the sub-channels with lower $\gamma_{q,\min}(r,m)$.
          Go to step 2
        end
      end
    end
  end
end
Step 4. Transmission:
Transmit the OFDMA frame.

Algorithm 15: The proposed bit and power allocation algorithm of the SRA strategy for SISO-AMC-OFDMA system.

5.7 Simulation Results and Discussion

In this Section, the performance of the proposed SRA strategy based SISO-AMC-OFDMA system is presented and compared with conventional approaches. The SISO-AMC-OFDMA system considers the simulation parameters shown in Table 2.1 with a total transmission power of 50 W. The investigated systems have been tested over different ITU channel profiles as expressed in Table 2.4. Moreover, most of the simulation results are achieved for $Q = 10$ queues.

In the simulation results, dynamic and fixed sub-channelling techniques of four SISO-AMC-OFDMA systems are compared as follows:

1. AMC-OFDMA-dynamic sub-channelling for scheduling and optimised resource allocation (DSORA) system that adopts the proposed dynamic sub-channelling based scheduling and optimised resource allocation strategy.

2. AMC-OFDMA-dynamic sub-channelling for scheduling and decoupled resource allocation (DSDRA) system that uses the proposed dynamic sub-channelling based scheduling and decoupled resource allocation strategy.

3. AMC-OFDMA-fixed sub-channelling for scheduling and optimised resource allocation (FSORA) system that utilises the fixed sub-channelling based scheduling and optimised resource allocation strategy.

4. AMC-OFDMA-fixed sub-channelling for scheduling and decoupled resource allocation (FSDRA) system, which considers the fixed sub-channelling based scheduling and decoupled resource allocation strategy.

5. AMC-OFDMA-dynamic sub-channelling for optimised resource allocation (DORA) system that employs the dynamic sub-channelling based optimised resource allocation combined with the FIFO scheduling method [78].

6. AMC-OFDMA-dynamic sub-channelling for decoupled resource allocation (DDRA) system, which uses the FIFO scheduling algorithm and the decoupled approach of the resource allocation.

7. AMC-OFDMA-fixed sub-channelling for optimised resource allocation (FORA) system that adopts the fixed sub-channelling based optimised resource allocation and FIFO method.

8. AMC-OFDMA-fixed sub-channelling for decoupled resource allocation (FDRA) system, which considers the fixed sub-channelling based decoupled resource allocation with FIFO scheduling method.

Fig. 5.3 compares the average throughput of the eight considered systems. The simulated average system throughput is evaluated for $N_{fr} = 1 \times 10^6$ transmitted OFDMA frames in terms of the effective bandwidth, B_{eff}, based on (2.45).

It is apparent from this figure that the performance of the proposed SRA strategy for both dynamic and fixed sub-channelling methods is shown to exceed the other approaches. This enhancement is the results of using the proposed scheduling algorithm that exploits the multiuser diversity efficiently over different queues. Additionally, the selection of the best user, which can maximise the average system throughput, in each queue can yield a high flexibility of applying the proposed resource allocation algorithms. On the other hand, the systems that adopt the FIFO scheduling method sort the users based on the arriving time, in which the multiuser diversity is moderately exploited. Furthermore, the selection of higher MCS levels and the suitable power value for each sub-channel can guarantee a successful and high rate of transmission of data with the lowest BER. The eight investigated systems avoid transmission in low SNR sub-channels in order to save power for other sub-channels and prevent any data loss.

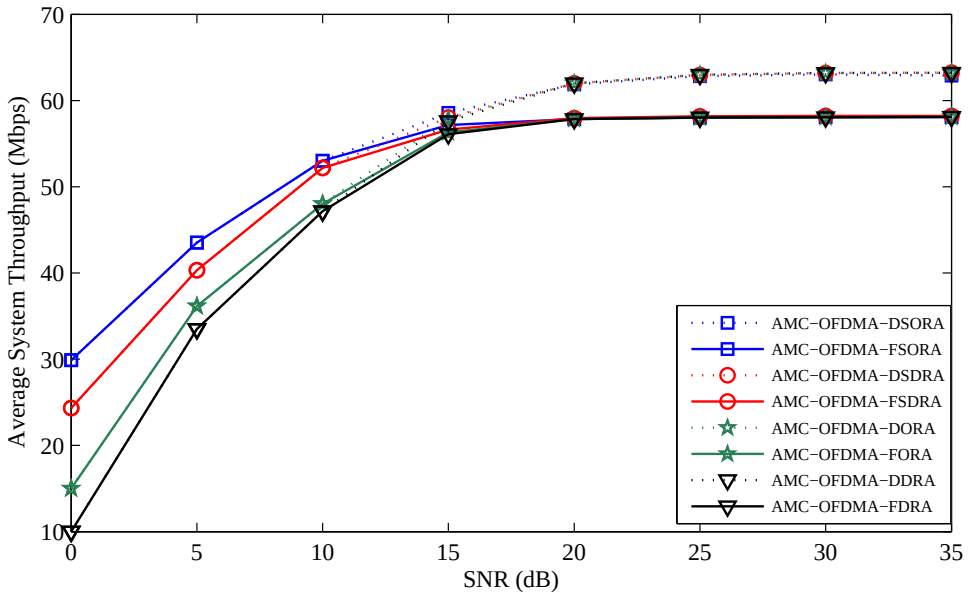

Figure 5.3: Average system throughput of the investigated conventional and SRA based AMC-OFDMA systems.

Fig. 5.4 demonstrates the average system spectral efficiency, ρ_{av} for the investi-

gated schemes. The term ρ_{av} is evaluated as a function of the spectral efficiency of the scheduled users, $\rho_{av_q}(r,m)$, as

$$\begin{aligned}\rho_{av} &= \frac{1}{N_{fr}}\sum_{g=1}^{N_{fr}}\rho_{av_g} \\ &= \frac{1}{N_{fr}}\sum_{g=1}^{N_{fr}}\frac{1}{Q}\sum_{q=1}^{Q}\sum_{r=1}^{R(q)}\sum_{m=1}^{M}\beta(q,r)\varphi(q,m)\rho_{av_q}(r,m).\end{aligned} \tag{5.41}$$

where ρ_{av_g} is the average information spectral efficiency for the g-th OFDMA frame. The performance of the AMC-OFDMA-DSORA system is shown to achieve a gain between 0.1-1.3 bps/Hz over other schemes. Additionally, the performance of the AMC-OFDMA-FSORA is increased by 0.1-0.8 bps/Hz in comparison with the rest.

It is evident that the significant improvement in the performance of the AMC-OFDMA systems that adopt DSORA, FSORA methods over the other investigated schemes is due to the exploitation of multiuser diversity. This diversity can lead to selecting the user with the best channel conditions that allow the assigned sub-carriers to carry more data bit streams. In contrast, the utilisation of FIFO scheduling methods by some of the considered systems enforces the resource allocation algorithms to choose medium and low level of MCSs in order to reduce the required power values. This is due to the inferior exploitation of the multiuser diversity in comparison with the proposed SRA strategy.

The throughput outage probability, P_{out}, of the compared system has been presented in Fig. 3.5. Based on (2.46), P_{out} is computed as an average value over N_{fr} transmitted frames.

It is observed from Fig. 5.5 that the AMC-OFDMA-FSORA system achieves lowest throughput outage probability amongst the other fixed sub-channelling based schemes. In addition, the AMC-OFDMA-DSORA system is shown to obtain a significant performance improvement in comparison with AMC-OFDMA-DSDRA, AMC-OFDMA-DORA and AMC-OFDMA-DDRA approaches. In other words, the proposed SRA strategy can achieve a close performance to the upper expected throughput bound, which can be evaluated following (2.47).

As highlighted in Chapter 3, the optimised resource allocation systems of DSORA, FSORA, DORA and FORA outperform the other approaches that adopt the decoupled resource allocation method. However, these systems can be more costly in

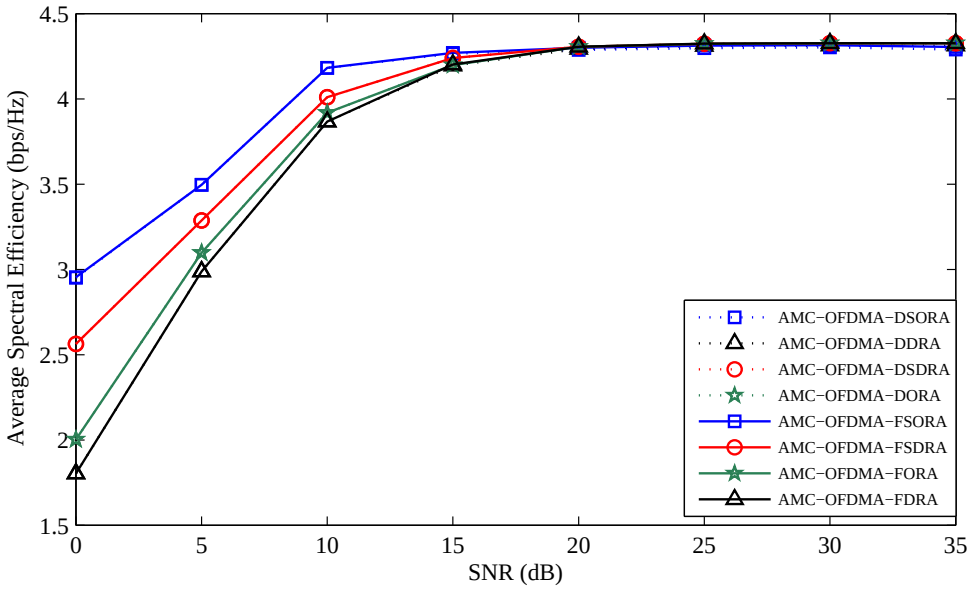

Figure 5.4: Average spectral efficiency for the investigated conventional and SRA based AMC-OFDMA systems.

terms of searching complexity, which is the result of using a huge number of iterations to obtain the optimal user, bit and power allocation over the transmitted OFDMA frame.

Fig. 5.6 shows the average throughput performance of the considered systems in terms of the number of the utilised queues at an assigned BS for an average SNR values of 5, 15, 25 and 35 dB. This figure demonstrates the multiuser diversity effects on the performance of the investigated systems. It is apparent that the performance of the AMC-OFDMA-DSORA and AMC-OFDMA-FSORA systems is improved significantly with the increase in the queues number more than other approaches. Moreover, the performance of the investigated systems is kept the same after 30 queues as the diversity saturation threshold is reached. As mentioned earlier, the scheduling algorithm for the proposed SRA strategy utilises the multiuser diversity to select the best user in each queue for every transmission time, T. In contrast, the degradation in the performance of the AMC-OFDMA-DDRA and FDRA systems in comparison with the other approaches is the result of employing the decoupled resource allocation with the FIFO scheduling method.

A statistical study of the usage ratio of the considered MCS options by the investigated systems is illustrated in Fig. 5.7. These results are computed for SNR values of 5, 15, 25 and 35 dB and over transmission time of 1.7 min. As explained in Chapter 2, the employed MCS options are sorted from the lowest, which is null

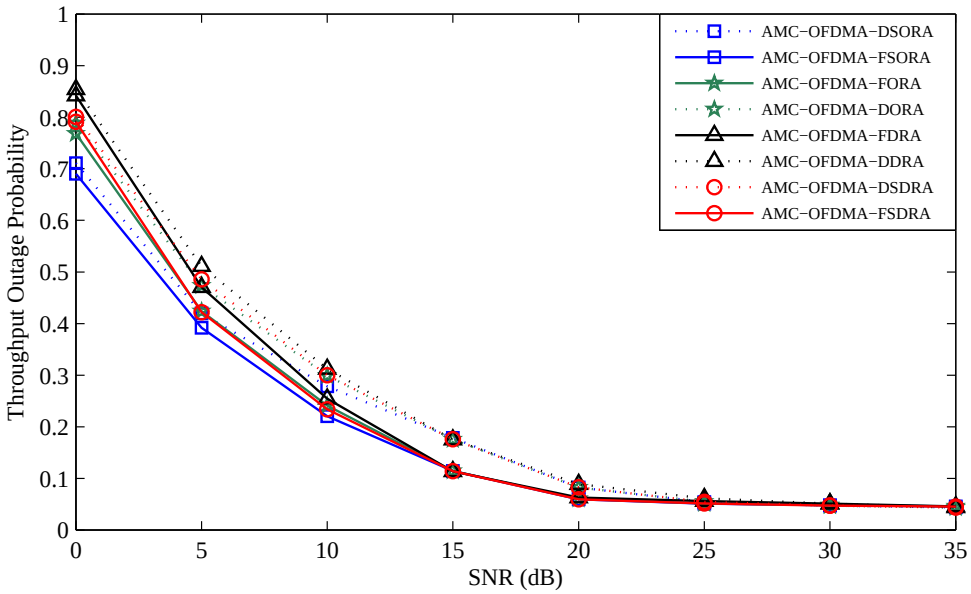

Figure 5.5: Throughput outage probability for the investigated conventional and SRA based AMC-OFDMA systems.

transmission, to the highest level, i.e. 64-QAM combined with 3/4 convolutional coding rate. In other words, the utilised ten MCS options are numbered from '1' to '10'.

It is apparent from Fig. 5.7 that the AMC-OFDMA-SORA and AMC-OFDMA-SDRA systems select the higher MCS options more than other schemes. This is due to the employment of the proposed user scheduling algorithm of the SRA strategy. At the same time, the optimised and decoupled resource allocation approaches aim to maximise the average system throughput by assigning the transmitted sub-carriers to the higher MCS option, in which the power constraints and the channel conditions are satisfied. It is also noted that most of the investigated systems choose the middle MCS options of 2-7 with the low SNR values and the options of 8-10 with high SNR ranges.

In contrast, this figure can clearly demonstrate the dynamic MCS selection of the employed AMC method over different systems, channel conditions and SNR values. Moreover, Fig. 5.7 illustrates the exploiting of the available MCSs by the proposed SRA strategy efficiently in comparison with the rest of systems. Therefore, the aim of increasing the average system throughput is achieved by implementing SRA.

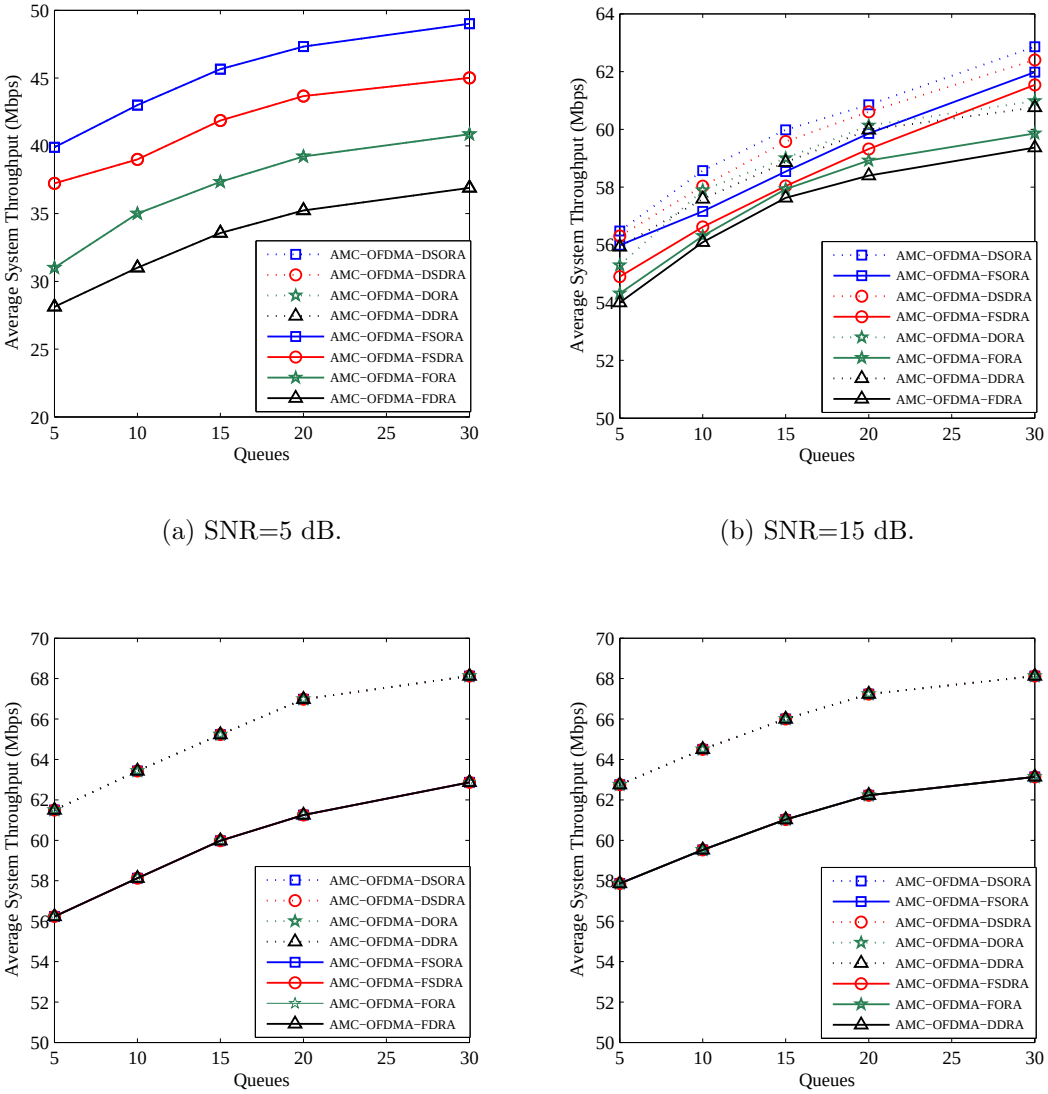

(a) SNR=5 dB.

(b) SNR=15 dB.

(c) SNR=25 dB.

(d) SNR=35 dB.

Figure 5.6: Throughput v.s. users for the investigated conventional and SRA based AMC-OFDMA systems.

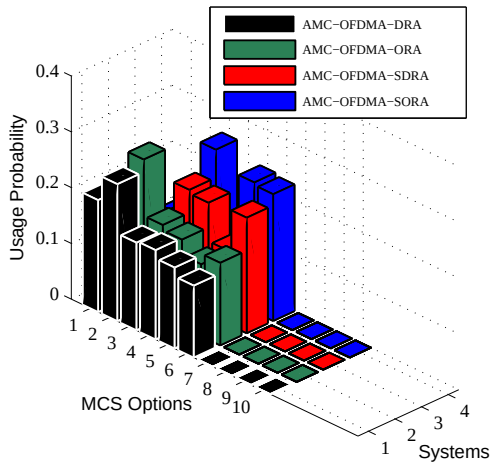

(a) SNR=5 dB.

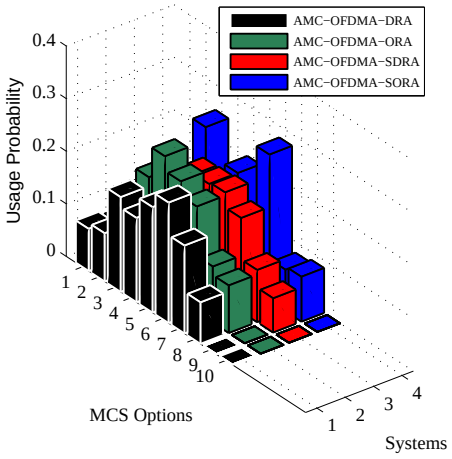

(b) SNR=15 dB.

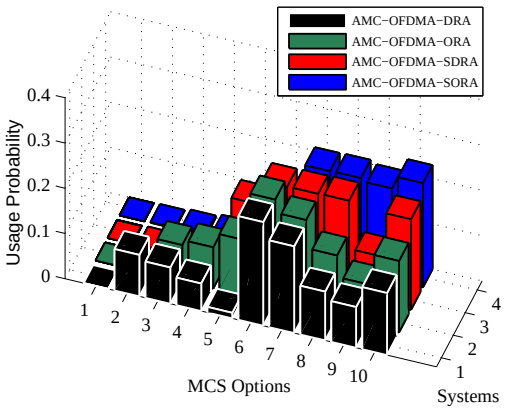

(c) SNR=25 dB.

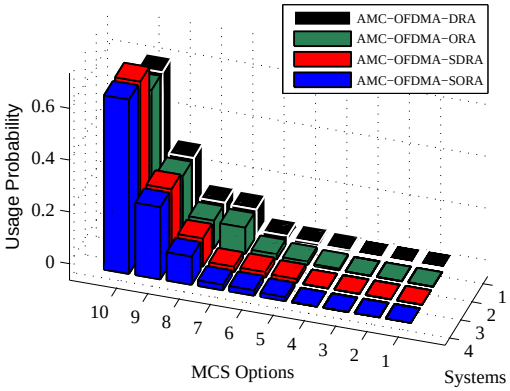

(d) SNR=35 dB.

Figure 5.7: Usage probability of the utilised MCS options for the investigated conventional and SRA based AMC-OFDMA systems.

5.8 Chapter Summary

A cross-layer scheduling and resource allocation strategy for SISO-AMC-OFDMA systems has been proposed in this Chapter in order to maximise the average system throughput as a function of the spectral efficiency and the BER. In addition, a developed software engineering life cycle model has been presented to design the proposed strategy. This life cycle model provided the SRA strategy with high scalability, extendibility and portability to address the problems of system updating and communication traffic. The transmitter of the investigated SISO-AMC-OFDMA system divided the data sub-carriers of the OFDMA frame into groups assigned to sub-channels each of which was assigned to a scheduled user. The proposed SRA strategy exhibited two main algorithms, scheduling and resource allocation, that worked subsequently in order to reduce the mathematical complexity of the investigated convex maximisation problem. At the data link layer, the proposed scheduling algorithm arranged the users in queues depending on their priorities and consequently selected the best user that could maximise the system throughput of each queue according to the corresponding CSI. The scheduling algorithm achieved fair services for all users with different priorities and utilised the empty queues to serve users from high levels. The resource allocation algorithm, which worked at the MAC layer, exploited the multiuser channel diversity to allocate the user, related data bit streams and the transmission power amongst the utilised sub-channels, considering relevant CSI and power constraints. This algorithm considered changeable coding rates based on the selected MCS options using AMC methods. Different ITU channel profiles have been considered in this Chapter. The simulation results have compared the performance of the proposed SRA strategy with other conventional approaches for the investigated SISO-AMC-OFDMA system. These results showed that the proposed system outperformed the other investigated systems due to the efficient exploitation of multiuser diversity.

Chapter 6

Conclusion and Future Work

Recently, the SISO and MIMO practical communication systems have considered the multi-carrier wireless techniques, such as OFDM for single user and OFDMA for multiuser, in order to overcome the transmission problems of single-carrier approaches. These problems can be summarised by ISI and the selectivity of the fading channels. However, the OFDM and OFDMA systems suffer from the ICI and PAPR issues, which are the results of Doppler shift and FFT operation, respectively. In addition, these systems have not efficiently exploited the channel capacity due to the change of the transmission conditions, such as the utilised channel profiles, speed mobility and available resources. The poor exploiting of the channel capacity results in a significant reduction in the system throughput performance. In order to sort this problem, AMC technology has been combined with OFDM and OFDMA systems. AMC-OFDM/OFDMA systems can adapt to different transmission environments by selecting the suitable modulation types, FEC methods and the coding rates.

In contrast, the cross-layer resource allocation strategies have been widely employed by the AMC-OFDM/OFDMA systems to improve the throughput performance. These strategies have allocated the available resources, i.e. user diversity, transmission power and information bits, optimally over the sub-carriers in order to satisfy the required QoS and the related channel conditions.

On the other hand, AMC-OFDMA systems have utilised the user scheduling algorithms along with the resource allocation strategies to exploit the multiuser channel diversity. User scheduling algorithms have managed the servicing of different users depending on distinct parameters, such as priority and arrival time.

The motivation behind this research was to improve the average throughput of SISO and MIMO based AMC-OFDM/OFDMA systems by proposing efficient algorithms. The key objective was to design SISO and MIMO based OFDM/OFDMA based on AMC, resource allocation and user scheduling strategies in order to maximise average system throughput.

This thesis proposed three strategies, i.e. AMC, resource allocation and user scheduling, for SISO and MIMO systems that considered the OFDM and OFDMA wireless transmission technologies. These strategies were designed based on different developed software engineering life cycle models. The developed models have considered the cyclic evolutionary life cycle methodology as is exhibited the required feedback information.

The proposed AMC strategy exhibited two main parts, i.e. fixed and dynamic sub-channelling. Fixed sub-channelling AMC distributed the data and pilot sub-carriers into sub-channels depending on the measured coherence bandwidth for OFDM and the number of users for OFDMA. Then, it selected the suitable MCS option for each sub-channel based on the SNR value of such sub-channel. In contrast, dynamic sub-channelling AMC considered the same procedure of fixed sub-channelling method, yet the number of data and pilot sub-carriers within each sub-channel could be changed by implementing the proposed pilot adjustment scheme. This scheme reduced the number of pilots required for channel estimation in each sub-channel individually depending on the measured coherence bandwidth, the variance of the SNR fluctuation values of the involved sub-carriers and the minimum SNR. The redundant pilots were replaced by additional data sub-carriers in order to improve the average system throughput. It should be noted that the proposed AMC strategy employed two MCS scenarios, each of which included ten MCSs of LDPC and convolutional based coding rates of 1/2, 2/3 and 3/4 combined with QPSK, 16-QAM and 64-QAM as well as no transmission option.

In terms of the proposed cross-layer resource allocation strategy, a modified throughput maximisation problem was mathematically formulated as a function of spectral efficiently and BER. This problem has been solved using Lagrange multipliers optimisation method. Furthermore, the proposed resource allocation strategy aimed to maximise the average system throughput by allocating the users, transmission power and information bits amongst the considered sub-channels assigned to different users. This was carried out by presenting two solution approaches, i.e.

optimised and decoupled. The optimised approach provided an optimal solution to the investigated maximisation problem on the cost of high computational complexity. Moreover, the decoupled approach produced a low complexity solution with an acceptable degradation in the throughput performance compared to the optimised approach particularly for low SNR values. The proposed strategy considered both parts of the proposed AMC method along with convolutional based MCS scenario. Therefore, the variable coding rate was adopted as an important metric rather than employing the fixed coding rate or uncoded schemes. This strategy was basically designed for SISO-OFDMA system, and then it was expanded to work with MIMO-OFDMA approach. Two resource allocation strategies were introduced for MIMO systems. The first one considered the allocation of the resources at each transmitted antenna based on the best SISO link between each transmit antenna and the received antennas in terms of channel conditions. Moreover, the second strategy adopted the SVD or eigen mode based transmission.

In contrast, the proposed cross-layer user scheduling strategy aimed at improving the throughput maximisation target by managing the information bit streams of different users. It sorted the involved users in queues depending on the user priorities and then selected the optimal user in each queue, in which the average system throughput was maximised. It also assigned more bandwidth for high priority users by filling the empty queues with them. This strategy was combined with both approaches of the proposed resource allocation algorithms and AMC method in order to exploit the multiuser channel diversity, transmission power and channel capacity efficiently.

It is important to note that the combination of the proposed strategies led to produce comprehensive wireless communication systems that address the transmission problems. Additionally, these systems could work over different channel profiles and transmission conditions by allocating the resources over the sub-carriers and exploiting the multiuser channel diversity.

The OFDM and OFDMA systems based on the proposed strategies have been tested over different ITU channel profiles. The users were divided into three categories and each of which adopted distinct channel profile along with the related mobility speed in order to simulate the physical situations of the involved users. In contrast, numerous simulation results were presented in this thesis based on the introduced systems. In these results, the performance of the investigated systems that

considered the proposed strategies has been compared with different conventional approaches. In terms of the proposed AMC strategy, the throughput performance of this strategy was compared with the traditional AMC technology that selected the same MCS option for all sub-channels based on the minimum SNR value amongst the sub-carriers of the transmitted OFDM/OFDMA frame. It was apparent that the proposed AMC-OFDM/OFDMA system outperformed the other approach significantly over all SNR values. On the other hand, the throughput performance of the SISO and MIMO based AMC-OFDMA systems that employed both approaches of the proposed resource allocation strategy was improved significantly in comparison with other two conventional approaches. This throughput enhancement was the results of exploiting multiuser diversity and the optimal allocation of the available resources, i.e. users, transmission power and information bits. Throughout the simulation results, the behaviour of the AMC-OFDMA system that utilised the combination of the proposed user scheduling, resource allocation and AMC strategies has been studied and compared with the FIFO scheduling method based schemes. It was reported that this system showed a superior performance in comparison with other systems that adopted FIFO scheduling method combined with the proposed resource allocation strategy. The improvement in the throughput performance was achieved by the utilised user scheduling algorithm that selected one user in each queue with best conditions. This was to increase the channel diversity and offer a high flexibility to the dynamic change of the considered MCS options over the sub-channels within each transmitted OFDMA frame.

Future Work

This research project concentrated primarily on maximising the average system throughput of the single-cell downlink transmission based wireless SISO and MIMO systems that employed the OFDM and OFDMA techniques. However, the future work should consider both the downlink and uplink multiuser communication for single and multi-cell mobile networks. In this project, the PAPR issue has not been considered. Therefore, the future work should tackle this problem using the traditional well known methods, such as SLM and PTS, or by proposing a novel approach.

In contrast, the ICI and synchronisation problems, which are the results of

Doppler shift and spread effects, should be considered in order to produce complete wireless systems that can address the expected transmission challenges. It is worth reporting the use of more advanced channel estimation methods is expected to improve the performance of the proposed systems. These methods can mitigate the estimated channel MSE, which yields a significant reduction in the BER.

In terms of MIMO system, the future work should consider the channel estimation in order to provide a practical MIMO system. If the channel estimation is adopted, the proposed pilot adjustment scheme can be expanded to work with the MIMO technology. This scheme can further improve the average system throughput. Additionally, more efficient MIMO receivers, such as minimum mean square error (MMSE) and ML, are recommended to be utilised in the future work to significantly degrade the effects of the multi-antenna interference. On the other hand, the PAPR, ICI and synchronisation problems for MIMO systems should be considered and sorted using the traditional and efficient methods.

The tackling of long service waiting time problem of the proposed user scheduling strategy should be considered in future work to overcome this highlighted drawback. Additionally, the consideration of the queue state conditions and the length of the data packets should be adopted to achieve practical systems.

Finally, the computational complexity of the proposed strategies should be studied. From this study, the units that require a high cost should be replaced by alternative solutions that can significantly reduce the corresponding complexity.

References

[1] M. Mirabito and B. Morgenstern, *The New Communications Technologies*. Oxford, UK: Elsevier Inc, 2004.

[2] E. Lee and D. Messerschmitt, *Digital Communication*. Massachusetts, USA: Kluwer Academic Publishers, 1994.

[3] J. Proakis and M. Salehi, *Digital Communications*. New York, USA: The McGraw-Hill Companies, Inc, 2008.

[4] J. Kurzweil, *An Introduction To Digital Communications*. New York, USA: John Wiley and Sons, Inc, 2000.

[5] A. Goldsmith, *Wireless Communications*. Cambridge, UK: Cambridge University Press, 2005.

[6] M. Ibnkahla, *Signal Processing for Mobile Communications*. Florida, USA: CRC Press LLC, 2005.

[7] J. Proakis and D. Manolakis, *Digital Signal Processing*. New Jersey, USA: Pearson Education, Inc, 2007.

[8] Y. G. Li and G. Stuber, *Orthogonal Frequency Division Multiplexing for Wireless Communications*. New York, USA: Springer Science+Business Media, Inc, 2006.

[9] H. Liu and G. Li, *OFDM-Based Broadband Wireless Networks*. New Jersey, USA: John Wiley and Sons, Inc, 2005.

[10] J. Proakis, *Digital Communications*. McGraw Hill, 2001.

[11] J. Proakis and M. Salehi, *Fundamentals of Communication Systems*. New Jersey, USA: Pearson Education, Inc, 2005.

[12] M. Silva, "Introducing software quality engineering into a telecommunications development environment," *IEEE J. Sel. Areas Commun.*, vol. SAC-4, pp. 1026–1031, Oct. 1986.

[13] D. Edelstein, P. Sullo, and L. Boguchwal, "Making software engineering happen in a telecommunications R and D organization," *IEEE J. Sel. Areas Commun.*, vol. 8, pp. 283–290, Feb. 1990.

[14] D. Petriu, C. Shousha, and A. Jalnapurkar, "Architecture-based performance analysis applied to a telecommunication system," *IEEE Trans. Software Engineer.*, vol. 26, pp. 1049–1065, Nov. 2000.

[15] N. Mansurov and R. Probert, "A scenario-based approach to the evolution of telecommunications software," *IEEE Commun. Mag.*, pp. 94–100, Oct. 2001.

[16] H. Sun, J. Han, and H. Levendel, "Availability requirement for a fault-management sever in high-availability communication systems," *IEEE Trans. Rel.*, vol. 52, pp. 238–244, Jun. 2003.

[17] N. Ford and M. Woodroffe, *Introducing Software Engineering.* Hertfordshire, UK: Prentice Hall, Inc, 1994.

[18] H. Vliet, *Software Engineering.* West Sussex, England: John Wiley and Sons, Inc, 2000.

[19] D. Kim, B. Jung, H. Lee, D. Sung, and H. Yoon, "Optimal modulation and coding scheme selection in cellular networks with hybrid-ARQ error control," *IEEE Trans. Wireless Commun.*, vol. 7, pp. 5195–5201, Dec. 2008.

[20] K.-B. Song, A. Ekbal, S. Chung, and J. Cioffi, "Adaptive modulation and coding (AMC) for bit-interleaved coded OFDM (BIC-OFDM)," *IEEE Trans. Wireless Commun.*, vol. 5, pp. 1685–1694, Jul. 2006.

[21] T. Keller and L. Hanzo, "Adaptive multicarrier modulation: A convenient framework for time-frequency processing in wireless communications," *IEEE Proceeding of the IEEE*, vol. 88, pp. 611–640, May 2000.

[22] B. C. Jung, J. K. Kwon, H. Jin, and D. K. Sung, "Sub-band spreading technique for adaptive modulation in OFDM systems," *Journal of Communications and Networks*, vol. 10, pp. 71–78, 2008.

[23] J. S. Harsini, F. Lahouti, M. Levorato, and M. Zorzi, "Analysis of non-cooperative and cooperative type II hybrid ARQ protocols with AMC over correlated fading channels," *IEEE Trans. Wireless Commun.*, vol. 10, pp. 877–889, Mar. 2011.

[24] R. Zhang and L. Cai, "Joint AMC and packet fragmentation for error control over fading channels," *IEEE Trans. Veh. Technol.*, vol. 59, pp. 3070–3080, Jul. 2010.

[25] T. Kwon and D.-H. Cho, "Adaptive-modulation-and-coding-based transmission of control message for resource allocation in mobile communication systems," *IEEE Trans. Veh. Technol.*, vol. 58, pp. 2769–2782, Jul. 2009.

[26] M. Lei and P. Zhang, "Subband bit and power loading for adaptive OFDM," in *Proc. IEEE VTC-Fall Conference*, May 2003, pp. 1482–1486.

[27] X. Wang, Q. Liu, and G. Giannakis, "Analyzing and optimizing adaptive modulation coding jointly with ARQ for QoS-guaranteed," *IEEE Trans. Veh. Technol.*, vol. 56, pp. 710–720, Mar. 2007.

[28] H. Fu and D. Kim, "Scheduling performance in downlink WCDMA networks with AMC and fast cell selection," *IEEE Trans. Wireless Commun.*, vol. 7, pp. 2580–2591, Jul. 2008.

[29] L. Caponi, F. Chiti, and R. Fantacci, "Performance evaluation of a link adaptation technique for high speed wireless communication systems," *IEEE Trans. Wireless Commun.*, vol. 6, pp. 4568–4575, Dec. 2007.

[30] K. Ishihara, Y. Takatori, and M. Umehira, "Comparison of SCFDE and OFDM with adaptive modulation and coding in nonlinear fading channel," *IET Electron. Letter*, vol. 43, Feb. 2007.

[31] W. Zhang, X.-G. Xia, and P. Ching, "Optimal training and pilot pattern design for OFDM systems in rayleigh fading," *IEEE Trans. Broadcast.*, vol. 52, pp. 505–514, Dec. 2006.

[32] X. Fu and H. Minn, "Modified data-pilot-multiplexed schemes for OFDM systems," *IEEE Trans. Wireless Commun.*, vol. 6, pp. 730–737, Feb. 2007.

[33] G. Taubock and F. Hlawatsch, "A compressed sensing technique for OFDM channel estimation in mobile environment: exploiting channel sparsity for reducing pilots," in *Proc. IEEE ICASSP Conference*, May 2008, pp. 2885–2888.

[34] X. Cai and G. B. Giannakis, "Error probability minimizing pilots for OFDM with M-PSK modulation over Rayleigh-fading channels," *IEEE Trans. Veh. Technol.*, vol. SAC-4, pp. 1026–1031, Oct. 1986.

[35] W. Zhang, X.-G. Xia, P. C. Ching, and W.-K. Ma, "On the number of pilots for OFDM system in multipath fading channels," in *Proc. IEEE ICASSP Conference*, May 2004, pp. 381–384.

[36] O. Simeone and U. Spagnolini, "Adaptive pilot pattern for OFDM systems," in *Proc. IEEE ICC Conference*, Jun. 2004, pp. 978–982.

[37] J.-C. Kim, J.-Y. Hwang, and Y. Han, "Dynamic subchannelization for adaptation to multipath fading in mobile WiMAX," in *Proc. IEEE PIMRC Conference*, Sep. 2007, pp. 1–5.

[38] B. Devillers, J. Louveaux, and L. Vandendorpe, "Bit and power allocation for goodput optimization in coded parallel subchannels with ARQ," *IEEE Trans. Signal Process.*, vol. 56, pp. 3652–3661, Aug. 2008.

[39] I. Stupia, L. Vandendorpe, F. Giannetti, V. Lottici, and N. D'Andrea, "Power allocation for goodput optimization in BICM-OFDM systems," in *Proc. IEEE ICC Conference*, May 2008, pp. 3604–3608.

[40] R. Duran, J. Louveaux, and L. Vandendorpe, "Goodput optimization bit and power allocation for OFDM transmission with relaying," in *Proc. IEEE ISSPIT Conference*, Dec. 2007, pp. 1116–1120.

[41] M. Hasna and M.-S. Alouini, "Optimal power allocation for relayed transmissions over rayleigh-fading channels," *IEEE Trans. Wireless Commun.*, vol. 3, pp. 1999–2004, Nov. 2004.

[42] J. Wang and J. Liu, "An iterative power allocation algorithm in OFDM system based on power relaxation," in *Proc. IEEE ICME Conference*, Jul. 2005.

[43] Y. Zhang and C. Leung, "Subchannel power loading schemes in multiuser OFDM systems," *IEEE Trans. Veh. Technol.*, vol. 58, pp. 5341–5347, Jul. 2009.

[44] H. Moon and D. Cox, "Efficient power allocation for coded OFDM systems," *IEEE Trans. Commun.*, vol. 57, pp. 943–947, Apr. 2009.

[45] M. Ibrahimi and B. Liang, "Efficient power allocation in cooperative OFDM system with channel variation," in *Proc. IEEE ICC Conference*, May 2008, pp. 3022–3028.

[46] M. Talebi and B. Khalaj, "Distributed power allocation for OFDM wireless ad-hoc networks based on average consensus," in *Proc. IEEE ICCS Conference*, Oct. 2006, pp. 1–5.

[47] Z. Xu and L. Liu, "Power allocation for multi-band OFDM UWB communication networks," in *Proc. IEEE VTC-Fall Conference*, Sep. 2004, pp. 368–372.

[48] A. Biagioni, R. Fantacci, D. Marabissi, and D. Tarchi, "Adaptive subcarrier allocation schemes for wireless OFDMA systems in WiMAX networks," *IEEE J. Sel. Areas Commun.*, vol. 27, pp. 217–225, Feb. 2008.

[49] G. Kulkarni, S. Adlakha, and M. Srivastava, "Subcarrier allocation and bit loading algorithms for OFDMA-based wireless networks," *IEEE Trans. Mobile Comput.*, vol. 4, pp. 652–662, Nov. 2005.

[50] A. Gotsis, D. Komnakos, and P. Constantinou, "Dynamic subchannel and slot allocation for OFDMA networks supporting mixed traffic: Upper bound and a heuristic algorithm," *IEEE Commun. Lett.*, vol. 13, pp. 576–578, Aug. 2009.

[51] I. Wong and B. Evans, "Optimal resource allocation in the OFDMA downlink with imperfect channel knowledge," *IEEE Trans. Commun.*, vol. 57, pp. 232–241, Jan. 2009.

[52] ——, "Optimal downlink OFDMA resource allocation with linear complexity to maximize ergodic rates," *IEEE Trans. Wireless Commun.*, vol. 7, pp. 962–971, Mar. 2008.

[53] G. Li and H. Liu, "Resource allocation for OFDMA relay networks with fairness constraints," *IEEE J. Sel. Areas Commun.*, vol. 24, pp. 2061–2069, Nov. 2006.

[54] D. Kivanc, G. Li, and H. Liu, "Computationally efficient bandwidth allocation and power control for OFDMA," *IEEE Trans. Wireless Commun.*, vol. 2, pp. 1150–1158, Nov. 2003.

[55] G. Li and H. Liu, "Downlink radio resource allocation for multi-cell OFDMA system," *IEEE Trans. Wireless Commun.*, vol. 5, pp. 3451–3459, Dec. 2006.

[56] Y. Zhang and C. Leung, "Resource allocation in an OFDM-based cognitive radio system," *IEEE Trans. Commun.*, vol. 57, pp. 1928–1931, Jul. 2009.

[57] C. Yui, R. Cheng, K. Ben-Letaief, and R. Murch, "Multiuser OFDM with adaptive subcarrier, bit, and power allocation," *IEEE J. Sel. Areas Commun.*, vol. 17, pp. 1747–1758, Oct. 1999.

[58] S. Choudhury and J. Gibson, "Throughput optimization for wireless LANs in the presence of packet error rate constraints," *IEEE Commun. Lett.*, vol. 12, pp. 11–13, Jan. 2008.

[59] Y. Li and W. Ryan, "Mutual-information-based adaptive bit-loading algorithms for LDPC-coded OFDM," *IEEE Trans. Wireless Commun.*, vol. 6, pp. 1670–1680, May 2007.

[60] H. Zhu, "Radio resource allocation for OFDMA systems in high speed environments," *IEEE J. Sel. Areas Commun.*, vol. 30, pp. 748–759, May 2012.

[61] N. Ksairi and F. G. sur Yvette, "Resource allocation for downlink cellular OFDMA systemspart I: Optimal allocation," *IEEE Trans. Signal Process.*, vol. 58, pp. 720–734, Feb. 2010.

[62] S. Boyd and L. Vandenberghe, *Convex Optimization.* Cambridge, UK: Cambridge University Press, 2004.

[63] J. Xu, S.-J. Lee, W.-S. Kang, and J.-S. Seo, "Adaptive resource allocation for MIMO-OFDM based wireless multicast systems," *IEEE Trans. Broadcast.*, vol. 56, pp. 98–102, Mar. 2010.

[64] H. Li, H. Luo, X. Wang, C. Lin, and C. Li, "Fairness-aware resource allocation in OFDMA cooperative relaying network," in *Proc. IEEE ICC Conference*, Jun. 2009, pp. 1–5.

[65] C. Sung, K. Shum, and C. Ng, "Fair resource allocation for the gaussian broadcast channel with ISI," *IEEE Trans. Commun.*, vol. 57, pp. 1381–1388, May 2009.

[66] M. Tao, Y.-C. Liang, and F. Zhang, "Resource allocation for delay differentiated traffic in multiuser OFDM systems," *IEEE Trans. Wireless Commun.*, vol. 7, pp. 2190–2201, Jun. 2008.

[67] H. Zhu and J. Wang, "Chunk-based resource allocation in OFDMA systems-part i: Chunk allocation," *IEEE Trans. Commun.*, vol. 57, pp. 2734–2744, Sep. 2009.

[68] L. Weng and R. Murch, "Cooperation strategies and resource allocation in multiuser OFDMA systems," *IEEE Trans. Veh. Technol.*, vol. 58, pp. 2331–2342, Jun. 2009.

[69] P. Chan, E. Lo, V. Lau, R. Cheng, K. Ben-Letaief, R. Murch, and W. Mow, "Performance comparison of downlink multiuser MIMO-OFDMA and MIMO-MC-CDMA with transmit side information - multi-cell analysis," *IEEE Trans. Wireless Commun.*, vol. 6, pp. 2193–2203, Jun. 2007.

[70] E. Lo, P. Chan, V. Lau, R. Cheng, K. Ben-Letaief, R. Murch, and W. Mow, "Adaptive resource allocation and capacity comparison of downlink multiuser MIMO-MC-CDMA and MIMO-OFDMA," *IEEE Trans. Wireless Commun.*, vol. 6, pp. 1083–1092, Mar. 2007.

[71] Y.-H. Pan, K. Ben-Letaief, and Z. Cao, "Dynamic spatial subchannel allocation with adaptive beamforming for MIMO/OFDM systems," *IEEE Trans. Wireless Commun.*, vol. 6, pp. 2097–2107, Nov. 2004.

[72] D.-K. Hwang and R. Whang, "Efficient detection ordering scheme for MIMO transmission using power control," *IEEE Signal Process. Lett.*, vol. 16, pp. 715–718, Aug. 2009.

[73] Y.-H. Pan and S. Aissa, "Dynamic resource allocation with beamforming for MIMO OFDM systems: Performance and effects of imperfect CSI," *IEEE Trans. Wireless Commun.*, vol. 6, pp. 4249–4255, Dec. 2007.

[74] T. F. Maciel and A. Klein, "On the performance, complexity, and fairness of suboptimal resource allocation for multiuser MIMO/OFDMA systems," *IEEE Trans. Veh. Technol.*, vol. 59, pp. 406–419, Jan. 2010.

[75] N. Aboutorab, W. Hardjawana, and B. Vucetic, "A new resource allocation technique in MU-MIMO relay networks," *IEEE Trans. Veh. Technol.*, vol. 60, pp. 3485–34 900, Sep. 2011.

[76] W. Ho and Y.-C. Liang, "Optimal resource allocation for multiuser MIMO-OFDM systems with user rate constraints," *IEEE Trans. Veh. Technol.*, vol. 58, pp. 1190–1203, Mar. 2009.

[77] K. Seong, R. Narasimhan, and J. M. Cioffi, "Queue proportional scheduling via geometric programming in fading broadcast channels," *IEEE J. Sel. Areas Commun.*, vol. 24, pp. 1593–1602, Aug. 2006.

[78] Z. Kong, Y.-K. Kwok, and J. Wang, "A low-complexity QoS-aware proportional fair multicarrier scheduling algorithm for OFDM systems."

[79] J. Huang, V. Subramanian, R. Agrawal, and R. Berry, "Downlink scheduling and resource allocation for OFDM systems," *IEEE Trans. Wireless Commun.*, vol. 8, pp. 288–296, Jan. 2009.

[80] M. Ergen, S. Coleri, and P. Varaiya, "QoS aware adaptive resource allocation techniques for fair scheduling in OFDMA based broadband wireless access systems," *IEEE Trans. Broadcast.*, vol. 49, pp. 362–370, Dec. 2003.

[81] H. Seo and B. Lee, "Proportional-fair power allocation with CDF-based scheduling for fair and efficient multiuser OFDM systems," *IEEE Trans. Wireless Commun.*, vol. 5, pp. 978–983, May 2006.

[82] W. Huang and K. Ben-Letaief, "A cross-layer resource allocation and scheduling for multiuser space-time block coded MIMO/OFDM systems," in *Proc. IEEE ICC Conference*, May 2005, pp. 2655–2659.

[83] R. Elliott and W. Krzymien, "Downlink scheduling via genetic algorithms for multiuser single-carrier and multi-carrier MIMO systems with dirty paper coding," *IEEE Trans. Veh. Technol.*, vol. 58, pp. 3247–3262, Sep. 2009.

[84] M. Fathi, H. Taheri, and M. Mehrjoo, "Cross-layer joint rate control and scheduling for OFDMA wireless mesh networks," *IEEE Trans. Veh. Technol.*, vol. 59, pp. 3933–3941, Oct. 2010.

[85] D. W. K. Ng, E. S. Lo, and R. Schober, "Secure resource allocation and scheduling for OFDMA decode-and-forward relay networks," *IEEE Trans. Wireless Commun.*, vol. 10, pp. 3528–3540, Oct. 2011.

[86] J. Huang, V. Subramanian, R. Agrawal, and R. Berry, "Joint scheduling and resource allocation in uplink OFDM systems for broadband wireless access networks," *IEEE J. Sel. Areas Commun.*, vol. 27, pp. 226–234, Feb. 2009.

[87] K. Choi, D. Jeong, and W. Jeon, "Packet scheduler for mobile communications systems with time-varying capacity region," *IEEE Trans. Wireless Commun.*, vol. 6, pp. 1034–1045, Mar. 2007.

[88] S. Nam, H.-C. Yang, M.-S. Alouini, and K. Qaraqe, "Performance evaluation of threshold-based power allocation algorithms for down-link switching-based parallel scheduling," *IEEE Trans. Wireless Commun.*, vol. 8, pp. 1744–1753, Apr. 2009.

[89] S. Chung and A. Goldsmith, "Degrees of freedom in adaptive modulation: A unified view," *IEEE Trans. Commun.*, vol. 49, pp. 1561–1571, Sep. 2001.

[90] T. Moon, *Error Correction Coding.* New Jersey, USA: John Wiley and Sons, Inc, 2005.

[91] K.-C. Chen and J. R. B. de Marca, *Mobile WiMAX.* West Sussex, England: John Wiley and Sons, Inc, 2008.

[92] Y. Zhang and H.-H. Chen, *Mobile WiMAX: Toward broadband wireless metropolitan area networks.* Book News Inc., 2008.

[93] H. Meyr, M. Moeneclaey, and S. Fechtel, *Digital Communication Receivers.* West Sussex, England: John Wiley and Sons, Inc, 1998.

[94] D. Tse and P. Viswanath, *Fundamentals of Wireless Commuications.* Cambridge, UK: Cambridge University Press, 2005.

[95] J. Parsons, *The Mobile Radio Propagation Channel.* West Sussex, England: John Wiley and Sons, Inc, 2000.

[96] X. Huang, H.-C. Wu, and Y. Wu, "Novel pilot-free adaptive modulation for wireless OFDM systems," *IEEE Trans. Veh. Technol.*, vol. 57, pp. 3863–3867, Nov. 2008.

[97] L. Lihua, Z. Mingyu, W. Haifeng, and Z. Ping, "LDPC coded AMC based on decoding iteration times for OFDM systems," in *Proc. IEEE VTC Spring Conference*, May 2008, pp. 1157–1161.

[98] C. Snow, L. Lampe, and R. Schober, "Error rate analysis for coded multicarrier systems over quasi-static fading channels," *IEEE Trans. Commun.*, vol. 55, pp. 1736–1746, Sep. 2007.

[99] T. May, H. Rohling, and V. Engels, "Performance analysis of viterbi decoding for 64-DAPSK and 64-QAM modulated OFDM signals," *IEEE Trans. Commun.*, vol. 46, pp. 182–190, Feb. 1998.

[100] J. Andrews, A. Ghosh, and R. Muhamed, *Fundamentals of WiMAX: Understanding Broadband Wireless Networking.* Massachusetts, USA: Pearson Education, Inc, 2007.

[101] J. Heo, Y. Wang, and K. Chang, "A novel two-step channel-prediction technique for supporting adaptive transmission in OFDM/FDD systems," *IEEE Trans. Veh. Technol.*, vol. 57, pp. 188–193, Jan. 2008.

[102] "Guidelines for the evaluation of radio transmission technologies for IMT-2000," *Recommendation ITU-R M.1225.*

[103] S. Song and A. Singer, "Pilot-aided OFDM channel estimation in the presence of the guard band," *IEEE Trans. Commun.*, vol. 55, pp. 1459–1465, Aug. 2007.

[104] D. Bertsekas, *Constrained Optimization and Lagrange Multiplier Methods.* Massachusetts, USA: Athena Scientific, 1996.